

For Reference

NOT TO BE TAKEN FROM THIS ROOM

Ex LIBRIS
UNIVERSITATIS
ALBERTAENSIS



THE UNIVERSITY OF ALBERTA

FORMATION AND REACTION OF MONOVALENT
CARBON INTERMEDIATES

by



GERHARD J. A. KENNEPOHL

A THESIS

SUBMITTED TO THE FACULTY OF GRADUATE STUDIES AND RESEARCH
IN PARTIAL FULFILMENT OF THE REQUIREMENTS FOR THE DEGREE
OF DOCTOR OF PHILOSOPHY

DEPARTMENT OF CHEMISTRY
UNIVERSITY OF ALBERTA
EDMONTON, CANADA

FALL, 1972



Digitized by the Internet Archive
in 2022 with funding from
University of Alberta Libraries

<https://archive.org/details/Kennepohl1972>

thesis
72F-52D

UNIVERSITY OF ALBERTA

FACULTY OF GRADUATE STUDIES AND RESEARCH

The undersigned certify that they have read, and recommend
to the Faculty of Graduate Studies and Research for acceptance, a
thesis entitled

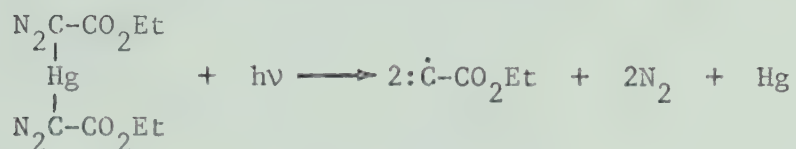
FORMATION AND REACTION OF MONOVALENT CARBON INTERMEDIATES
submitted by

GERHARD J. A. KENNEPOHL

in partial fulfilment of the requirements for the degree of Doctor
of Philosophy.

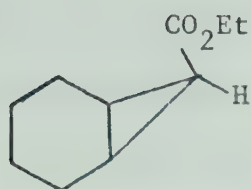
ABSTRACT

The monovalent carbon species carbethoxymethyne ($:\dot{\text{C}}\text{-CO}_2\text{Et}$) has been generated by the photolysis of diethyl mercurybisdiazoacetate,

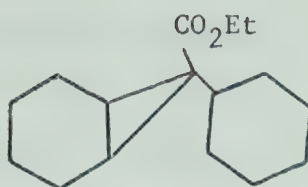


and its reactions have been investigated in solutions of cyclohexene, *cis*- and *trans*-butene-2, pyrrole, benzene, and hexafluorobenzene. Ground state doublet carbyne formed in the photolysis was found to insertively attack C-H bonds and to add stereospecifically to the olefinic double bonds yielding an alkyl and a cyclopropyl radical, respectively.

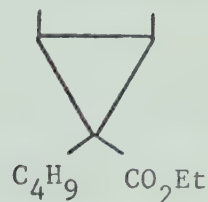
The intermediacy of the cyclopropyl radicals in the addition reactions leads to characteristic products and their yields demonstrated the extent of carbyne intervention. Thus hydrogen abstraction of the intermediate radical in cyclohexene and *cis*-butene-2 gave increased yields of the less stable isomers ethyl endo-norcarane-7-carboxylate (a) and ethyl *cis*-2,3-dimethylcyclopropane-*cis*-carboxylate (b) while reactions with the solvent yielded ethyl norcarane-7-cyclohexyl-7-carboxylate (c), ethyl norcarane-7-(3'-cyclohexenyl)-7-carboxylate (d), ethyl butyl-*cis*-2,3-dimethylcyclopropane carboxylate (e), and ethyl butenyl-*cis*-2,3-dimethylcyclopropane carboxylate (f):



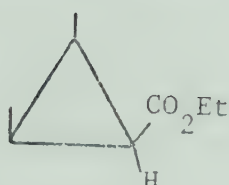
(a)



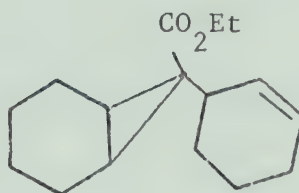
(c)



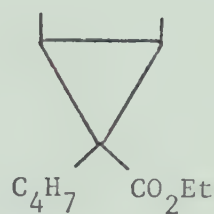
(e)



(b)

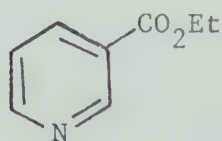


(d)

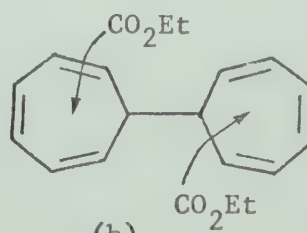


(f)

Addition of carbethoxymethyne ($:\dot{\text{C}}-\text{CO}_2\text{Et}$) to pyrrole and benzene resulted in ring expansion to give ethyl pyridine-3-carboxylate (g) and ethyl cycloheptatriene-carboxylate dimer (h):



(g)



(h)

Longer wavelength photolysis of the source compound leads only to N_2 loss in a stepwise fashion and the formation of singlet state mercury carbene which is capable of insertion and stereospecific additions as evidenced by the formation of stable mercury adducts. Cleavage of the C-Hg linkage of the source compound resulted in the formation of ethyl diazoacetate which was observed and monitored during the photolysis by infrared spectroscopy. The reactions of

carbethoxymethyne ($:\dot{\text{C}}-\text{CO}_2\text{Et}$) were compared to those of the corresponding carbethoxymethylene in each solvent system.

The effect of photonic energy of irradiation on the product distribution and the relative importance of the primary modes of decomposition were examined and the complexity in the overall mechanism discussed.

ACKNOWLEDGEMENTS

The author wishes to express his gratitude to Dr. O. P. Strausz for his constant encouragement and guidance throughout the course of this work.

Special thanks go to Dr. E. M. Lown for helpful advice and preparation of the manuscript.

The author is indebted to Dr. Thap DoMinh, Dr. F. X. Garneau, Dr. G. Frater, Dr. B. Kim, Mr. V. Sidhu, Mr. A. Clement and L. Torok-Both of the photochemistry group for invaluable help and experimental assistance.

The assistance of the technical staff of the Department of Chemistry, especially Mr. R. N. Swindlehurst, G. Bigam, Dr. A. M. Hoff and their associates is appreciated.

Special tribute is due to Mrs. R. Tarnowski for her diligent efforts in typing of this thesis.

The financial assistance provided by the University of Alberta and the granting of a leave of absence by Gulf Oil Canada Limited is gratefully acknowledged.

The author would like to express his gratitude to his wife, Evmarie, whose devotion and unceasing cooperation have made this work possible.

TABLE OF CONTENTS

	<u>Page</u>
ABSTRACT.....	i
ACKNOWLEDGEMENTS.....	iv
LIST OF TABLES.....	viii
LIST OF FIGURES.....	x
 CHAPTER 1. INTRODUCTION.....	 1
1.1 Subject, Definitions and Nomenclature.....	1
1.2 History and Review.....	2
1.3 Theoretical Aspects.....	21
1.4 Objectives and Outline.....	26
 CHAPTER 2. EXPERIMENTAL.....	 28
2.1 Apparatus and Instrumentation.....	28
2.2 Materials.....	36
2.3 Photolysis.....	39
2.4 Thermolysis.....	42
2.5 Analysis.....	43
 CHAPTER 3. PHOTOLYSIS OF DIETHYL MERCURYBISDIAZOACETATE.....	 47
3.1 Reaction and Observations.....	47
3.2 Product Description.....	48
3.3 Effect of Wavelength.....	53
3.4 Relative Stability of the Mercury-Adduct, [7].....	 55

TABLE OF CONTENTS (cont'd)

	<u>Page</u>
3.5 Intermediacy of EDA.....	56
3.6 Effects of Oxygen and Temperature.....	63
3.7 Discussion.....	66
 CHAPTER 4. PHOTOLYSIS OF DIETHYL MERCURYBISDIAZOACETATE IN <i>CIS-</i> AND <i>TRANS</i> -BUTENE-2.....	 80
4.1 Results.....	81
4.2 Discussion.....	87
4.3 Summary.....	94
 CHAPTER 5. PHOTOLYSIS OF DIETHYL MERCURYBISDIAZOACETATE IN PYRROLE.....	 95
5.1 Solvent Properties and Carbene Reactions of Pyrrole.....	 95
5.2 Results.....	97
5.3 Discussion.....	103
 CHAPTER 6. REACTIONS OF CARBETHOXYMETHYLENE AND CARBETHOXY- METHYNE WITH AROMATIC SOLVENTS.....	 109
6.1 Carbene Reactions.....	109
6.1.1 Photolysis of EDA in Benzene.....	109
6.1.2 Photolysis of EDA in Hexafluorobenzene (HFB)	115
6.2 Carbyne Reactions.....	130

TABLE OF CONTENTS (cont'd)

	<u>Page</u>
6.2.1 Results of the Photolysis of DMDA in Benzene.....	130
6.2.2 Results of the Photolysis of DMDA in Hexa- fluorobenzene (HFB).....	134
6.2.3 Discussion.....	137
CHAPTER 7. SUMMARY AND CONCLUSION.....	143
BIBLIOGRAPHY.....	148
APPENDIX A.....	156
APPENDIX B.....	158
APPENDIX C.....	161
APPENDIX D.....	162

LIST OF TABLES

<u>Table</u>	<u>Page</u>
I Simple Non-tetravalent Carbon Intermediates.....	2
II Rydberg States of CH.....	6
III Molecular Constants of CH in Its Various Electronic States.....	9
IV Rate Constants for the Reactions of CH with Different Substances.....	16
V Rate Constants for the Reaction of CCl and CBr with Substrate (298 \pm 3°K).....	18
VI Combined Gas Chromatographical and Mass Spectral Analysis for Products [1] - [7].....	50
VII Molecular Weights, I.R. and N.M.R. Spectra for Compounds [1] - [7].....	52
VIII Product Yield Variation as a Function of Wavelength..	54
IX Effect of Wavelength on Product Ratios.....	54
X Comparison of Yields from the Photolysis of DMDA and [7] in Cyclohexene.....	57
XI Product Yields from the Photolysis of [7] in the Absence of Oxygen.....	57
XII Concentration Measurements of DMDA and EDA during Photolysis.....	58
XIII Thermolysis of DMDA in the Absence and Presence of Oxygen.....	65
XIV Combined Gas Chromatographical and Mass Spectral Analysis for Products [10] - [17].....	83

LIST OF TABLES (cont'd)

<u>Table</u>	<u>Page</u>
XV Molecular Weights, I.R. and N.M.R. Spectra for Compounds [10] - [17].....	85
XVI Yields of Products [10] - [14] from the Photolysis of EDA and DMDA in <i>cis</i> - and <i>trans</i> -butene-2.....	88
XVII Wavelength Dependence of the Yields of [14] - [17]...	88
XVIII I.R. and N.M.R. Spectra for [18] and [19].....	99
XIX Combined Gas Chromatographical and Mass Spectral Analysis for Products [18] - [22].....	101
XX Per cent Yield of [18] and [19] from the Photolysis of DMDA and EDA in Pyrrole.....	102
XXI Mass Spectra of $C_7F_6HCO_2Et$ Isomers, Products [38] - [46].....	119
XXII Proton and Fluorine N.M.R. Data.....	120
XXIII Product Yields from the Photolysis of EDA in HFB Solution.....	126
XXIV Mass Spectra of Products [49] - [53].....	132
XXV Molecular Weights, I.R. and N.M.R. Spectra for Compounds [49] - [53].....	133
XXVI Analytical Data for Products [1] - [7].....	157
XXVII Concentration and Absorbance Measurements for EDA and DMDA.....	159
XXVIII Product Yields for [14] - [17].....	161
XXIX Analytical Data for the Photolysis of DMDA and EDA in Pyrrole.....	163

LIST OF FIGURES

<u>Figure</u>		<u>Page</u>
1	Potential Curves of Known Electronic States of CH....	5
2	Energy-level Diagram of the Observed Electronic States of CH Free Radicals.....	5
3	Correlation of Rate Constants with Ionization Potential for the Reaction of CCl with • Alkenes, o Halogenalkanes and ▲ Alkynes.....	20
4	Correlation Diagram for the Addition of Methyne to Ethylene.....	24
5	Modified Bulb-to-Bulb Distillation Apparatus.....	30
6	Photolysis Reaction Vessels: Immersion Well Assembly (a); Pyrex Reaction Vessel (b); Quartz Tube (c); and Quartz Tube with Attached I.R. Cell (d).....	32
7	Cut-off Range for Various Filters.....	34
8	Concentrations of DMDA ■ and EDA ● during the Photolysis with Vycor Filtered Light.....	59
9	Concentrations of DMDA ■ and EDA ● during the Photolysis with Corex Filtered Light.....	60
10	Concentrations of DMDA ■ and EDA ● during the Photolysis with Pyrex Filtered Light.....	61
11	Concentrations of DMDA ■ and EDA ● during the Photolysis with Uranium Glass Filtered Light.....	62
12	Reaction Scheme I.....	71

LIST OF FIGURES (cont'd)

<u>Figure</u>		<u>Page</u>
13	Reaction Scheme II.....	73
14	U.V. Spectra of DMDA and the Mercury Adduct [7].....	75
15	Reaction Scheme III.....	90
16	Reaction Scheme IV.....	91
17	Reaction Scheme V.....	107
18	Reaction Scheme VI.....	113
19	U.V. Spectrum of Product [38].....	123
20	U.V. Spectrum of Product [45].....	125
21	Reaction Scheme VII.....	141
22	Calibration Curves for EDA and DMDA.....	160

CHAPTER 1

INTRODUCTION

1.1 Subject, Definitions and Nomenclature

Ever since the concept of the tetravalency of carbon was formulated more than a century ago, the non-tetravalent carbon species have played an extraordinary role in organic chemistry. One such species is monovalent carbon, the subject of this study.

A carbon species which has only one covalent bond to an adjacent group or, more precisely, only one substituent bonded by a covalent bond is defined here as a "monovalent carbon." There are also three non-bonding orbitals which contain three electrons among them and two additional valence electrons which are shared in the one covalent bond. The definition is consistent with the well established terminology for other non-tetravalent carbon transients such as divalent and trivalent carbon which are linked to two and three adjacent groups respectively by covalent bonds. Thus, monovalent carbon is a member of the homologous series of simple non-tetravalent carbon intermediates which are summarized in Table I. Monovalent carbon is named "carbyne" by analogy with the well accepted "carbene" nomenclature. The suffixes -ylidyne and -ylidene respectively have been approved by the International Union of Pure and Applied Chemistry (IUPAC; B 5.11 and B 5.12) Organic Nomenclature Committee but the "carbyne" nomenclature will be used here because it

is in most cases preferred for its simplicity, clearness, and consistency with the "carbene" nomenclature in use today.

TABLE I

Simple Non-tetravalent Carbon Intermediates

Species		Valency	No. of valence electrons	No. of unshared electrons
Carbanion	>C:^-	trivalent	8	2
Radical	$\text{>C}\cdot$	trivalent	7	1
Carbonium	>C^+	trivalent	6	0
Carbene	>C:	divalent	6	2
Carbyne	$\text{-}\dot{\text{C}}\text{:}$	monovalent	5	3
Atomic carbon	$\text{:}\dot{\text{C}}\text{:}$	zero valent	4	4

1.2 History and Review

The chemistry of carbon atoms as well as di- and tri-valent intermediates has been thoroughly explored. The extent and significance of research involving di- and trivalent species is reflected in the enormous amount of literature and hence needs no further comment. Atomic carbon chemistry has also developed to an extensive and rapidly expanding field. Especially in the last two decades, many publications have appeared describing production methods and chemical reactions of atomic carbon. Its presence has been detected and its intervention postulated in numerous energetic

reactions including nuclear transformation¹, pulse radiolysis², carbon arcs³, explosion of graphite filament⁴, shock heating⁵, plasma decomposition⁶, microwave discharge⁷, photolysis⁸, flash photolysis⁹ and chemical reaction¹⁰.

Surveying the chemistry of carbon intermediates, one immediately realizes that monovalent carbon has been neglected. Indeed little is known on the formation, physical characterization properties and chemical reactivities of these species as it will be evident from the brief review presented in the subsequent paragraphs.

Occurrence, Spectra, and Reactions of Methyne. Astrophysical studies have, at the beginning of this century, suggested and confirmed the existence of CH, methyne, which is the simplest carbyne transient. Its prominent bands have been detected in the spectra of stellar atmospheres including the sun and interstellar atmospheres¹¹. There exists, also, a group of peculiar carbon stars which are characterized by unusually strong CH bands (λ : 4300^oÅ, 3900^oÅ) and comparatively weak C₂ bands¹². Methyne has also been observed and studied utilizing one of the oldest methods of obtaining spectra of free radicals, by producing it in high temperature flames. In the flame of the ordinary Bunsen burner CH amongst other diatomic free radicals has been detected by emission spectroscopy. Other more sophisticated methods to produce methyne include atomic flame, electric discharge and the decomposition of stable parent compounds by irradiation with ultraviolet light. The analysis of the emission spectrum of CH in the visible and near ultraviolet regions was mostly accomplished by the early work of

Hulthén¹³, Kratzer¹⁴, Fortrat¹⁵, Mulliken¹⁶, and Hori¹⁷. While Kratzer (1924) and Mulliken (1927) studied in detail the first two known bands (λ : 4300Å, 3900Å) in the spectrum of CH, Hori (1929) provided the theoretical interpretation of the third band (λ : 3143Å) which was originally observed by Fortrat. All three band systems terminate in the $^2\Pi$ ground state of the molecule. The upper states of the three systems are A $^2\Delta$, B $^2\Sigma^-$, and C $^2\Sigma^+$. In further work Gerö¹⁸ succeeded in observing the species CD. Shidei¹⁹ noted the breaking off of the rotational structure with predissociation of the B $^2\Sigma^-$ state of CH and CD from which Gerö determined reliable dissociation energies^{18,20}. It was not until 1952 that Norrish, Porter and Thrush²¹ observed the first absorption spectrum of CH in the laboratory. They photographed the three systems A-X, B-X and C-X in the combustion of acetylene initiated by the flash photolysis of NO_2 . Subsequently, several groups applied greatly improved methods to produce much stronger spectra for quantitative measurement, such as the flash photolysis of diacetylene by Callomon and Ramsay²² and the flash photolysis of diazomethane by Herzberg²³ et al. An improved value for the dissociation energy of CH (and CD) was obtained and a number of electronic transitions (Figure 1) were found in the vacuum ultraviolet, including a Rydberg series starting at 1370Å which supplied an ionization potential of 10.64 eV. In a recently (1970) published book dealing with the spectra and structure of simple free radicals, Herzberg²⁴ has described the Rydberg states of CH (Table II) and the fine structure of the CH band at 3630Å, from which an energy level diagram of the known electronic states (Figure 2)

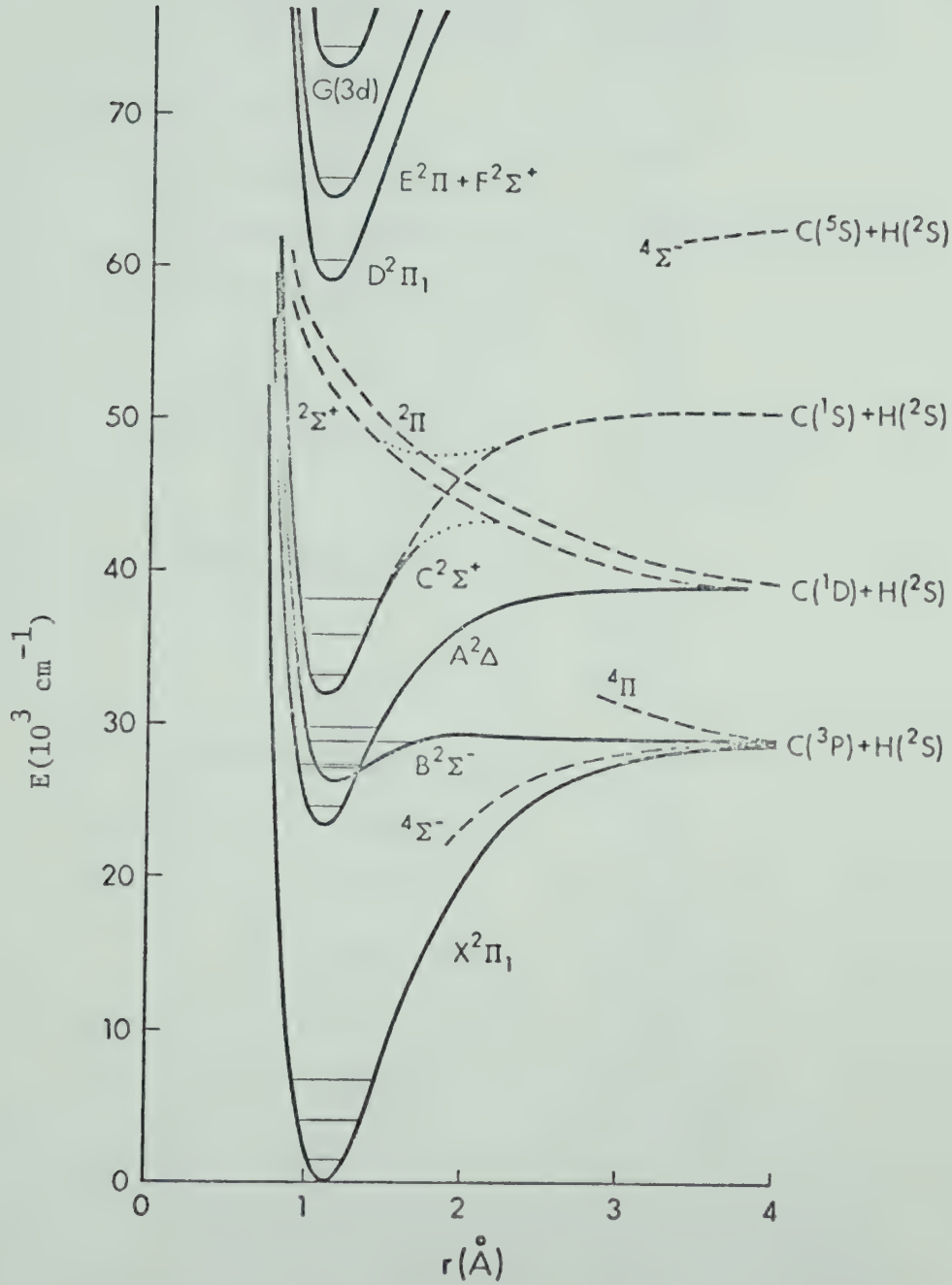


FIGURE 1: Potential Curves of Known Electronic States of CH

TABLE II

Rydberg States of CH

Electron Configuration	States
$1s\sigma^2 2s\sigma^2 2p\sigma^2 2p\pi$	<i>X</i> $^2\Pi$
$1s\sigma^2 2s\sigma^2 2p\sigma^2 3s\sigma$	$^2\Sigma^+$
$1s\sigma^2 2s\sigma^2 2p\sigma 2p\pi 3s\sigma$	<i>E</i> $^2\Pi$, $^2\Pi$, $^4\Pi$
$1s\sigma^2 2s\sigma^2 2p\sigma^2 3p\sigma$	<i>F</i> $^2\Sigma$
..... $3p\pi$	$^2\Pi$
$1s\sigma^2 2s\sigma^2 2p\sigma 2p\pi 3p\sigma$	$^2\Pi$, $^2\Pi$, $^4\Pi$
..... $3p\pi$	$^2\Sigma^+$, $^2\Sigma^-$, $^2\Delta$, ...
$1s\sigma^2 2s\sigma^2 2p\sigma^2 3d\sigma$	$^2\Sigma^+$
..... $3d\pi$	<i>G</i> $^2\Pi$
..... $3d\delta$	$^2\Delta$
$1s\sigma^2 2s\sigma^2 2p\sigma^2 ns\sigma$	$^2\Sigma^+$
..... $np\sigma$	$^2\Sigma^+$
..... $np\pi$	$^2\Pi$
..... $nd\sigma$	$^2\Sigma^+$
..... $nd\pi$	$^2\Pi$
..... $nd\delta$	$^2\Delta$
$1s\sigma^2 2s\sigma^2 2p\sigma^2 p\pi ns\sigma$	$^2\Pi$, $^2\Pi$, $^4\Pi$

The states designated by italic letters added to the Greek symbol have been observed [Herzberg and Johns (ref. 23)]. In addition some of the states with $n = 4, 5, 6$ have been found.

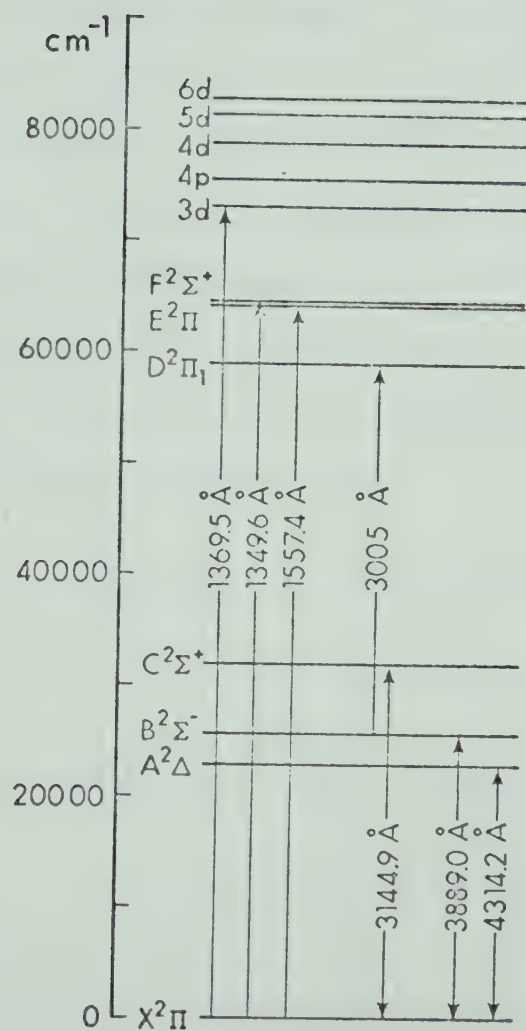
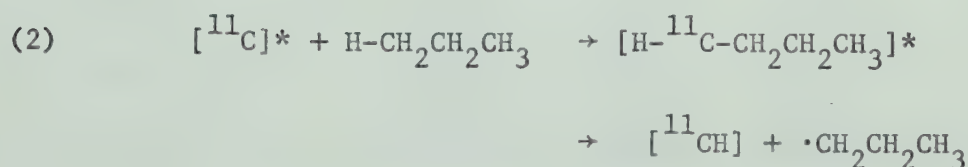
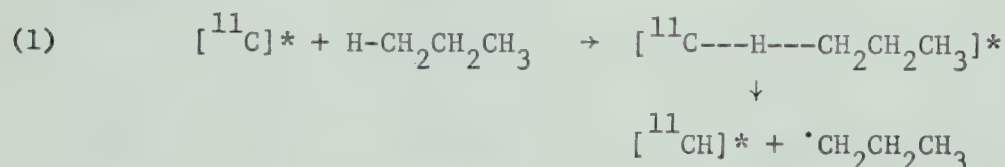


FIGURE 2: Energy-level Diagram of the Observed
Electronic States of CH Free Radicals

and molecular constants of CH in its various electronic states (Table III) could be derived. Although the presence of methyne in numerous energetic reactions has been unambiguously documented by spectroscopic means, only very few studies of its reactions have been made to date. Initially, this intermediate was vaguely alluded to, and postulated to be a possible alternative transient in the reactions of "hot" carbon atoms with saturated hydrocarbons²⁵⁻²⁸. Wolff²⁹ considers two possible modes of formation of methylene-¹¹C from the encounter of recoil carbon atom-11 with hydrocarbon substrates, involving either H-atom abstraction upon the first reactive encounter (1) or bond formation by insertion into the carbon-hydrogen bond and subsequent decomposition (2) of the energized radical:



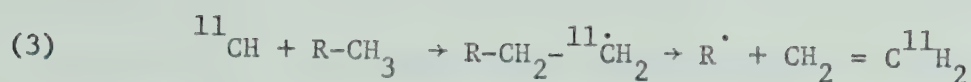
In principle, methyne could react to form many of the products which are observed in free carbon atom chemistry. In the formation of the two predominant products, acetylene and ethylene, methyne has been suggested as a possible precursor²⁸⁻³⁰. One can visualize that ethylene-¹¹C is primarily formed from an intermediate arising from insertion of ¹¹CH into primary carbon-hydrogen bonds followed by C-C bond rupture:

TABLE III

Molecular Constants of CH in its Various Electronic States

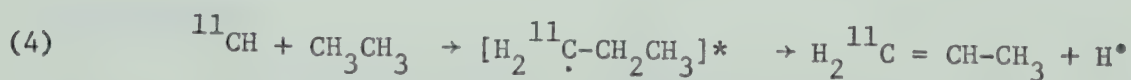
State	T_0	$G(\frac{1}{2})$	B_0	r_0
na	82788			
$6d$	82726			
na	81545			
$5d$	81271			
na	81006			
$4d$	78660			
$4p$	75550			
$3d(^2\Sigma, ^2\Pi, ^2\Delta)$	72960			
$F ^2\Sigma^+$	64531.5		12.17	1.221
$E ^2\Pi$	64211.7		12.6	1.2_0
$D ^2\Pi_1$	58981.0		13.7	1.1_2
$C ^2\Sigma^+$	31778.1	2612.5	14.2466	
$B ^2\Sigma^-$	25698.2	1794.9	12.645	
$A ^2\Delta$	23217.5	2737.4	14.577	
$X ^2\Pi_r$	0	2732.50	14.190	

The states marked 'na' are not assigned.



Insertion into secondary carbon-hydrogen bond cannot lead to ethylene without hydrogen migration and scission of two carbon-carbon bonds and may therefore be discounted. Acetylene is presumably formed in a solvent cage by direct insertion of ${}^{11}\text{C}$ and subsequent decomposition of the reaction complex because the yields of this product are unaffected by the addition of scavengers such as iodine³⁰. In contrast, the ethylene and ethane yields decrease upon addition of iodine indicating that the immediate precursors were radicals presumably CH , which escaped the solvent cage. Furthermore, labeling experiments have also ruled out the possibility that ${}^{11}\text{CH}$ may contribute significantly towards acetylene formation.

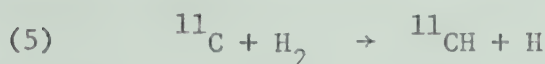
The formation of propylene- ${}^{11}\text{C}$ has also been rationalized in terms of ${}^{11}\text{CH}$ insertion. Only ethane and those hydrocarbons which contain an ethyl group give substantial yields of propylene- ${}^{11}\text{C}$. The formation of propylene- ${}^{11}\text{C}$ from ethane occurs by ${}^{11}\text{CH}$ insertion with only a single carbon-hydrogen bond being broken instead of a carbon-carbon bond:



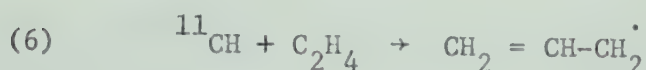
The complex is believed to be sufficiently energetic to meet additional energy requirements for such a rupture. There has been no lack of variety in the choices of gaseous and liquid hydrocarbons used as targets for interaction with recoil carbon. Trends in product

distribution especially yields of $[C_2H_4 + C_2H_6]$ and $[C_2H_4 + C_2H_6]/[C_2H_2 + C_2H_4 + C_2H_6]$ have been related to degree of saturation, hydrogen availability at the insertion site, and branching. Still, to this point in time, as reviewed by Wolfgang^{31,32} in 1965, it was difficult to assess the extent of methyne intervention and to distinguish among the reactions of C, CH and CH_2 intermediates.

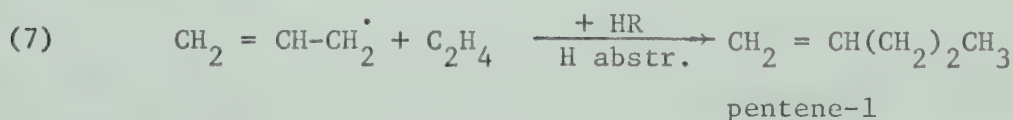
More convincing evidence for the apparent production of methyne in the reactions of free carbon atoms was presented in 1966 by Wolfgang et al.^{33,34}. When translationally excited (hot) ^{11}C was produced in mixtures of H_2 and C_2H_4 one of the products, pentene-1, could not easily be explained by the intermediacy of ^{11}C , $^{11}CH_2$, or $^{11}CH_3$. Methyne formed from carbon and hydrogen appeared to be, however, a reasonable precursor. Insertion of ^{11}CH into the π or



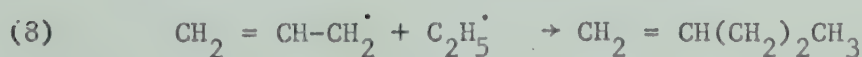
C-H bond, by analogy with carbenes, yield the allyl radical which



subsequently adds to ethylene. Pentene-1 is then formed by H-abstraction:

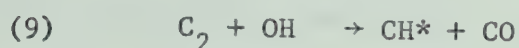


A combination reaction with a free ethyl radical will also lead to pentene-1:

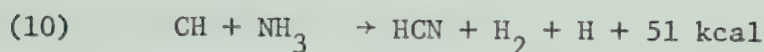


Both mechanisms are probably operative. The amount of CH formed was then estimated through yields of pentene-1. It was further noted that an increase in hydrogen pressure of the system gave increased yield of pentene-1 and therefore increased production of CH. In addition to free carbon atom chemistry, there are also a few recent studies of methyne formation and reactions in highly energetic reactions such as (a) atomic flames, (b) shock waves, (c) flash-photolysis, and (d) pulse radiolysis.

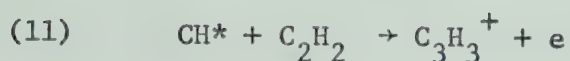
(a) The occurrence and mechanism of methyne formation in



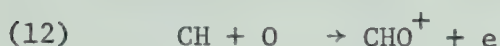
atomic flames advanced by Gaydon³⁵ is generally accepted. The first study of reactions of methyne in flames was reported by Safrany et al.³⁶ in 1964. They observed production of HCN when NH_3 was added upstream from a $\text{C}_2\text{H}_2 - \text{O}_2$ reaction flame, suggesting the following reaction:



An estimated upper limit of $k = 6 \times 10^7 \text{ l mol}^{-1} \text{ sec}^{-1}$ was recorded for the reaction which is the first reported rate constant for methyne. Calcote et al.^{37a} have postulated methyne in low pressure high temperature flames using a mass spectrometer and Langmuir probe techniques for identification. The CH transient is involved in a proposed mechanism for the formation of an important primary ion, C_3H_3^+ , which is dominant in most hydrocarbon combustion fronts:

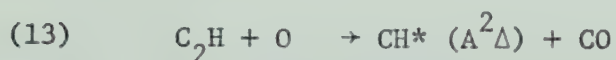


In addition to chemi-ionization, Fontiju et al.^{37b} observed chemiluminescence in a study of the $\text{O} + \text{C}_2\text{H}_2$ reaction in a Wood-Bonhoeffer system. Experiments which allowed identification and measurement of individual ions as well as measurements of relative chemiluminescence intensity, suggest the intervention of ground and excited states in the chemi-ionization mechanism:



The addition of free radical scavengers NO or O_2 decreased the total ion concentration and light emission, indicating that free radicals initially produced in the reaction $\text{O} + \text{C}_2\text{H}_2$ are precursors of the ionizing and light emitting species.

(b) Glass et al.^{37c} have found that the high temperature oxidation of acetylene in shock tubes proceeds by fast chain branching reactions involving methyne. The suggested step for the production of electronically excited CH :



is novel and not consistent with the earlier Gaydon mechanism, (9). The discrepancy is attributed to the difference in the experimental conditions of the two experiments.

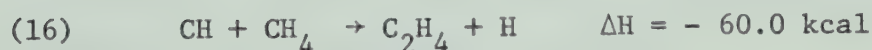
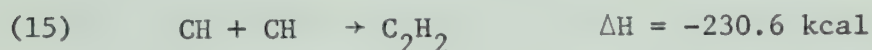
(c) Flash-photolysis in the vacuum ultraviolet of methane and mixtures of $\text{CH}_4\text{-CD}_4$ was undertaken in 1966 by Braun et al.³⁸ Complete product analysis including isotopic distribution of hydrogen, ethane and the major hydrocarbon product, ethylene, led to

the conclusion that CH plays a major role in the photolysis. The origin of methyne was explained by two possible mechanisms both involving CH_2 formed in the primary act. It could be formed by the secondary photolysis of CH_2 ;

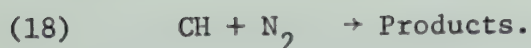
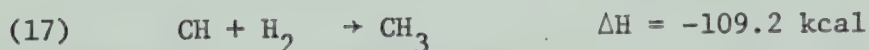


or by unimolecular decomposition of vibrationally excited CH_2 . The identification of methyne could be substantiated by the known transitions of CH in absorption, i.e. $\text{C } ^2\Sigma^{-1} \leftarrow \text{X } ^2\Pi$ and $\text{A } ^2\Delta \leftarrow \text{X } ^2\Pi$.

In a subsequent paper Braun³⁹ reported absolute rate constants for the reactions of CH, utilizing flash photolysis in the ultraviolet and kinetic spectroscopy: this is the first intensive kinetic study of the monovalent carbon species, CH, on record. The decay curve for methyne exhibited first order reaction. The mechanism for CH disappearance was believed to involve two possible reactions:



The addition of hydrogen and nitrogen to methyne were also studied:



(d) Additional rate constants were published in 1971 by

Bosnali and Perner⁴⁰ who reacted $\text{CH}(^2\Pi)$ with methane and several other compounds. The $\text{CH}(^2\Pi)$ radical was produced by pulse radiolysis and re-examined by kinetic absorption spectroscopy. The rate constants for the reaction of methyne with various compounds reported by Braun, Safrany, Bosnali and Perner (Table IV) show considerable deviations.

Formation and Reactions of Halomethynes. Besides the simplest monovalent carbon species, methyne, there are a few recent studies with halogen and nitrile mono-substituted carbon species. The spectra and transitions of these diatomic radicals, CF, CCl, CBr, and CCN, have been studied and assigned, but are not as detailed and comprehensive as those for methyne. The emission spectra for the diatomic radicals CF and CCl have been known over 20 years, and details of their earlier studies and spectral assignments were summarized by Pearse and Gaydon (1965).⁴¹ A more detailed study of the emission spectrum of CF which consists of two major band systems $A \ ^2\Sigma \rightarrow X \ ^2\Pi$ and $B \ ^2\Sigma^+ \rightarrow X \ ^2\Pi$ in the 1975 to 2965 Å region was given by Porter et al.⁴² Analysis of the rotational structure of 18 bands, dissociation energies and a graph showing potential energy curves were also given.

Simons and Yarwood⁴³⁻⁴⁵ (1961-1962) have observed the formation of carbon monohalides CF, CCl, CBr during flash photolysis of molecules containing halogeno-methyl groups. They proposed a mechanism for the formation of CF, CCl, and CBr via decomposition of energized halogen-methyl radicals

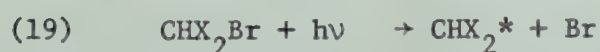
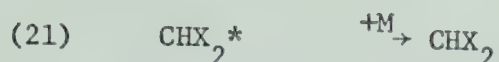
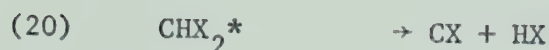


TABLE IV

Rate Constants for the Reaction of CH with
Different Substances ($298 \pm 3^\circ\text{K}$)

Substance	k ltr. mol ⁻¹ sec ⁻¹	Reference
CH ₄	$(2.01 \pm 0.05) \times 10^{10}$ 1.5 $\times 10^9$	40 39
C ₃ H ₈	$(8.2 \pm 2) \times 10^{10}$	40
<i>n</i> -C ₄ H ₁₀	$(7.8 \pm 0.7) \times 10^{10}$	40
C ₂ H ₄	$(6.9 \pm 0.6) \times 10^{10}$	40
C ₂ H ₂	$(4.5 \pm 0.9) \times 10^{10}$	40
H ₂ O	$(2.7 \pm 0.2) \times 10^{10}$	40
NH ₃	$(5.9 \pm 0.9) \times 10^{10}$ 6 $\times 10^7$	40 36
N ₂	$(6.1 \pm 3) \times 10^8$ 4.3 $\times 10^7$	40 39
H ₂	$(1.05 \pm 0.12) \times 10^{10}$ 6.2 $\times 10^8$	39 39
O ₂	2.4 \pm $\times 10^{10}$	40
CO	2.9 $\times 10^9$	40



where X = halogen and M = N₂, Ar, or SF₆. The mechanism was deduced from the observed variation of product yields with photon energy input, flash intensity, and total pressure under isothermal conditions. New absorption systems of CCl and CBr radicals following flash-photolysis of organic halides were assigned and advanced by Dixon and Kroto⁴⁶ in 1963 and recently by Tyerman⁴⁷. Jacox and Milligan^{48,49} were able to study infrared and ultraviolet spectra of CF and CCl isolated in argon and nitrogen matrices, and Carrington and Howard⁵⁰ the gas phase electron resonance spectrum and dipole moment of CF. The absorption spectrum of the free radical CCN was discovered by Merer and Travis⁵¹ in the flash photolysis of diazoacetonitrile. Three electronic transitions were assigned for band systems between 3500Å and 4700Å.

The only reported reaction of monovalent carbon halides is that of chloromethyne, CCl, by Tyerman^{52,53} in 1969. Similarly to earlier studies by Braun et al.^{38,39} of methyne itself in the vacuum ultraviolet flash photolysis of methane, Tyerman utilized kinetic spectroscopy to monitor the rate of removal of CCl when reagents were added to flashed mixtures containing halogenated hydrocarbons. Rate constants for the reaction of CCl and CBr⁵⁴ radicals with olefins, alkynes, chloroalkanes, hydrogen, and oxygen were determined (Table V).

TABLE V

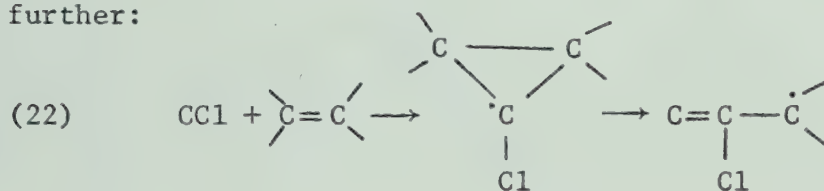
Rate Constants for the Reaction of CCl and CBr with
with Substrate ($298 \pm 3^\circ\text{K}$)

Compound	$10^{-8} \times k \text{ (ltr.} \times \text{mole}^{-1} \times \text{sec}^{-1})$	
	CCl*	CBr**
hydrogen	0.3 ± 0.1	<0.03
nitrogen	<0.015	<0.004
oxygen	25 ± 3	13 ± 0.5
methane	-	<0.03
propane	1.0 ± 0.15	-
i-butane	-	<0.03
cyclohexane	2.3 ± 0.3	-
chloroform	2.2 ± 0.1	-
ethylene	3.3 ± 0.4	4.2 ± 1
propene	25 ± 2.5	-
iso-butene	155 ± 11	-
butene-1	-	86 ± 10
t-butene-2	96 ± 8	170 ± 25
vinyl fluoride	-	4.7 ± 0.3
acetylene	1.1 ± 0.1	<0.5
propyne	24 ± 2	-

* Reference 53.

** Reference 54.

The fact that saturated hydrocarbons react with CCl and CBr considerably slower than do olefins was interpreted to mean that attack of the electrophilic monovalent carbon species on the π -bond system of olefins is preferred over insertion and abstraction reactions. A good correlation of ionization potentials and rates of reactions (Figure 3) with olefins is also an indication of π -system involvement which may lower the energy of the transition complex with increasing electron density. The mechanism of reaction with olefins has been suggested to be symmetrical addition of the radical to the double bond, forming a cyclopropyl radical which would carry sufficient excess energy to rearrange to an alkyl radical and react further:



However, it must be conceded that it is impossible to suggest an actual reaction mechanism from the reported rate constants alone. No further detailed kinetic mechanistic studies have been reported to date on the family of monovalent carbon intermediates. The difficulty in generating transients under conditions amenable for mechanistic interpretation is still the major problem in the study of carbynes and the likely major reason for the scarcity of information on these carbon intermediates. Hitherto, nobody has recognized the possibilities of mercury-diazo compounds as useful sources of carbynes. In 1967 a program for the systematic study of monovalent carbon intermediates was started in this laboratory utilizing the

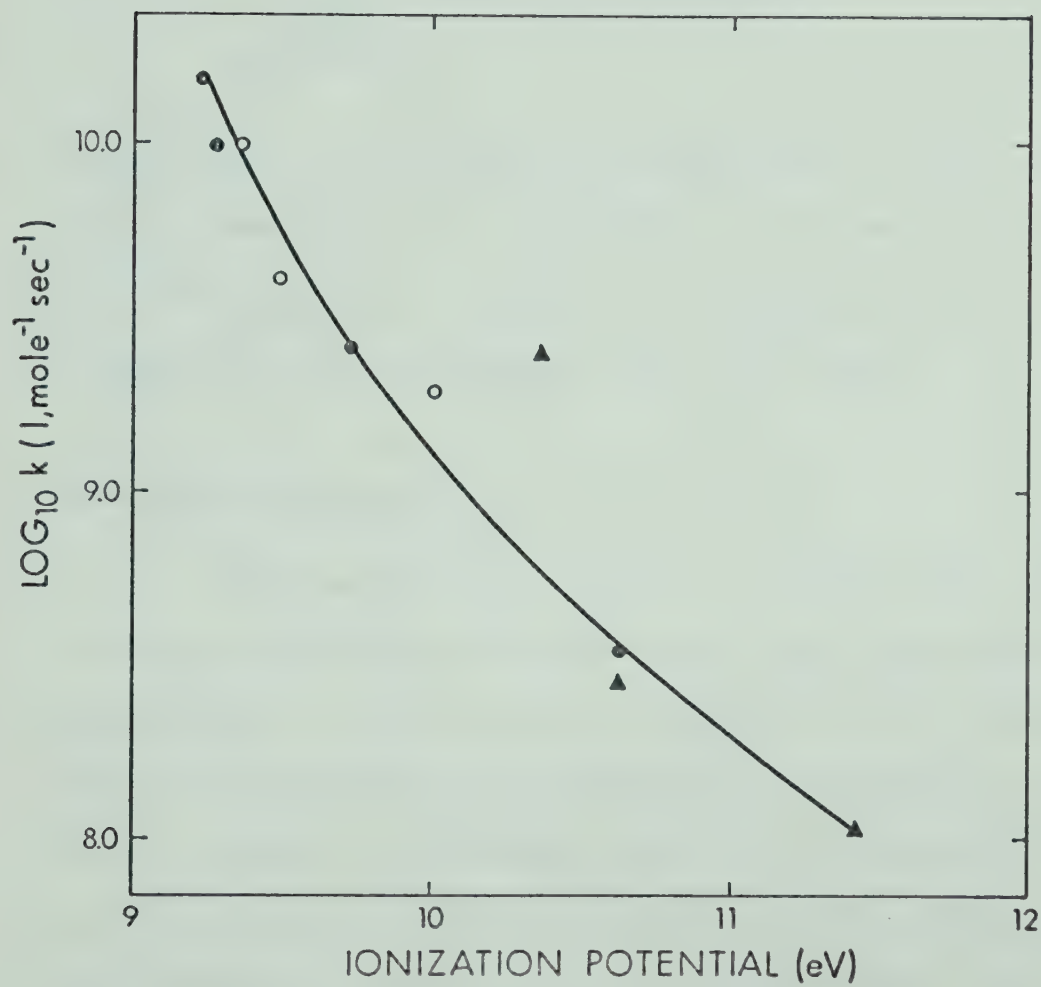
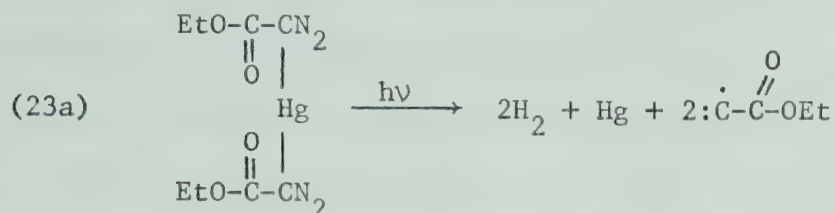


FIGURE 3: Correlation of Rate Constants with Ionization Potential for the Reaction of CCl with ● Alkenes, ○ Halogenalkenes and ▲ Alkynes.

photochemical decomposition of diethyl mercury bisdiazooacetate, DMDA. Carbethoxymethyne was suggested as the reactive intermediate in the photochemical decomposition of DMDA^{55a,b}.



Indeed, photolysis of DMDA in fluorolube glass at -196°C generated a single symmetrical e.s.r. signal with no hyperfine structure at $g = 2.000$ indicating the presence of a doublet ground state species containing no protons adjacent to the radical site.

1.3 Theoretical Aspects

Carbynes have five valence electrons and thus methyne itself is isoelectronic with the nitrogen atom. The ground electron configuration is characterized by the distribution: $1\sigma^2 2\sigma^2 2p^3$. Two of the three non-bonding p-orbitals are degenerate and depending on the splitting of the orbital energy levels as compared to the electron repulsion energies, the ground electronic state may either be a doublet or a quartet. In fact the ground state of all the four carbynes CH, CF, CCl and CBr, whose u.v. spectra are known is a doublet Π state and the excitation energy of the lowest excited quartet state of methyne has been estimated to lie 28 kcal/mole above the $X^2\Pi$ ground state.⁵⁶ To date the quartet states of carbynes have not been observed experimentally. Substituents could alter the

orbital energy levels and invert the energy of the $X^2\Pi$ ground state and the lowest quartet state, $\alpha^4\Sigma^+$. In the case of the carbenes, methylene has a triplet ground state, but introduction of a single halogen atom, carboalkoxy or aryl group lowers sufficiently the energy of the first excited orbital to bring the singlet state energy below the orbitally excited triplet. These relations for carbenes are expressed by Hoffmann's empirical rule⁵⁷ that when the optimum σ^2 configuration has an EHMO energy less than 1.5 eV below the σp configuration at the same $\angle C$: angle then the ground state is likely to be the triplet. The computed EHMO energy difference for methyne is somewhat above 1.5 eV and since the ground state is known to be a doublet it seems that Hoffmann's rule is also applicable to carbynes. On this basis the ground state of the carbethoxymethyne which is the main concern of the present study, should have a $^2\Pi$ ground state and the lowest excited quartet state should lie at ≥ 28 kcal/mole.

Chemical Behavior. Doublet and quartet carbynes are paramagnetic, featuring one and three unpaired electrons and may in some respects be compared with a radical and tri-radical respectively. However, the fact that 3 electrons occupy orbitals on the same carbon atom may give rise to some peculiarities with respect to chemical behaviour. Thus, the doublet carbyne possesses an unpaired electron like a radical and at the same time a non-bonding pair of electrons comparable to a singlet carbene or carbanion. Furthermore, carbynes are electron deficient, and as such exhibit electrophilic

character as do most known carbenes. However, the electrophilic nature as well as the stability of the carbyne radical is greatly influenced by the electron-withdrawing ability of the adjacent group. To establish the main chemical characteristics including stereochemical behaviour and to correlate chemistry with structural parameters using the rules of spin multiplicity and orbital symmetry conservation is the immediate task of carbyne chemistry. Comparison with carbene and atomic carbon chemistry may be of assistance. The principal reactions observed in singlet carbene chemistry are concerted insertion into the C-H or C-X bonds of paraffins, olefins and haloalkanes (C-F bond excepted) and single step stereospecific cycloaddition to olefins, acetylenes and aromatics^{58,59}. These processes are facile because they conserve the spin and orbital angular momenta^{60,61}. It has been indicated on the basis of EMO calculations and molecular orbital symmetry correlations, Figure 4, that the symmetric approach of the doublet ground state methyne in the addition to ethylene is forbidden by both spin and orbital symmetry.⁶²

The question of "stereoselectivity" in carbyne chemistry is best discussed by analogy with carbene and atomic carbon chemistry. In the stereospecific addition reactions of unsymmetrical carbenes to olefins that have no center of symmetry nor a twofold symmetry axis along the C=C bond (e.g. *cis*-butene-2), two modes of *cis* addition are possible. Discriminating between the two possible ways, the stereoselective carbene produces two different adducts designated as *syn* and *anti*. Carbyne and atomic carbon are not stereoselective

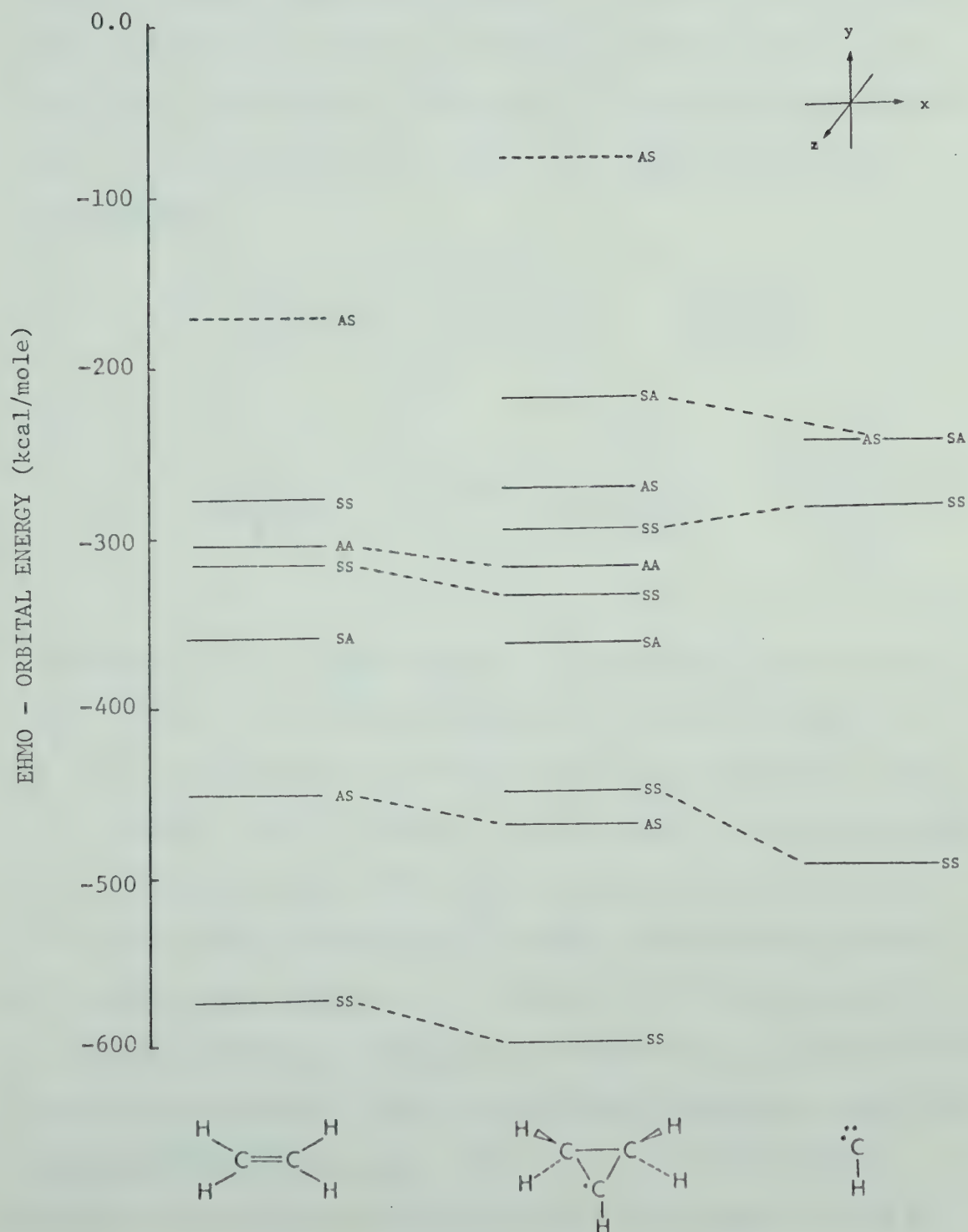
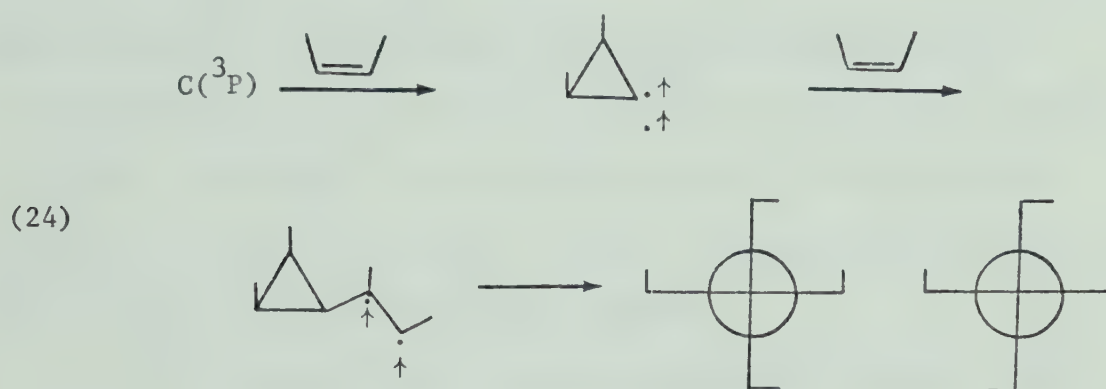


FIGURE 4: Correlation Diagram for the Addition of Methyne to Ethylene

in the same sense in that the discrimination does not occur in the primary addition reaction. Thus Skell^{3a} reports stereospecific addition of ground state atomic carbon (³P) to *cis*-butene-2, which yields, in the first step, an intermediate carbene, triplet *cis*-dimethylcyclo-propylidene, which then in a subsequent reaction adds non-stereospecifically to the substrate to give two different spiro-pentenenes.

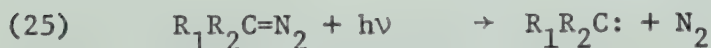


The primary step of carbyne addition is expected to give a cyclopropyl radical in which the stereochemical information content of the parent olefin would be maintained but without additional content of the reaction itself. However, new information would be impressed in the subsequent H-atom abstraction of the cyclopropyl radical and in this sense stereoselectivity of carbynes and therefore the ratio of isomeric adducts may be quite relevant in the characterization and chemical behaviour of carbynes. Stereospecific and stereoselective features can, of course, only be meaningfully considered provided hot molecule rearrangements do not occur; this in the liquid phase, geometrical isomerization of products can be discounted in view of high collision frequencies and consequent rapid deactivation.

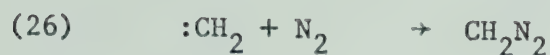
1.4 Objectives and Outline

As it has been discussed in the preceding sections, in the few studies addressed to the problems of carbyne chemistry, carbynes were generated by secondary photolysis or cracking of primary photolysis products or by high temperature thermolyses rendering kinetic analyses extremely difficult. The objectives of the present work were twofold: first, it appeared to be desirable to examine the possibility of developing a simple photochemical source of carbynes which would make quantitative kinetic-mechanistic studies possible, and second, to explore the chemistry of carbynes with a variety of substrates by means of product characterization and quantitative kinetic analysis of product yields.

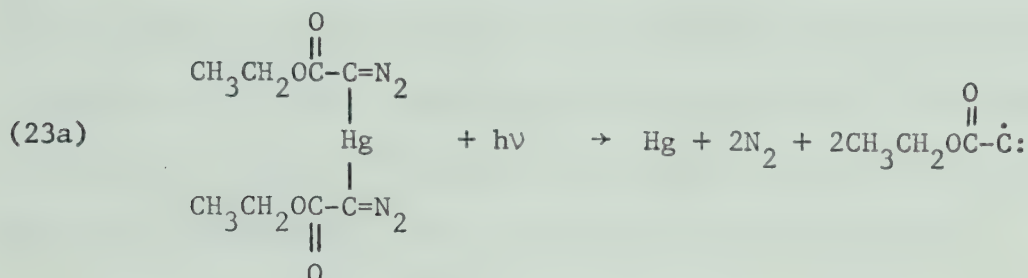
As mentioned above diethyl mercurybisdiazoacetate, DMDA, appeared to be a promising source material. This compound contains two extremely labile linkages, $C=N_2$ and $C-Hg$. The strength of the diazo carbon linkage is of the order of 25-30 kcal and photolysis of diazo compounds in the near u.v. is a widely used method of generating carbenes:



Similarly, the $Hg-C$ bond strength lies within the same range or slightly higher,^{63,64} and absorption in the range 2200-2600Å leads to the efficient production of alkyl radicals from the corresponding mercurials.⁶⁹⁻⁷¹ For the reaction



Von Büнау⁶⁸ has estimated $\Delta H = -47$ and -36 kcal/mole for singlet and triplet state methylene, respectively. Therefore, photolysis of DMDA at 2537Å (112 kcal/mole) could lead to the overall primary decomposition,



with the production of $^2\Pi$ ground state carbethoxymethyne. Therefore DMDA has been photolyzed in various solvents involving olefins and aromatics and the detailed reaction mechanism of product formation investigated. A number of different mercury-diazo compounds whose syntheses were described by Do Minh et al.⁶⁹ in 1968 were also considered as potential carbyne precursors.

Following a description of the general experimental procedures, the results and discussion for the solvents cyclohexene, *cis*- and *trans*-2-butene, pyrrole, and benzene will be presented.

CHAPTER 2

EXPERIMENTAL

2.1 Apparatus and Instrumentation

A great variety of apparati and instruments had to be used because of the many different materials and products encountered throughout this work. Some apparati were modified or specially built to accommodate the particular requirements. A brief description of each apparatus and instrument used is listed below.

A conventional high vacuum system was constructed for handling gaseous products, condensing and degassing low boiling solvents (e.g. butenes), and vacuum distillation of high boiling products. A pressure of 10^{-6} torr could be realized by a two-stage mercury diffusion pump backed by a mechanical Duo Seal Vacuum Pump (W. M. Welch Manufacturing Co.). Pressures were measured by a mercury manometer, Pirani gauge tubes (Consolidated Vacuum Corp.), a McLeod gauge, and a MKS Baratron Type 77 electronic pressure meter capable of measuring absolute pressures in the range 10^{-5} to 30 torr. In addition to a U-trap distillation train for product purification, the system had an analysis section which consisted mainly of a Toepler pump, a gas burette, and a gas chromatographic (g.c.) analysis system. Non-condensable gases (N_2 , CO) were passed through the Toepler pump and measured in the gas burette from where they could be introduced into the evacuated sample loop of the

g.c. system or collected in a removable glass bulb for mass spectral or infrared analysis. The g.c. analysis system consisted of a Gow-Mac TR2B temperature regulated thermal conductivity cell maintained at 180°C and a filament current of 150 mamp. The power supply was a Gow-Mac 999-C. The chromatograms were recorded by a Sargent Recording Potentiometer Model (SR).

A Nester-Faust Adiabatic Annular spinning band distillation column was available for efficient distillation and difficult separations. The still was vacuum jacketed and silvered making it adiabatic. The band, which acts as a packing, was driven through a vacuum septum, and this seal allowed a vacuum better than 20 microns.

A Büchi Rota vapor was employed in connection with a standard water aspirator for distillation and rapid flash-evaporation of solvents under reduced pressure.

A modified bulb-to-bulb distillation apparatus (Fig. 5) was designed and used with good success especially for the distillation of high boiling unstable mercury adducts. The distillation bulb (diameter 2 to 4 cm) contained a magnetic stirrer and was completely submerged in the oil bath except for the septum. The traps were conveniently cooled with small Dewar flasks containing a suitable slush or liquid nitrogen. After completion of the distillation the trap and the distillation bulb were separated and weighed on an analytical balance with and without content to obtain the yield of product and residue.

A Fisher-Johns melting point apparatus was used for all melting points (m.p.) which, along with all boiling points (b.p.), are reported uncorrected.

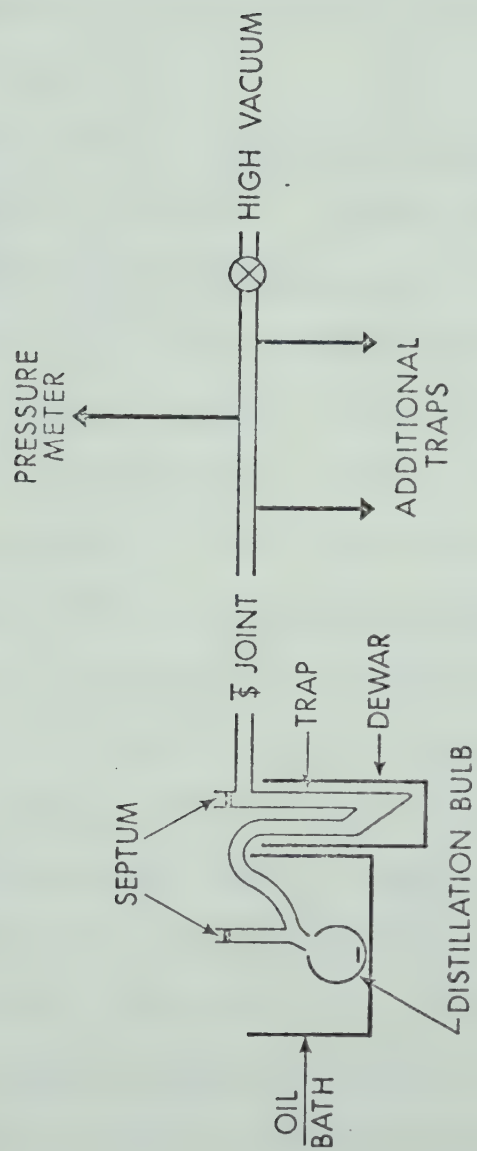


FIGURE 5: Modified Bulb-to-Bulb Distillation Apparatus

A thermogravimetric analyser (model 950, E. I. du Pont Nemours and Company Inc.) was used to study the thermal decomposition of DMDA.

The photolysis lamp assembly consisted of a Hanovia 450 W medium pressure mercury arc (No. 679 A 36) connected to a step-up voltage transformer.

Several types of photolysis reaction vessels, Figs. 6a,b,c,d, were used throughout this work. All were used in connection with a cylindrical immersion well assembly (a), (Fig. 6a) which is described by Calvert and Pitts⁷⁰. The immersion well held the mercury arc and the required cylindrical cut-off filter sleeves. The inlet and outlet of the quartz cooling jacket were connected to a cold water line. The immersion well assembly (a) was fitted with an appropriate ground glass joint into a 200 ml pyrex reaction vessel (b) (Fig. 6b) which was purged with nitrogen through a sintered glass inlet at the bottom of the vessel. The vessel had also a side arm with a standard T 24/40 joint which was mounted with a 12 inch condenser. For constant temperature operation the vessel was immersed into a 3.5 liter beaker which was filled with cooling liquid (water or ice-water) and had a side arm as overflow. The geometrical arrangement of the immersion vessel assembly with the mercury arc in the center permitted only one-half of the total volume (~100 ml) to be irradiated directly in a cylindrical mantel of about 0.5 cm thickness. To facilitate adequate circulation and mixing of the solute of the dead space into the effective irradiation area a magnetic stirrer was used in addition to a brisk stream of nitrogen. Quartz tubes (c) (Fig. 6c)

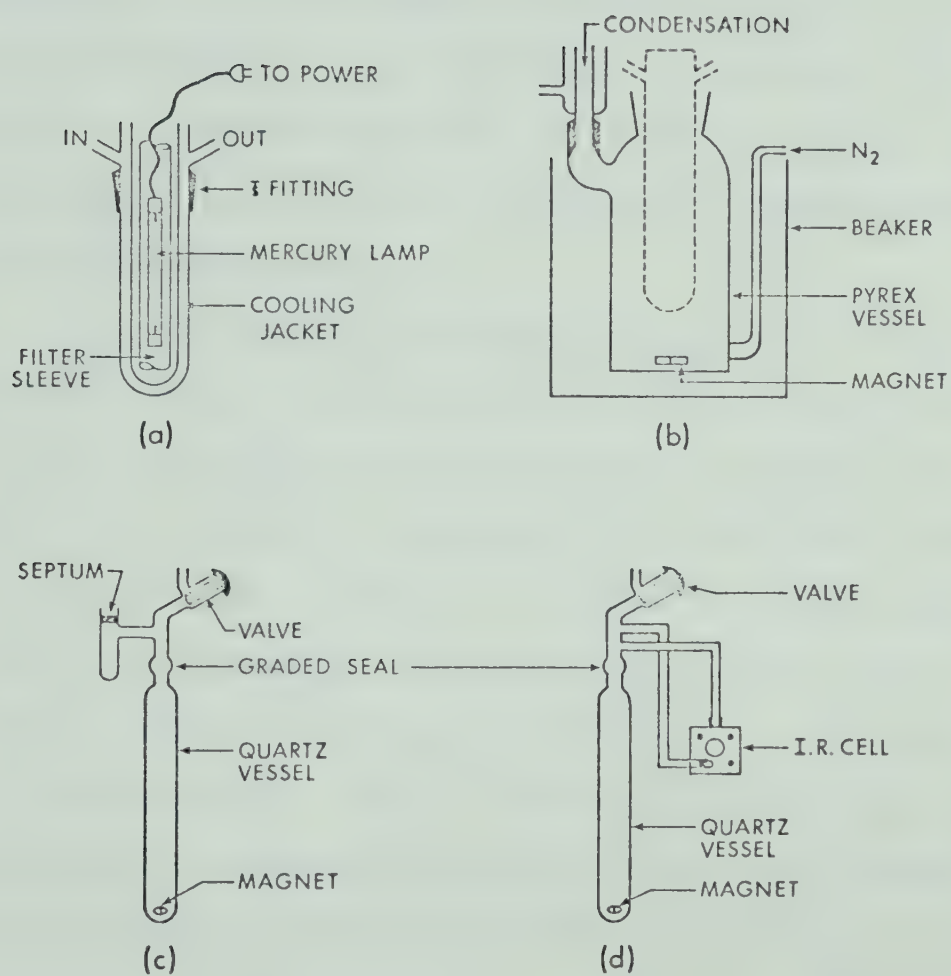


FIGURE 6: Photolysis Reaction Vessels: Immersion Well Assembly (a); Pyrex Reaction Vessel (b); Quartz Tube (c); and Quartz Tube with Attached I.R. Cell (d).

sealed with a Rotaflow valve (Quickfit, TF 2/24) and a sidearm with septum for removing the test samples with a syringe, were used for the irradiation of degassed samples and samples containing a liquified gas as solvent. The teflon stem of the Rotaflow valve could be removed for addition and removal of solids or a magnetic stirrer. Two sizes of tubes were employed: 30 ml (16 mm diameter), and 120 ml (38 mm diameter). For constant temperature operation the photolysis tubes (c) were immersed into the 3.5 liter cooling bath together with the immersion well assembly (a).

A quartz tube with an attached i.r. cell (d) was constructed to monitor the extent of DMDA disappearance and EDA formation during photolysis. Kovar seals were soldered to the two openings of a standard sodium chloride i.r. cell, and then attached via 4 mm diameter pyrex tubing to the photolysis tube above the graded pyrex-quartz seal. By shifting and turning the whole assembly, the loop with the i.r. cell could be flushed and filled with the reaction mixture for measurement. Thus i.r. measurements could be performed during photolysis using condensed gases as solvents (e.g. butenes), without concentration changes due to solvent evaporation, and also air was excluded from the system.

Several different cylindrical filter sleeves were inserted into the immersion well surrounding the mercury arc to eliminate the lower wavelengths of the arc. Fig. 7 displays the cut-off range for various filters, determined with a Perkin-Elmer (Model 202) ultraviolet-visible spectrophotometer.

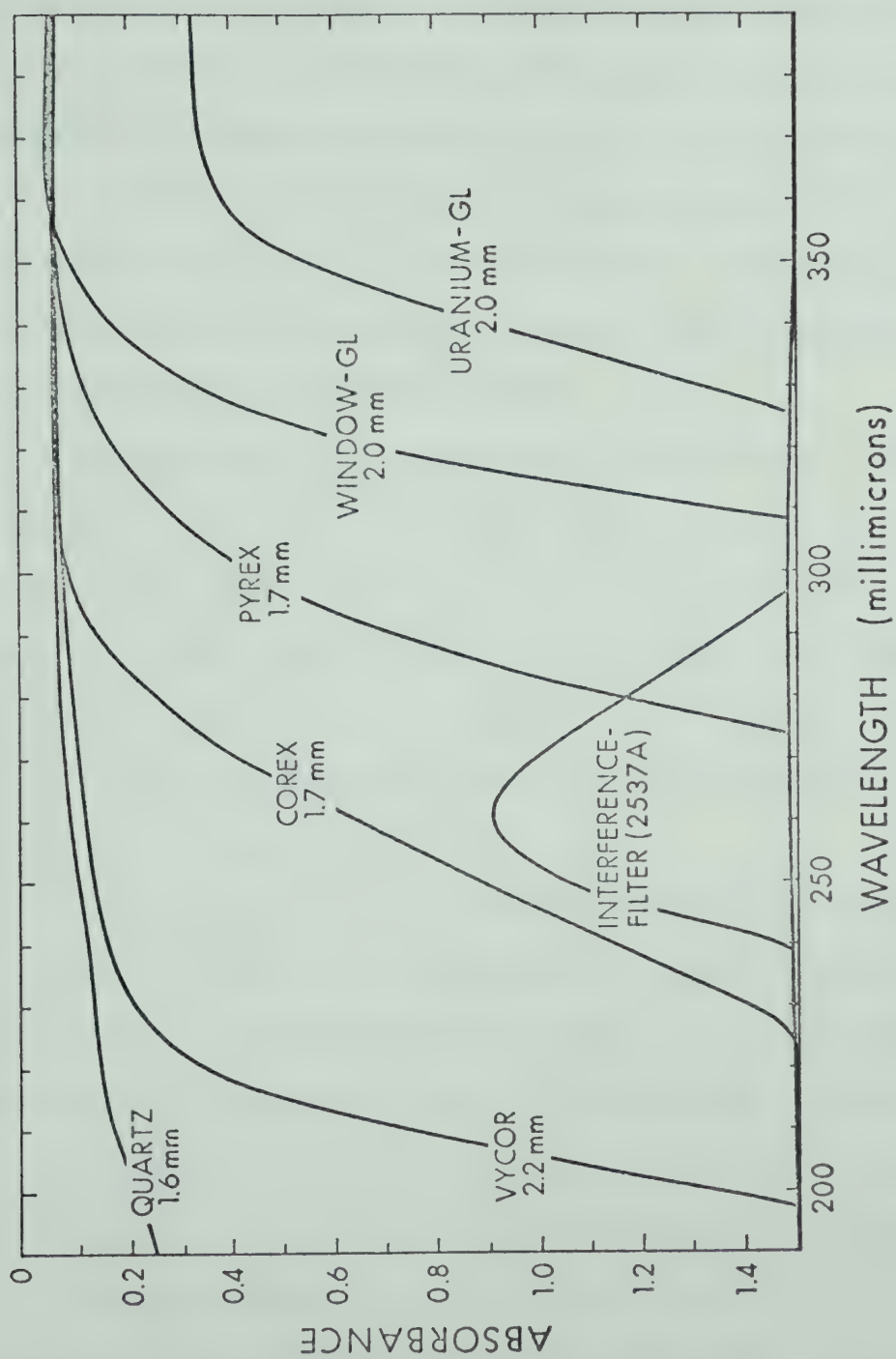


FIGURE 7: Cut-off Range for Various Filters

Gas chromatography (g.c.) was carried out with three different instruments in addition to the previously mentioned g.c. unit of the high vacuum system. A Varian Aerograph (Model 90P) was mostly used for preparative work. The instrument was modified to accommodate an effluent splitter in order to collect thermally unstable products. Hewlett-Packard's research chromatographs model 5750B and model 7620A served as analytical instruments. Both instruments were equipped with flame ionization detectors, dual column and automated temperature programming systems.

The infrared (i.r.) spectra were recorded with a Perkin Elmer (model PE-421) and a Perkin-Elmer Infracord (model PE-6137) spectrophotometer. The polystyrene 1601 cm^{-1} band was used as a reference. The PE-421 was employed for quantitative measurement because of its sensitivity and versatility, which allowed very slow scan rates and a scale expansion by changing the gear ratio (e.g. gear ratio of 1 to 4 gave 100\AA per cm).

The ultraviolet (u.v.) absorption spectra were measured in "spectro" grade solvents with a Cary 14 and a Cary 15 recording spectrophotometers. An MTS Fortran H program was used for the analysis of electronic spectra using the Gaussian approximation to resolve the spectral envelope into component peaks. The program was designed by Drs. E. D. Day, D. R. McTavish and R. G. Cavell.

The mass spectra (m.s.) were determined with an A.E.I. MS-9 double-focusing high resolution mass spectrometer operated at 70 eV, and an A.E.I. MS-12 mass spectrometer in combination with g.c. analysis. Peak measurements were made with perfluorotributylamine

as reference at a resolving power of 15,000.

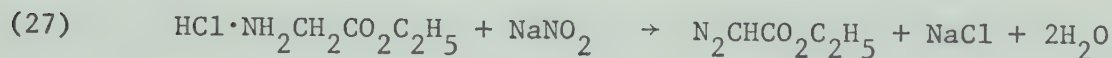
The nuclear magnetic resonance (m.n.r.) spectra were recorded on Varian A-56/60 and A-100 spectrometers. Proton spectra were measured with tetramethylsilane, and fluorine spectra with trichlorofluoromethane as reference standards.

2.2 Materials

Commercially available chemicals of "Reagent" grade were used without further purification unless otherwise specified.

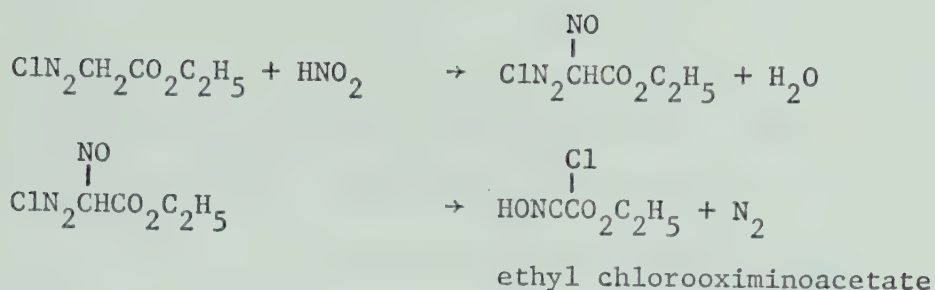
Preparation of Ethyldiazoacetate, EDA

EDA was used as starting material for DMDA and also as a source of carbethoxycarbene in control experiments. The procedure reported in the latest edition of "Organic Synthesis"⁶⁹ was followed for the preparation of EDA. The method quotes "high boiling esters" as main contaminants in the product fraction and it was observed that one such "high boiling ester" was dicarbethoxyfuroxan. The formation of this byproduct in the synthesis of ethyldiazoester by the action of sodium nitrite on glycine ethylester hydrochloride can

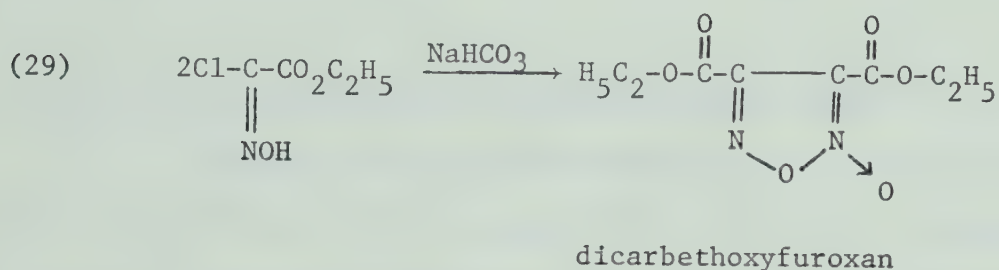


be derived from the following considerations: Skinner⁷⁷ has found that glycine ester hydrochloride and sodium nitrite, in the presence of hydrochloric acid, form the ester of chlorooximino acid according to





According to Wieland⁷³ chlorooximinoacetate condenses in the cold to dicarbethoxyfuroxan with great facility when treated with sodium bicarbonate:



Dicarbethoxyfuroxan was easily chromatographed (15 ft x 1/8 inch column of 12% XE 60 on Chromosorb W, 40-60 mesh, column temperature: 170°C, flow: 60 ccm per minute, retention time 26 minutes). The elemental analyses calculated for $\text{C}_8\text{H}_{10}\text{N}_2\text{O}_6$ and found were:

calculated: 41.7%C; 4.3% H; 12.2%N

found: 43.1%C; 4.7% H; 10.8%N

Reported^{74,75} and observed properties were in good agreement:

b.p.: 90°/0.1 torr

m.s.: m/e 29 (base peak); 230 (parent); 215 (P-CH₃)

200 (P-2CH₃ and P-NO); 185 (P-OC₂H₅)

i.r. (CCl_4): 1740 cm^{-1} (C=O); 1620 cm^{-1} (C=N)

n.m.r. (CCl_4): τ 8.63 and τ 8.59 (triplet, CH_3)

τ 5.58 and τ 5.54 (quartet, $-\text{CH}_2-$)

Distilled EDA purchased from Aldrich Chemical Co., did not contain a detectable amount of dicarbethoxyfuroxan. However, in the subsequent synthesis of DMDA, freshly prepared EDA appeared more suitable.

Preparation of Diethyl Mercurybisdiazoacetate, DMDA

The reaction of yellow mercuric oxide and EDA as described by Buchner⁷⁶ was used to prepare DMDA in 85% yield. It was noticed that the exclusion of air, moisture, and light reduced the decomposition of freshly formed DMDA in solution. Decomposition, as readily seen by deposition of black metallic mercury, also occurred when the cooling of the exothermic reaction was insufficient. Thus violent and almost instant decomposition occurred several times when the heat of reaction was not controlled adequately. The initiation of the reaction with purchased or stored EDA appeared difficult and often took more than three hours. A crystalline product of sulphur-like yellow color was obtained by recrystallization from ethyl ether.

Analytical data of DMDA:

m.p.: $103-104^\circ\text{C}$

m.s.: calculated and found parent peak m/e 428 ($\text{C}_8\text{H}_{10}\text{N}_4\text{O}_4$
 Hg^{202}); base peak m/e 85 ($\text{C-CO}_2\text{C}_2\text{H}_5$)

i.r. (KBr): 2075 cm^{-1} (C=N_2); 1670 cm^{-1} (C=O).

u.v.: $\lambda_{\text{max}}^{\text{EtOH}}$ $264\text{ m}\mu$ (ϵ 22,000)

$$\lambda_{\max}^{\text{EtOH}} \quad 380 \text{ m}\mu \quad (\epsilon=107)$$

n.m.r. (CDCl_3): τ 8.75 (triplet path 7Hz; 6H; $-\text{CH}_3$)

τ 5.80 (quartet 7Hz; 4H; $-\text{CH}_2-$)

Solvent purification: All solvents used were checked by i.r. and g.c. analysis for impurities. *Cis*- and *trans*-butene-2 (Matheson) as well as hexafluorobenzene (Aldrich) had less than 0.1% total contaminant and were used without further purification. Cyclohexene (BDH "Reagent grade") was dried over potassium hydroxide pellets and then distilled under reduced pressure by spinning band chromatography. However, a check of the liquid residue of a 20 ml sample of purified cyclohexene by g.c. showed the presence of cyclohexanol, cyclohexenol, and cyclohexenone. These impurities were identified by comparison of g.c. retention times and combined g.c.-m.s. analysis. They are typical autoxidation products of cyclohexene. The level of contamination could be kept below 0.1% (including other unidentified oxidation products) by using freshly distilled solvent. Pyrrole (Eastman, practical) was always distilled immediately prior to photolysis because of the instability of this solvent towards oxygen. Benzene (Shawinigan, "Reagent" grade) was treated with sodium and then distilled under reduced pressure.

2.3 Photolysis

Because DMDA is a solid with a low vapour pressure at room temperature photolyses were carried out only in solution. In each

solvent, the photolysis of EDA was also carried out parallel to the photolysis of DMDA and the results compared. The experimental conditions such as wavelength, irradiation time, concentration, geometrical arrangement of reaction vessel and lamp, temperature and solvents were found to profoundly affect product yields. Therefore variables had to be carefully controlled and their effects explored.

Cut-off filters as described in section 2.1 fixed the lower wavelength limit and therefore the amount of energy dissipated to the system. A wavelength study was also done for the various solvent systems by interchanging the cut-off filter sleeves. The wavelength and the type of filters are reported together with the results for each photolysis experiment.

The irradiation time varied with wavelength, geometrical arrangement of the irradiation source, concentrations of DMDA and EDA, and solvent. It was monitored by the disappearance of the characteristic diazo bands in the i.r. Photolyses designed for product characterization analysis were always carried out to the complete disappearance of the diazo band. This was done by either removing a test sample with a syringe for i.r. analysis or using a photocell with the attached i.r. cell. Incomplete photodecomposition could result in non-photolytic decomposition of the remaining unstable DMDA in the work-up procedure. Excessive irradiation was avoided to keep secondary photolysis of the reaction products to a minimum. The irradiation times were reported with the results of each photolysis. They represent the times necessary to completely photolyze DMDA or EDA under the given

experimental conditions. The i.r. monitoring of DMDA and EDA was not only used to determine the end of the photolysis but also the extent of EDA intermediacy in the photolysis of DMDA. For this purpose ~0.1 gm samples were dissolved in 20 ml of cyclohexene and 1 ml samples withdrawn every 2-3 minutes during photolysis. The disappearance of DMDA was measured in a 0.2 mm sodium chloride cell while the intermediate EDA was determined in a 1 mm i.r. cell for higher intensity. The spectrophotometer (PE-421) was calibrated with samples of known amounts of DMDA and EDA.

The low solubility of DMDA in most solvents studied, limited the concentration of the solutions, e.g. cyclohexene, 0.4% *cis*- and *trans*-butene, 0.2%, benzene, 0.5%. Attempts to dissolve larger amounts by heating the solution resulted in precipitation of mercuric oxide and decomposition of DMDA. The amount of DMDA used in each photolysis is reported with the results together with size of vessel and temperature of cooling water.

In the general photolysis procedure the weighed amount of DMDA was put into a cleaned and dried reaction vessel together with the required amount of purified solvent and a teflon coated magnetic stirrer. When the 200 ml pyrex reaction vessel with the immersion well assembly was used, the DMDA was immediately dissolved by stirring (~30 minutes) and then the cooling water and the irradiation lamp were turned on. The cooling water varied from 16°C (winter) to 27°C (summer). Most runs were done at 18 - 20°C with the help of ice when required.

When the sealed quartz tubes were used, the reaction mixture,

solid DMDA plus solvent, was degassed by freezing with liquid nitrogen and evacuated on the high vacuum system two or three times. The DMDA was then dissolved and irradiated for the required time by positioning the tube within 2 cm of the immersion well assembly (section 2.1). Both the immersion well assembly and the reaction vessel were always placed in a 3.5 liter cooling vessel during the photolysis for constant temperature operation.

One further variation of the photolysis procedure was the use of liquified or condensed gases as solvents, i.e. *cis*- and *trans*-butene. A quartz tube with a Rotaflo valve was evacuated after addition of the required amount of DMDA and a magnetic stirrer. By cooling the quartz tube to -78°C with a dry ice-trichloroethylene slush the required amount of gas was condensed into the quartz tube from a gas cylinder which was also connected to the high vacuum system. The pressure was less than 30 torr and at room temperature slightly over 760 torr, which was well within the pressure resistance of the quartz tube used. For the removal of this solvent the reaction vessel was kept at 0°C (water-ice) and the gas was slowly distilled into a heavy wall pyrex storage tube kept at -78° (dry ice-trichloroethylene).

2.4 Thermolysis

The thermal decomposition of DMDA in various solvents was examined briefly. The photolysis tubes described in section 2.1 were used as reaction vessels. The tubes containing the reaction mixture were closed and immersed into a temperature controlled water

or oil bath. In a few cases the decompositions were carried out in sealed Carius tubes which were heated by a remote temperature controlled Gallenkamp tube furnace. A sample of pure DMDA was also decomposed using the Du Pont Thermogravimetric Analyser. About 20 mg of pure DMDA were put on the semi-micro balance and the weight of the sample was measured as a function of linearly increasing temperature.

2.5 Analyses

Product analyses of various photolysis and thermolysis reaction mixtures were for the most part a complicated and often lengthy task. Much time was consumed for development of adequate qualitative and quantitative analysis procedures for each solvent system which often contained a host of unavailable or unknown products. Non-condensable gases (N_2 , CO) were separated and determined prior to any work-up procedure. Utilizing the high vacuum system, the sample tube was frozen with liquid nitrogen and degassed. The non-condensable gases were collected with the Toepler pump assisted by an auxiliary mercury-diffusion pump. After measurement in the gas burette the gases were analysed on a 10 ft spiral glass column filled with molecular sieve (13X, Union Carbide).

In general, the work-up procedure consisted of separation of metallic mercury by decantation and filtration, removal of solvent by flash evaporation, and analysis of the solvent free reaction mixture. The recovered metallic mercury was weighed on an analytical balance. However, the technique of collecting small amounts of

mercury from the reaction vessels as well as additional precipitation of mercury from the reaction mixture during further processing introduced a considerable error, in the order of 10 - 15%.

The solvents were removed with the Büchi Rotavapor or, if solvent recovery was critical (e.g. hexafluorobenzene) by the use of standard semi-micro distillation equipment. Recovered solvent fractions were checked for light reaction products by g.c.

The remaining mixture of reaction products was submitted to fractionation via spinning band or bulb-to-bulb distillation followed by g.c. analysis of the different fractions. The residues including non-volatile reaction mixtures were analysed by liquid chromatography (l.c.) and thin-layer chromatography (t.l.c.). Whenever t.l.c. would not show distinct separation after repeated attempts with a number of different solvents the residue was considered polymeric and further analysis was abandoned. Often, insolubility of residues and tailing of m.s. analysis at increasing temperature, confirmed the presence of polymeric materials.

Product samples of total amount 200 mg or less were not subjected to distillation prior to g.c. analysis. The total sample, after evaporation of most of the solvent was made up to a known volume (e.g. 10 ml, using a volumetric vial) to be used as stock solution. The concentration of the various products was then determined by withdrawing aliquots (0.5 to 10 μ l) from the stock solution for direct comparison with standard solutions using an analytical research chromatograph. The standards were prepared from isolated, purified, and identified products. The concentrations of

the standards (using the same solvent) were approximately the same as those in the unknown samples to minimize or avoid errors due to potential loss or decomposition on the g.c. column. The procedure was found to be reproducible within $\pm 5\%$ by comparison of the integrated g.c. peak areas. Details of the g.c. columns used for each system and the conditions for programs are reported together with the results.

The isolation of the individual products was often hampered due to thermal instability of the products and the complexity of the reaction mixtures which were in most cases heavy and dark oils. As a first preliminary step the mixture was analysed by a combined g.c.-m.s. scan which in most cases gave the required parent peaks for the major components resolved by the g.c. program. After this preliminary identification the g.c. program was adapted to a preparative g.c. column and the individual products were collected - often with considerable loss - for structure confirmation by i.r., n.m.r., elemental analysis, m.p., etc. Effluent splitters were used in the collection of thermally unstable products. Some heavier and solid products such as mercury adducts, dimers and tetramers, were collected from l.c. and t.l.c. fractions by crystallization. The l.c. separations were performed in a quartz column (2 cm diameter, 60 cm length) packed with the required amount of silica gel for chromatographic adsorption (BDH, 60 - 120 mesh) and a trace of electric phosphor (Rotma-P-1, type 118-2-7, General Electric) which fluoresced when irradiated with a u.v. lamp (mineral-light, U.V.S.-11 Fisher Scientific). Separation and elution of the different fractions, which appeared as shadows, could be easily followed and

collected. For t.l.c. separation, glass plates (20 x 20 cm) were coated with 0.2 to 1 mm silica Gel G (E. Merck AG) according to Stahl. T.l.c. was also performed with precoated silica gel sheets (Eastman-Kodak).

CHAPTER 3

PHOTOLYSIS OF DIETHYLMERCURYBISDIAZOACETATE
IN CYCLOHEXENE3.1 Reaction and Observations

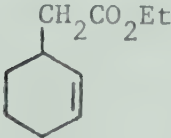
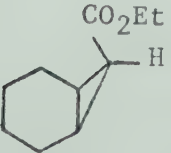
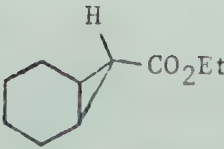
The first systematic study of chemically produced monovalent carbon was the photodecomposition of DMDA in cyclohexene. On photolysis of a solution of DMDA in cyclohexene, evolution of nitrogen especially around the core of the immersion well could be observed; within a few minutes the bright yellow solution turned cloudy and bleaching of the yellow color was apparent. Near the end of the photolysis, as indicated by the disappearance of the mercury-diazo band (30 minutes) metallic mercury settled to the bottom of the reaction vessel and the solution became transparent again. When smaller diameter quartz tubes were used, metallic mercury plated out like a silver mirror on the wall adjacent to the immersion well with the light source.

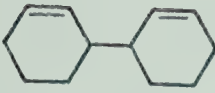
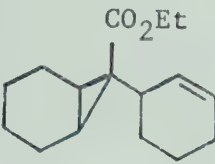
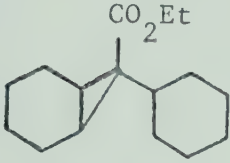
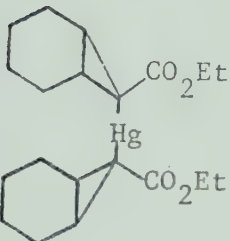
Seven major reaction products were detected in addition to nitrogen and mercury, presumably from insertion and addition reactions of intermediate radicals with solvent; significantly one of these contained mercury. Ethyldiazoacetate (EDA) was also formed in smaller amounts. The relative yields of all the reaction products were strongly dependent on the wavelength of irradiation and the presence of dissolved oxygen in the solvent.

The nature of the products was consistent with the intermediacy of carbethoxymethyne and the photolysis of DMDA therefore appeared to be a promising source of carbethoxymethyne radicals. In order to establish firmly the mechanistic details of the overall reactions it became imperative to characterize not only the reaction products but also their dependence upon photon energy and temperature. Some aspects of the oxygen-initiated reaction had to be also examined.

3.2 Product Description

Metallic mercury and nitrogen which result from the decomposition of DMDA could be easily isolated and identified (cf. Experimental, section 2.5). After evaporation of cyclohexene from the reaction mixture, the following seven additional products were separated and identified:

- | | | |
|-----|---|---|
| [1] |  | ethyl (3'-cyclohexenyl)acetate
(insertion product) |
| [2] |  | ethyl endo-norcarane-7-carboxylate
(endo addition product) |
| [3] |  | ethyl exo-norcarane-7-carboxylate
(exo addition product) |

- [4]  3,3'-bicyclohexenylyl
- [5]  ethyl norcarane-7-(3'-cyclohexyl)-7-carboxylate
- [6]  ethyl norcarane-7-cyclohexyl-7-carboxylate
- [7]  diethyl mercury bis-norcarane-7-carboxylate
(mercury adduct)

The retention times (t_R), molecular weights or parent peaks (m/e P), and the ten most intense mass peaks (m/e) for all seven products were determined by combined g.c.-m.s. analysis using three different g.c. programs (Table VI).

Products [1] to [6] were distilled by bulb-to-bulb distillation (cf. Experimental, section 2.1) at 100–110°/0.01 mm Hg, and then isolated from the distillate by preparative g.c. The fraction distilling at 175° – 200°C at 0.01 mm Hg contained the mercury adduct [7] which partially decomposed at that temperature as evidenced by appearance of metallic mercury. Upon cooling, the fraction gave a crystalline, white compound (m.p. 126 – 127°C; recrystallized from *n*-pentane).

TABLE VI
Combined Gas Chromatographical and Mass Spectral Analysis for Products [1] - [7]

Compound No.	t_R (minutes)	m/e (P)	m/e and (% of base peak)									
[1]	18 ^a	168 (14)	122 (40)	94 (44)	81 (52)	80 (100)	79 (96)	61 (44)	41 (28)	32 (56)	29 (24)	18 (26)
[2]	20.5 ^a	168 (18)	123 (40)	122 (56)	97 (40)	95 (42)	94 (65)	81 (70)	80 (96)	79 (100)	57 (52)	41 (46)
[3]	24 ^a	168 (40)	123 (56)	95 (70)	81 (57)	80 (97)	79 (77)	67 (84)	55 (68)	44 (75)	41 (65)	28 (100)
[4]	26 ^a	162 (<1)	81 (100)	80 (56)	79 (42)	77 (14)	67 (11)	55 (10)	53 (18)	41 (28)	39 (26)	27 (20)
[5]	21 ^b	248	167	81	80	79	78	44	41	32	29	28
(some [6] present)												
[6]	18 ^b	250 (31)	168 (12)	95 (13)	81 (23)	79 (14)	67 (16)	55 (15)	41 (20)	32 (17)	29 (16)	28 (100)
[7]	9 ^c	536 (<1)	167 (38)	93 (97)	80 (37)	79 (63)	77 (39)	41 (60)	39 (54)	31 (57)	29 (100)	27 (60)

^a column: 15 ft x 1/8 inch packed with 20% SE30 on Chromosorb W, 30-60 mesh.

program: from 110° - 180°C at 1° per minute with 6 minutes post injection delay; flow rate at 60 cc/minute.

^b column: as in a.

program: 180°C constant column temperature; flow rate at 60 cc/minute.

^c column: 10 ft x 1/8 inch packed with 10% SE30 on Chromosorb W.

program: 240°C constant temperature; flow rate 60 cc/minute.

Molecular weights, determined by m.s. measurements, the principal well defined peaks of i.r. and n.m.r. spectra of compounds [1] - [7] are reported in Table VII. The data are in agreement with the proposed structures. Compounds [1] to [4] have been characterized by Skell⁷⁷ in the photolysis of EDA in cyclohexene. The insertion product [1] gave positive unsaturation tests with bromine and catalytic hydrogenation. The low field multiplet at $\tau = 7.50$ in the n.m.r. spectrum may be assigned to a methinyl allylic proton. Irradiation on this proton produced significant changes in the splitting patterns of both the α -methylene and vinylic protons. Thus this structure is consistent with insertion into the allylic C-H linkage of cyclohexene. Compounds [5] to [7] are novel and do not occur in the photolysis of EDA in cyclohexene.

Examination of the n.m.r. spectra of the mother liquor in the separation of [7] indicated the presence of at least one other mercury compound, possibly two. They are tentatively assigned insertion [8] and mixed insertion-addition [9] mercury adducts:

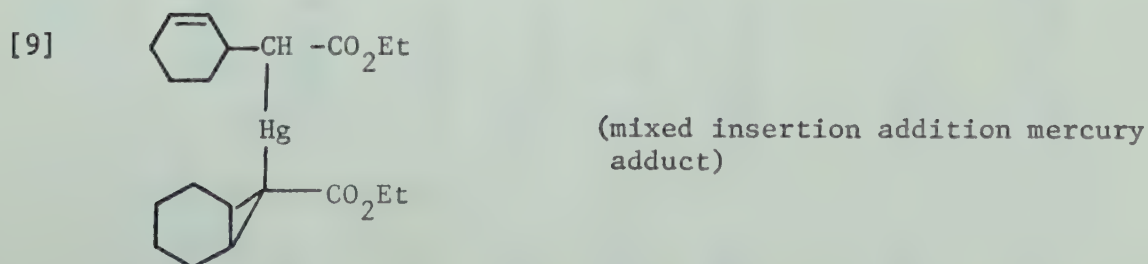
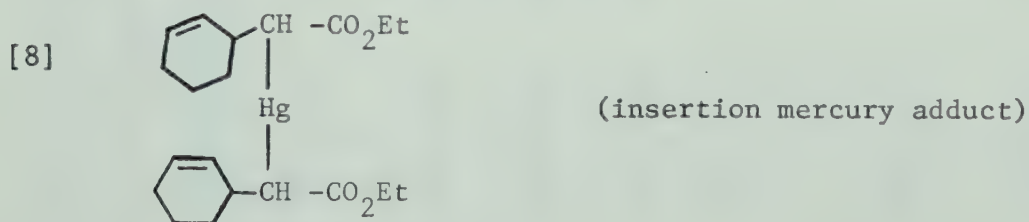


TABLE VII

Molecular Weights, I.R. and N.M.R. Spectra for Compounds [1] to [7]

Compound No.	Formula	M.Wt.		i.r. $\nu_{\text{max}}^{\text{CCl}_4(\text{cm}^{-1})}$	n.m.r. τ (CCl_4)
		calculated	measured		
[1]	$\text{C}_{10}\text{H}_{16}\text{O}_2$	168.1150	168.1153	3050(w); 1720(s)	8.80 (t, 3H); 7.90-9.00 (broad m, 6H); 7.85 (m, 2H); 7.50 (m, 1H); 5.93 (q, 2H); 4.42 (m, 2H)
[2]	$\text{C}_{10}\text{H}_{16}\text{O}_2$	168.1150	168.1151	3045(w); 1725(s)	8.80 (t, 3H); 8.10-9.05 (broad m, 11H); 5.95 (q, 2H)
[3]	$\text{C}_{10}\text{H}_{16}\text{O}_2$	168.1150	168.1151	3050(w); 1720(s)	8.80 (t, 3H); 7.65-9.05 (broad m, 11H); 6.00 (q, 2H)
[4]	$\text{C}_{12}\text{H}_{18}$	162.1409	162.1409	3020(w); 1642(w)	8.43 and 8.10 (2 broad m, 14H); 4.45 (m, 4H)
[5]	$\text{C}_{16}\text{H}_{24}\text{O}_2$	248.1776	-	3010(w); 2930(s); 1740(s)	8.78 (t, 7.0Hz, 3H); centered around 8.08 and 8.35 (2 broad m, 19H); 5.92 (q, 7.0 Hz, 2H); 4.40 (m, 2H)
[6]	$\text{C}_{16}\text{H}_{24}\text{O}_2$	250.1933	-	2930(s); 1718(s)	8.72 (t, 7.0 Hz, 3H); centered around 8.25 and 8.90 (2 broad m, 21H) 5.89 (q, 7.0 Hz, 2H)
[7]	$\text{C}_{20}\text{H}_{30}\text{O}_4\text{Hg}^{202}$	536.1850	536.1856	2980(w); 2928(s); 2853(s); 1700(s)	9.82 (t, 7.0 Hz, 6H); centered around 8.14 and 8.48 (2 broad m, 20H); 6.00 (q, 7.0 Hz, 4H)

Chromatography of the mother liquor by l.c. gave a main fraction with the following n.m.r. spectrum: τ 8.80 (τ , 7.0 Hz, 6H); τ centered around 8.20 (1 broad m, 16H); τ 5.98 (q, 7.0 Hz, 4H); τ 4.40 (m, 3-4H). This heavy, viscous oil could not be crystallized. However the low lying multiplet of τ 4.40 in the n.m.r. spectra gives strong evidence for an insertion mercury adduct, [8].

3.3 Effect of Wavelength

While measuring the products [1] to [7] quantitatively it was found that the wavelength of irradiation had a significant effect on their yields. For this reason irradiation was effected by using four different wavelength regions utilizing interchangeable cylindrical filter sleeves (cf. Experimental, section 2.1) in the immersion well of the photolysis lamp. The relative product yields of the photolysis of DMDA in cyclohexene at the four different wavelength regions are given in Table VIII. Shown are the theoretical yields, based on the starting material, DMDA, for the major products. The yields of the various products were determined by direct comparison with standards prepared from isolated, purified and identified products using analytical g.c. techniques (cf. Experimental, section 2.5). The detailed analytical data for the g.c. determination of products for the individual photolyses and the description of the standards is appended (Appendix A).

Table IX shows the effects of wavelength on product ratios. Several trends are noticeable. The insertion to combined endo plus

TABLE VIII

Product Yield Variation as a Function of Wavelength*

Compound No.	Percent Yield for the Wavelength			
	>2100Å (Vycor)	>2400Å (Corex)	>2800Å (Pyrex)	>3200Å (Uranium)
[1]	9.2	8.4	5.4	2.95
[2]	13.6	6.6	2.2	1.3
[3]	1.7	0.8	0.5	0.3
[5]	3.4	3.0	1.5	0.6
[6]	<u>2.7</u>	<u>1.9</u>	<u>0.5</u>	<u>0.1</u>
$\Sigma[1]-[6] \rightarrow$	30.6	20.7	10.1	5.3
[7]	16.4	27.0	38.6	37.6
Total Product	47.0	47.7	48.7	42.9
Hg (metallic) recovered	46	30	16	4

* average of three experiments.

TABLE IX

Effect of Wavelength on Product Ratios

Compound Ratio	Wavelength, Å			
	>2100 (Vycor)	>2400 (Corex)	>2800 (Pyrex)	>3200 (Uranium)
$[1]/([2] + [3])$ (Insertion/Endo + Exo)	0.6	1.2	2.0	1.8
$[2]/[3]$ (Endo/Exo)	8.2	8.2	4.4	4.3
$[7]/[1] + [2] + [3] + [5] + [6]$ (Hg-adduct/total insert. + add.)	0.54	1.30	3.82	7.09

exo product, i.e. $[1]/([2] + [3])$ increases with increasing wavelength. The endo to exo product ratio, $[2]/[3]$, which decreases from 8.2 to 4.3 with increasing wavelength, is considerably higher at all wavelengths than the values obtained from the photolysis of EDA in cyclohexene. Thus $[2]/[3] = 0.625$ was initially determined by Skell and Etter⁷⁷, and later repeated by Moser⁷⁸ who found a value of 0.53. An increase in light energy also resulted in a decrease of the ratio of mercury addition product to combined insertion plus addition products, i.e. $[7]/([1] + [2] + [3] + [5] + [6])$. Since the total amounts of organic products, including the mercury adduct, are nearly constant (~50%) it would appear that some products are formed at the expense of mercury adduct. The stability of [7] was therefore examined, to establish the importance of secondary photolysis or thermolysis of the mercury adduct.

3.4 Relative Stability of the Mercury-Adduct, [7]

Samples of [7] were photolyzed in cyclohexene, but metallic mercury was not observed during the time required to photolyze an equivalent sample of DMDA under the same experimental conditions. However, extended irradiation, especially at shorter wavelength ($>2100\text{\AA}$), resulted in some decomposition of the mercury-adduct with the appearance of [1], [2] and [3]. To establish the maximum degree of secondary product formation in the photolysis of DMDA samples of [7] were photolyzed, and the extent of disappearance of [7] as well as the formation of products [1], [2] and [3] (insertion, endo and exo

addition products, respectively) were determined quantitatively. The results are shown in Table X along with standard samples of DMDA. It is seen that the yields derived from photolysis of the mercury adduct are considerably lower than those from DMDA for the same irradiation time of 30 minutes.

In several additional experiments it was noticed that in the absence of O_2 , the predominant product of the photolysis of [7] was the endo-adduct [2]. This is shown in Table XI where the photolyses were performed in small quartz tubes which were carefully degassed prior to irradiation.

3.5 Intermediacy of EDA

In order to rationalize the intermediacy of EDA in the photolysis of DMDA, auxiliary experiments were performed in which the concentrations of these species were continuously monitored using the sharp infrared diazo bands at 2075 cm^{-1} and 2110 cm^{-1} in cyclohexene for DMDA and EDA respectively. Details of calibration procedures and measurements are appended (Appendix B). The wavelength and time dependence of EDA and DMDA concentrations are shown in Table XII and Figures 8 - 11.

Unfortunately, it was observed that the rate of photolysis was quite sensitive to the amount of light absorbed, i.e. to experimental conditions such as the rate of stirring, distance of the photolysis tube from light source, amount of light dispersed by suspended mercury formed during photolysis, etc. Therefore, the

TABLE X

Comparison of Yields from the Photolysis of DMDA and
[7] in Cyclohexene*

Filter (wavelength, Å)	starting material, mg	mg product			mg [7] recovered
		[1]	[2]	[3]	
Corex (>2400)	DMDA, 778	68	50	4	-
Corex (>2400)	[7], 310	3	3	4	310 ± 28
Vycor (>2100)	DMDA, 773	55	90	9	-
Vycor (>2100)	[7], 310	8	14	12	275 ± 28

* photolysis time of 30 min.

TABLE XI

Product Yields from the Photolysis of [7] in the
Absence of Oxygen

Photolysis cell diameter (mm)	Irradiation time (minutes)	% theoretical yields				
		[1]	[2]	[3]	[4]	[5]
8	64	<0.2	8.4	<0.2	2.6	<0.1
16	64	<0.2	4.9	<0.2	1.3	<0.1

TABLE XII
Concentration Measurements of DMDA and EDA during Photolysis

Irradiation time (minutes)	Concentrations (mole/ltr. $\times 10^{-3}$) for cut-off filters (λ)									
	Vycor ($\lambda > 2100\text{\AA}$)		Corex ($\lambda > 2400\text{\AA}$)		Pyrex ($\lambda > 2800\text{\AA}$)		Uranium ($\lambda > 3200\text{\AA}$)		DMDA	EDA
	DMDA	EDA	DMDA	EDA	DMDA	EDA	DMDA	EDA		
0	11.8 (11.8)*	1.0 (1.0)*	11.9	1.0	11.7	1.1	11.7	.75		
1	10.6	1.25(1.2)	11.8	1.25	11.3	1.3	-	0.9		
2	9.8 (10.1)	1.4 (1.3)	11.6	1.45	10.8	1.5	-	1.0		
3	9.0	1.45	10.3	1.6	10.2	1.7	11.2	1.2		
4	7.8 (8.25)	1.5 (1.5)	10.0	1.7	9.5	1.75	-	-		
5	-	(7.4)	-	1.75	-	1.8	-	-		
6	6.5	1.7	8.6	1.8	8.0	2.0	10.7	1.5		
8	5.25 (5.4)	1.6	7.5	1.95	-	-	-	-		
9	-	-	-	-	7.5	2.1	10.3	1.7		
10	3.9 (4.1)	1.5 (1.5)	6.7	2.0	-	-	-	-		
12	3.0	1.35	-	2.1	5.9	2.25	9.5	-		
15	1.8 (2.0)	1.1 (1.2)	5.2	1.95	5.2	-	9.0	1.8		
18	-	-	-	-	-	2.6	-	-		
20	-	-	-	2.0	-	-	-	-		
21	0.4	0.6	4.0	-	-	-	-	-		
22	-	-	-	-	-	-	-	-		
24	-	-	-	-	-	-	-	-		
30	0.1 (0.1)	0.1 (0.1)	-	-	3.1	2.25	-	-		
36	-	-	2.2	1.6	2.0	2.1	6.0	2.4		
			-	-	-	-	-	-		

*() duplicate measurement.

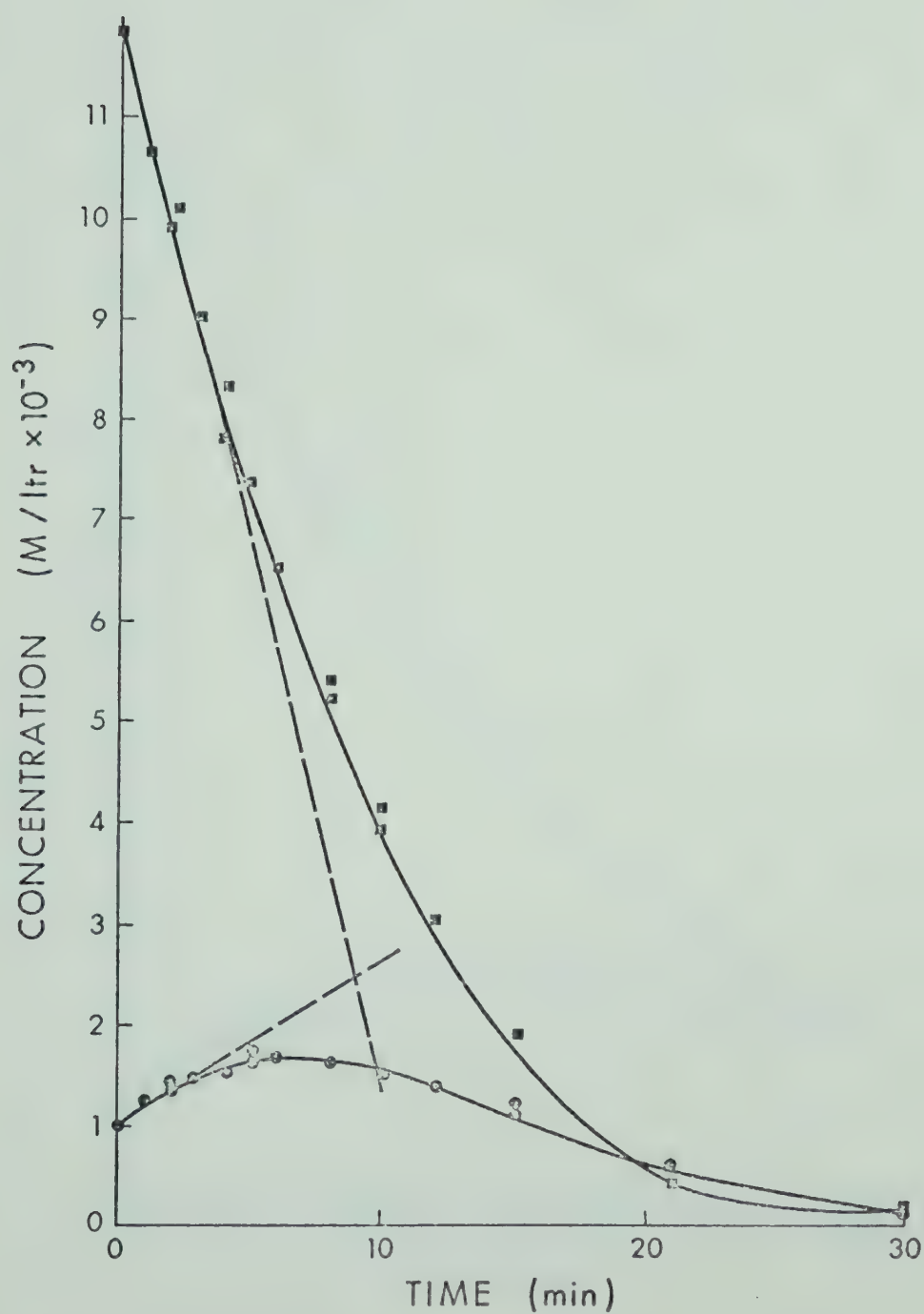


FIGURE 8: Concentrations of DMDA ■ and EDA ● during the Photolysis with Vycor Filtered Light

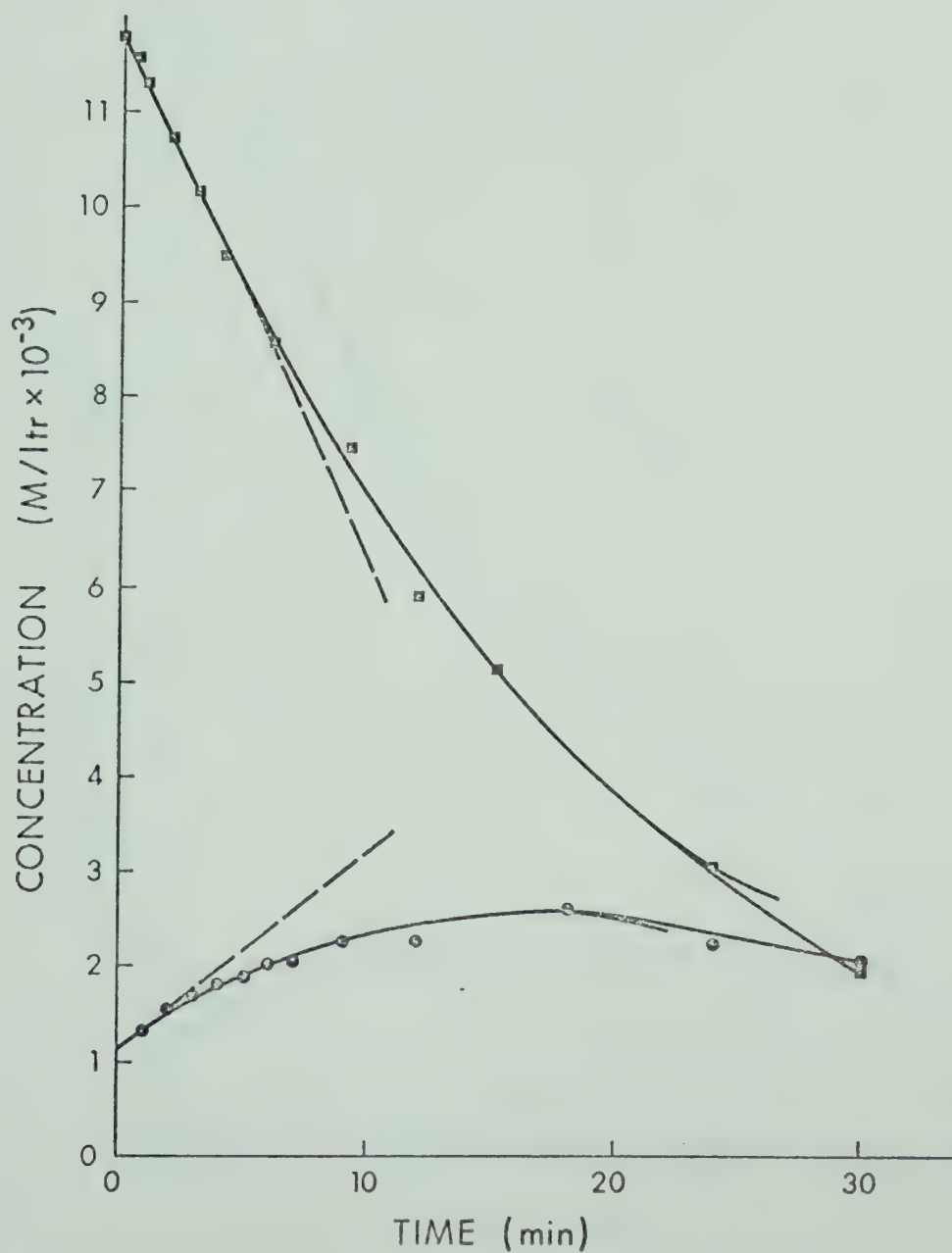


FIGURE 9: Concentrations of DMDA ■ and EDA ● during the Photolysis of Corex Filtered Light

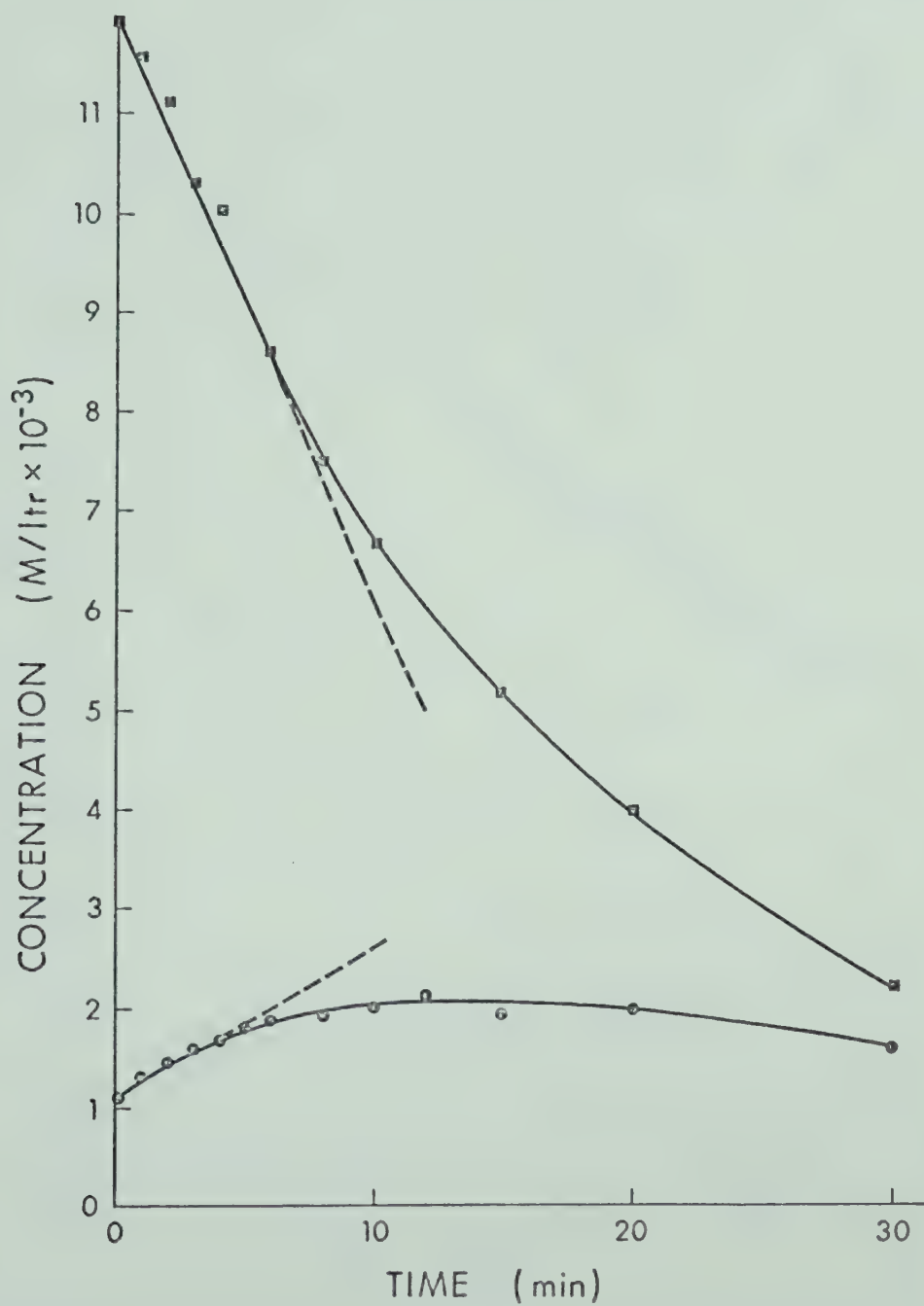


FIGURE 10: Concentrations of DMDA ■ and EDA ● during the Photolysis with Pyrex Filtered Light

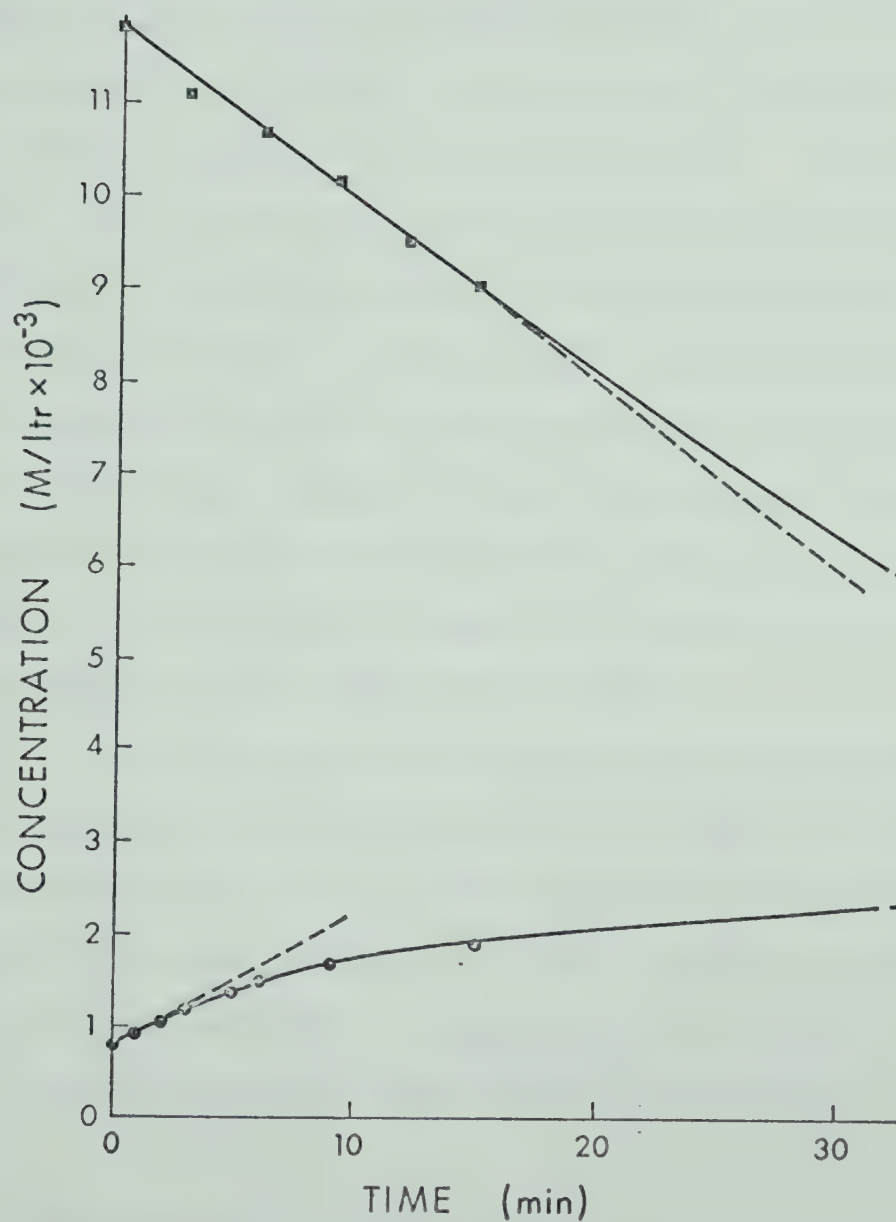


FIGURE 11: Concentrations of DMDA ■ and EDA ● during the Photolysis with Uranium Glass Filtered Light

results were not suitable for accurate rate determinations, but limited the evaluation of the data to a comparison of the relative rates of disappearance of DMDA and simultaneous formation of EDA in the initial stages of photolysis. Furthermore, EDA is also photolyzed under the given experimental conditions and the observed apparent rate of formation of EDA is probably a resultant curve of its formation and subsequent photolysis. It was assumed, however, that in the initial stages of the photolysis, secondary photolysis is negligible, and that the slope at this point is a fair assessment of the rate of EDA formation. From the relative rates of DMDA disappearance and EDA formation which were approximated from the initial slopes, the upper limit of EDA formation could be estimated. The importance of the intervention of EDA was found to increase with increasing wavelength of irradiation: 8% ($\lambda > 2100\text{\AA}$), 12% ($\lambda > 2400\text{\AA}$); 20% ($\lambda > 2800\text{\AA}$); 30% ($\lambda > 3200\text{\AA}$).

In spite of the fact that the solutions were always degassed and maintained at 18°C (at lower temperatures DMDA crystallizes out of solution) small amounts of EDA, 0.25 to 1.1×10^{-3} moles/liter, were always formed during dissolution of DMDA in cyclohexene prior to photolysis. Hence additional experiments were performed to study the effects of oxygen and temperature on the decomposition of DMDA.

3.6 Effects of Oxygen and Temperature

A solution of 0.1034 gm DMDA in 20 ml cyclohexene was degassed and kept in the dark at room temperature (24 - 25°C).

Infrared analysis after 24 hours showed that the concentrations of DMDA and EDA were unchanged. Subsequent irradiation of this probe resulted in decomposition of DMDA and simultaneous EDA formation as described above (section 3.5).

Addition of 4×10^{-3} moles of oxygen to a solution of 0.1073 gm of DMDA in 20 ml of cyclohexene effected moderate decomposition after one hour at room temperature.

The effects of oxygen and temperature on the decomposition of DMDA are summarized in Table XIII. The data clearly document the thermal stability of DMDA in cyclohexene in the absence of oxygen up to 145°C. In the presence of oxygen however, DMDA decomposes readily with increasing temperature, yielding about 50% EDA. Although detailed product analyses were not carried out, preliminary g.c. analysis showed large amounts of typical autoxidation products of cyclohexene, including cyclohexanol, cyclohexenol, cyclohexenone, and bicyclohexenyl. Only trace amounts (<1%) of insertion and addition products of cyclohexene could be verified.

The mercury was recovered as mercuric oxide, a greyish and flocculent precipitate which, in contrast to metallic mercury, dissolved easily in dilute hydrochloric acid. The mercuric ion was then identified as copper amalgam and mercuric sulfide.

Pure DMDA (23 mg) decomposed readily in a thermal analyzer under vacuum within 10 minutes in the temperature range of 105 to 125°C.

TABLE XIII

Thermolysis of DMDA in the Absence and Presence of Oxygen

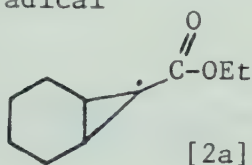
Temperature (°C)	Amount of Oxygen	Reaction Time (hrs.)	Concentration (mole/ltr. x 10 ⁻³)				Percent EDA produced ^a
			Initial		final		
			DMDA	EDA	DMDA	EDA	
25	nil	24	12.1	0.5	12.1	0.5	nil
80	nil	8	12.1	0.8	12.1	0.9	trace?
145	nil	3	12.1	1.0	12.0	1.2	trace
165 ^b	nil	1.5	11.9	1.0	<0.2	0.5	2
20	4 x 10 ⁻³ moles	1	12.1	0.5	11.6	1.2	70
80	7 x 10 ⁻³ moles	0.5	12.0	1.0	complete decomposition		
20	open to air	4	12.0	0.25	10.8	2.0	73
40	open to air	4	12.0	0.25	7.2	5.25	52
60	open to air	4	12.0	0.25	5.75	6.6	50
70	open to air	4	12.0	0.25	4.5	8.3	54

^a % EDA produced from decomposed DMDA.^b Carried out in Carius tube

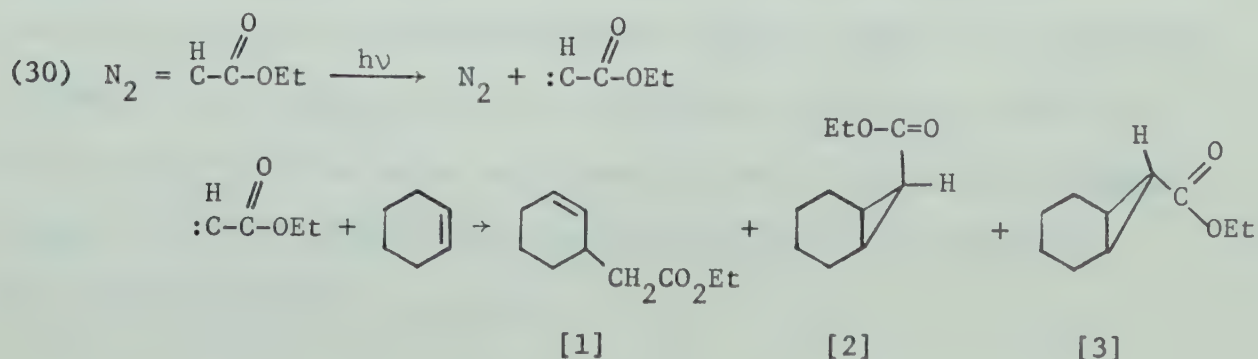
3.7 Discussion

The direct photolysis of DMDA in cyclohexene has yielded a number of characteristic reaction products, and also shown a great sensitivity of product distribution to experimental conditions. The subsequent discussion is intended to be an interpretation of these results in terms of various possible mechanisms with the emphasis on the elucidation of the conditions for predominant carbyne intermediacy and the characterization of the chemical behaviour of carbyne transients.

The most predominant and important feature is the involvement of the cyclopropyl radical

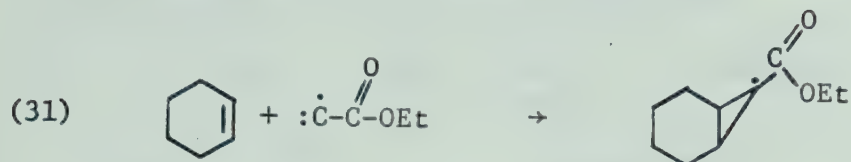


which is unequivocally demonstrated by the high endo- to exo-addition product ratio, [2]/[3]. Carbethoxymethylene from the photolysis of EDA in cyclohexene has been reported to give the same products:^{77,78}

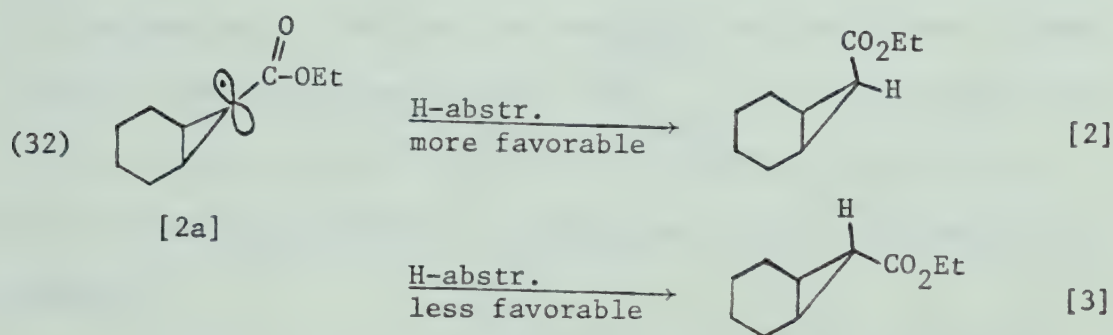


However, there is a notable difference. The endo/exo product ratio,

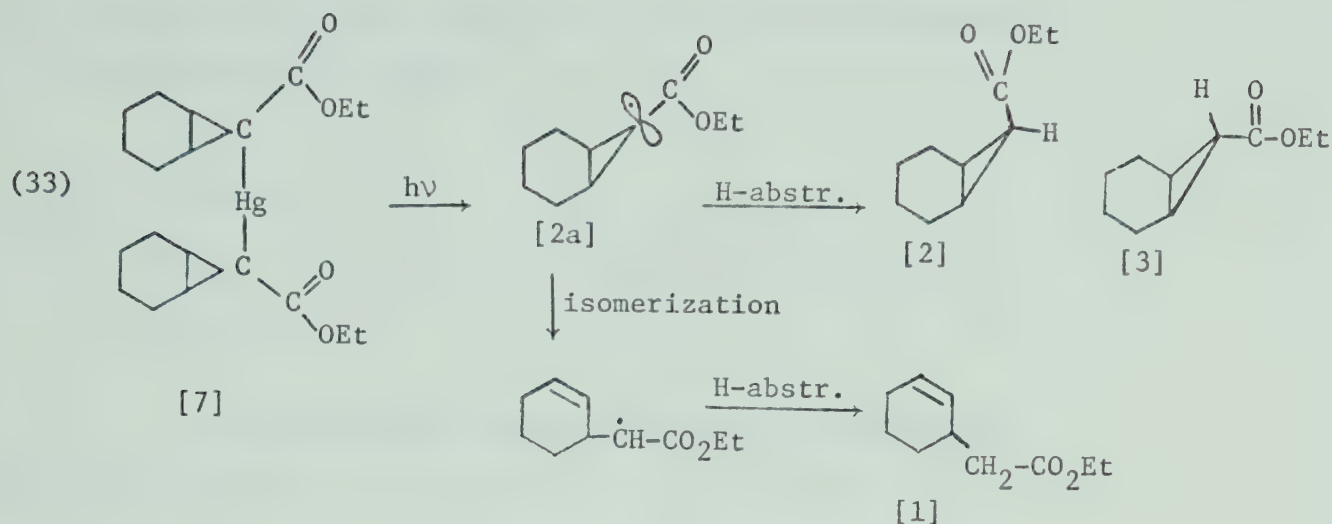
[2]/[3], was only 0.53^{78} which differs considerably from the value 8.4 observed in the photolysis of DMDA for the proposed addition of carbethoxymethyne to cyclohexene:



The fact that the less stable endo isomer is the predominant product here can be readily rationalized from steric considerations: thus the radical intermediate would be expected to react preferentially on the more exposed side of the p-orbital, in accordance with the proposed addition abstraction sequence:



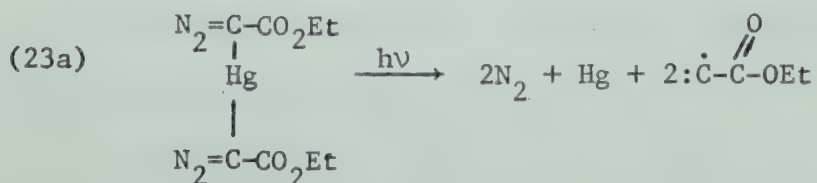
The cyclopropyl radical [2a] is also an intermediate in the photolytic decomposition of the mercury-adduct [7] which yields metallic mercury and predominantly endo-addition product [2]. Following cleavage of the carbon-mercury bonds hydrogen abstraction leads to the formation of <0.2% exo-addition product [3] and <0.2% of the insertion product [1], the latter being the manifestation of the occurrence of a slow isomerization reaction.



In view of the limited formation of [2a] via the photolysis of the mercury-adduct [7] (cf. Table X) all possible primary modes of decomposition of DMDA must be carefully considered here in order to ensure that carbethoxymethyne ($:\dot{\text{C}}-\text{C}(=\text{O})\text{OEt}$), the monovalent carbon species, is the only major possible route that may lead to the production of [2a] and hence be correlated to the endo-product [2] formation.

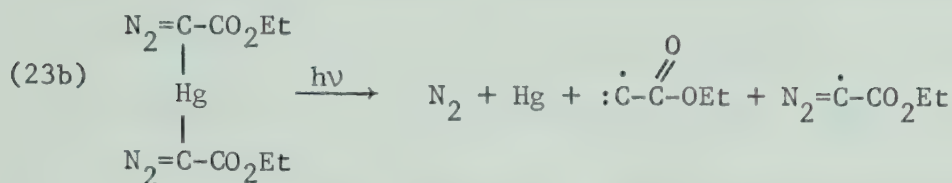
Primary steps that can be envisioned in the photolytic decomposition of DMDA involving monovalent, divalent and trivalent intermediates include:

a) simultaneous rupture of the carbon-nitrogen and carbon-mercury bonds leading to 2N_2 , Hg and carbethoxymethyne:

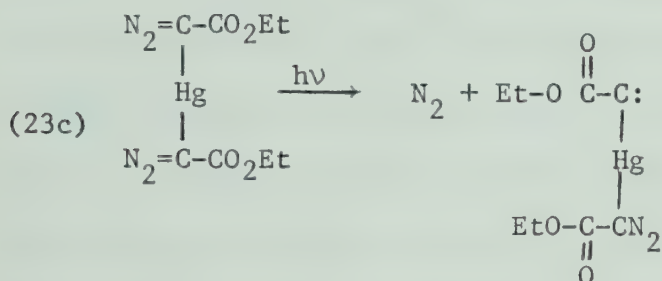


b) simultaneous cleavage of one carbon-nitrogen bond and

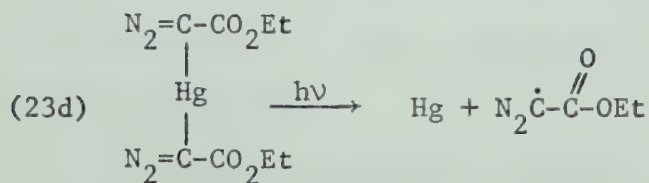
both carbon-mercury bonds yielding N_2 , Hg, carbethoxymethyne, and EDA radical ($N_2\dot{C}-CO_2Et$):



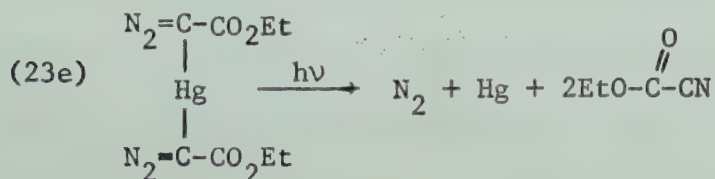
c) single carbon-nitrogen rupture to give a novel mercury carbene



d) mercury-carbon bond rupture to yield Hg and EDA radicals:



e) elimination of nitrogen between diazo groups of DMDA and simultaneous cleavage of the mercury-carbon bonds to form N_2 , Hg, and carboethoxy-nitriles:



Reactions of carbethoxymethyne: A mechanism involving carbyne formation is shown in Reaction Scheme I (Figure 12). The carbethoxymethyne formed by equations (23a) and (23b) may insert in the carbon-hydrogen bond, add to the double bond of cyclohexene, and also abstract hydrogen to give carbethoxymethylene. Based on criteria set forth by the spin conservation rule for the chemical behaviour of singlet and triplet carbenes, the doublet-state carbyne may be expected to undergo insertion and concerted addition reactions, and the quartet-state reagent, abstraction and stepwise addition. Insertion into the allylic carbon-hydrogen bond leads to the intermediate radical [1a] which, upon abstraction of hydrogen from the solvent, yields the final insertion product [1]. Addition of carbethoxymethyne produces the intermediate radical [2a] which, after abstraction of hydrogen from the medium, yields endo- and exo-addition products [2] and [3]. The predominance of the endo isomer is taken here as a strong evidence for the proposed reaction sequence involving the intermediacy of the radical [1a-2] and hence the intervention of carbethoxymethyne as the reactive intermediate of the photolysis.

Another interesting feature of the carbethoxymethyne addition reaction is the appearance of products [5] and [6], formed via addition of initially-formed radical [1a] to cyclohexene, followed by hydrogen abstraction and competitive disproportionation. A similar sequence was proposed by Wolfgang^{33,34} for the reaction of $\dot{\text{C}}\text{-H}$ with ethylene [cf. Introduction, section 1.3, equations (6) and (7)] to form an allyl radical which, after addition to another

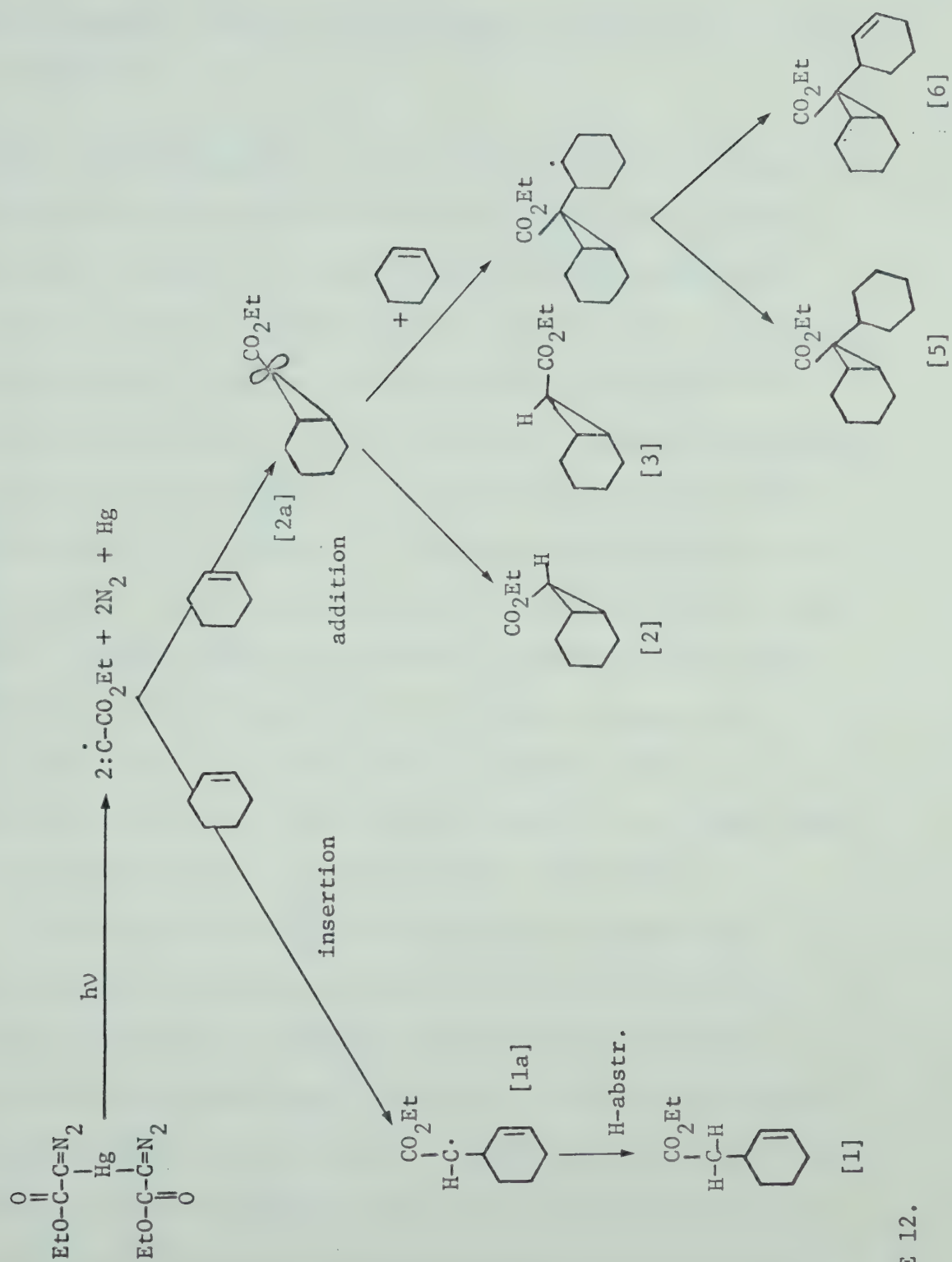


FIGURE 12.

substrate molecule, ethylene, and subsequent hydrogen abstraction, yields pentene-1.

Reactions of mercurycarbene. The presence of the mercury-adduct [7] among the reaction products and its strong wavelength dependence indicate the operation of an alternative mechanism involving the generation of a novel mercury carbene in a primary step. A proposed reaction sequence is outlined in Reaction Scheme II (Figure 13), which shows the formation of [7] in a two-step consecutive photolysis-addition sequence and includes at the same time a possible pathway for the formation of insertion [8] and mixed insertion-addition [9] mercury adducts. The primary step generating mercury-carbene, (23c), exhibits a distinct wavelength dependence reflected in the yields of [7] which increase from 16.4 to 37.6% with increasing wavelength of the irradiation source and a substantial decrease in the yields of [1] to [5], i.e. those products derived from primary steps (23a) and (23b) involving carbyne formation (Table VIII).

At this point it appears necessary to consider the possibility of secondary photolysis of [7] to give products [1] - [6] which have been thus far exclusively attributed to a mechanism involving the carbethoxymethyne intermediate. Some decomposition of [7] could be realized upon extended irradiation at shorter wavelength ($\lambda > 2100\overset{\circ}{\text{A}}$); however, a comparison of yields from the photolysis of DMDA and [7] in cyclohexene under the same experimental condition [cf. Table X] shows that the yields derived from the photolysis of [7] are considerably lower, for the same irradiation time.

Reaction Scheme II

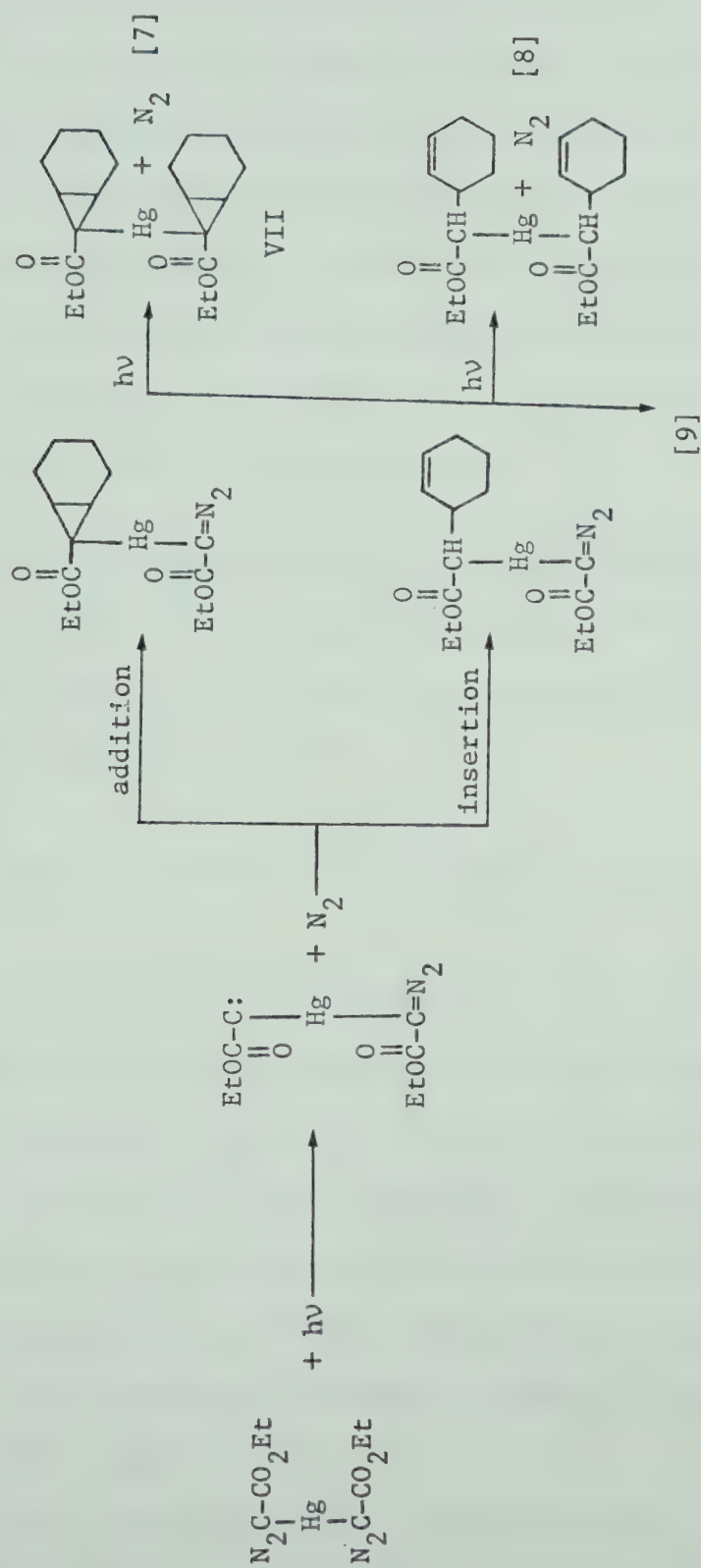
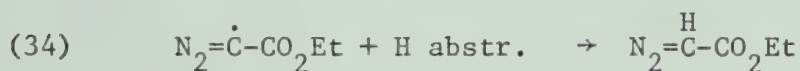


FIGURE 13

Furthermore, DMDA is a much stronger absorber than [7] as depicted in Figure 14 and henceforth secondary photolysis of [7] in the presence of DMDA competes unfavorably with the photolysis of DMDA. Thus, the amounts of products obtained in the photolysis of pure [7] are the maximum yields possible, and the actual contribution to the total yields of addition and insertion products via secondary photolysis of [7] is likely very much smaller and in any case not sufficient to account for the observed yields.

Reactions of the EDA radical ($\text{N}_2=\dot{\text{C}}-\text{CO}_2\text{Et}$): The intermediacy of the EDA radical which is formed in the photolysis of DMDA via primary steps (23b) and (23d), has been verified by direct i.r. monitoring of its characteristic product, EDA:



During the photolysis of DMDA however, EDA undergoes secondary photolysis, producing carbethoxymethylene which upon reaction with cyclohexene yields endo- and exo-addition products in the ratio of $[2]/[3] = 0.53^{78}$ (cf. equation 30). The intermediacy of the EDA radical therefore reduces the endo/exo product ratio obtained from the photolysis of DMDA. The tendency of increased EDA formation with increasing wavelength is reflected in the decrease of $[2]/[3]$ from 8.2 to 4.3.

The fate of the EDA radical is not necessarily exclusive formation of EDA via hydrogen abstraction, but one can also envision

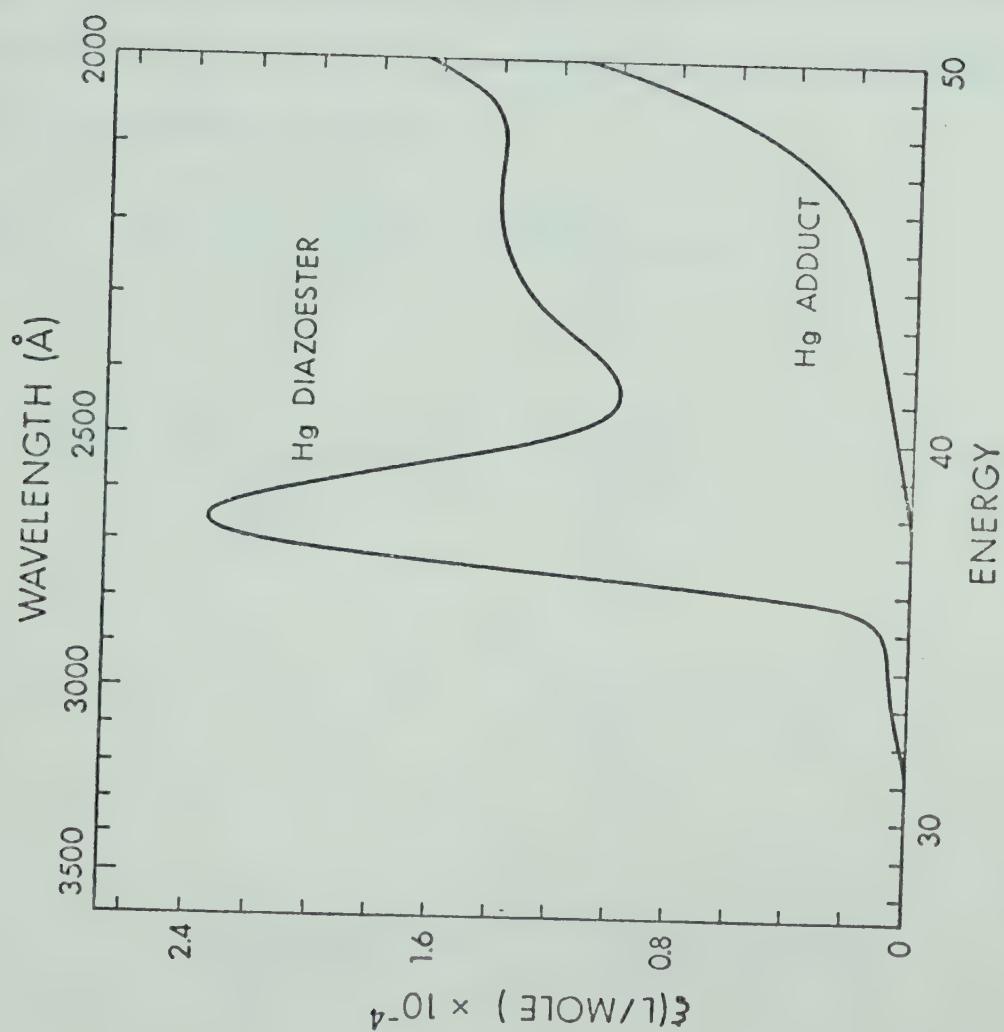
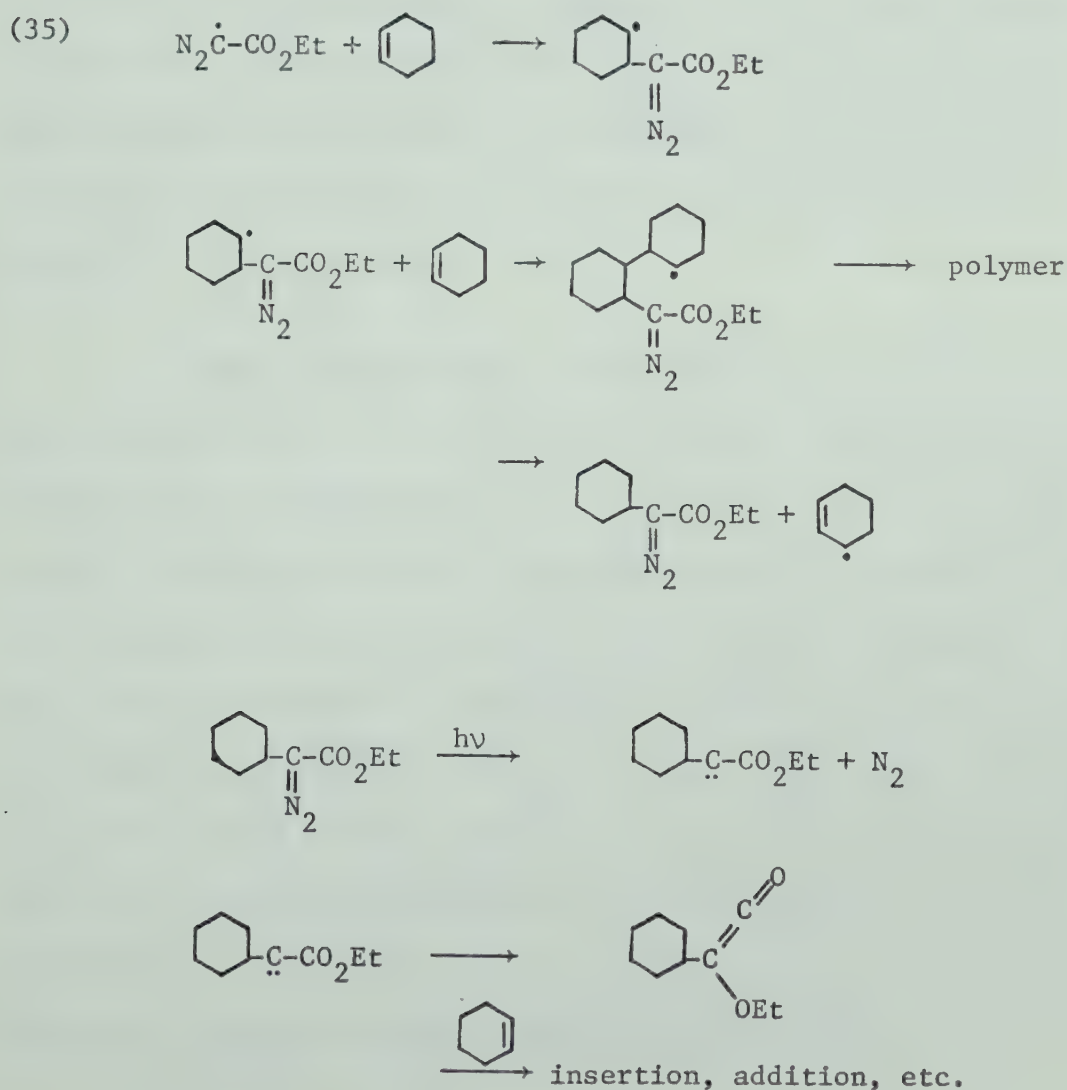


FIGURE 14: U.V. Spectra of DMDA and the Mercury Adduct [7]

a mechanism that involves scavenging of the EDA radical by cyclohexene. The analogous scavenging reaction for the cyclopropyl radical [2a], yielding products [5] and [6] (vide infra) was also observed in this system. Polymerization of the labile intermediates could result via secondary photolysis of the diazo group and an undefined sequence of radical reactions, and thus contribute to the observed polymeric residue:



Oxygen-initiated reaction: A further contribution to some low [2]/[3] ratios in the decomposition of DMDA is the interfering reaction of oxygen which apparently gives high yields (~50%) of EDA (cf. Table XIII). This dark reaction, once recognized, was naturally minimized or avoided by appropriate experimental procedures. By use of proper precautions a considerable reduction in EDA yields was achieved, resulting in high [2]/[3] ratios. The mechanism for the non-photolytic decomposition of DMDA was not investigated further. Observations, however, indicated a radical mechanism involving autoxidation of cyclohexene and intermediate oxide and peroxide radicals. Carbon-mercury cleavage by a free radical pathway is known.⁸⁰

Other intermediates: The primary step (23c) leading to carboethoxynitriles is not considered to play a role in the photolytic decomposition of DMDA because, due to the linearity of the carbon-mercury bonds in mercurials, the stereochemical arrangement of DMDA is unfavorable for one-step intramolecular nitrogen elimination. In fact, one can exclude the possibility of this or any similar primary step yielding nitrogen-containing compounds like nitriles, pyrazolines, or azines that might also result from an intramolecular mechanism^{81,82}, because all the diazo-nitrogen was recovered quantitatively (cf. experimental, section 2.5) and no nitriles or any other nitrogen-containing compounds could be isolated and identified.

Summary: The nature and distribution of products formed in the

photolysis of DMDA in the solvent cyclohexene, and their dependence upon wavelength, temperature and oxygen can be rationalized by postulating four types of primary processes (23a-d). Two of these lead to the production of carbethoxymethyne and increase in importance with increasing photon energy. Carbethoxymethyne reacts with cyclohexene via insertion and addition and the intervention of this novel intermediate as the principal reagent provides the only plausible and self-consistent rationalization for the observed characteristic products and their yield distribution. Since the reactivity of this monovalent carbon intermediate is completely unknown, the investigation was extended to include a variety of substrates.

Energetically, all outlined processes are feasible within the wavelength range used in this study. DMDA exhibits two absorption in the u.v. [$\lambda_{\text{max}}^{\text{EtOH}} = 3800\text{\AA}$ ($\epsilon \sim 107$) and 2640\AA ($\epsilon \sim 22,000$) which by analogy with diazoalkanes may be ascribed to $(\pi^* \leftarrow n)$ and $(\pi^* \leftarrow \pi)$ transitions respectively.⁷⁹ Irradiation in the (n, π^*) region apparently leads to the loss of one nitrogen molecule, leading to the formation of the mercury carbene, step (23c), ultimately recovered as the mercury adduct [7]. It would also appear that at longer wavelengths, owing to the relatively long lifetime of the energized molecule, the absorbed photon energy is efficiently randomized and C-Hg bond cleavage can occur selectively. Results show that at long wavelengths the mercury-adduct [7] yields and the intermediacy of EDA, which involve primary steps (23c) and (23d) respectively, are predominant. Finally, absorption in the higher energy region (π^*, π) leads to simultaneous cleavages of $\text{C}=\text{N}_2$ and C-Hg bonds, involving step (23a) and possibly (23b). Unfortunately the relative importance of these processes cannot be assessed precisely from the data, since the wavelength region of the actinic light is not well-defined. It can be stated with certainty however, that the processes leading to carbethoxymethyne formation increase with increasing photon energy, since the characteristic product ratio $[7]/[1]+[2]+[3]+[5]+[6]$ (vide infra) decreases from 7.09 to 0.54 and the endo/exo product ratio $[2]/[3]$ increases from 4.3 to 8.4.

CHAPTER 4

PHOTOLYSIS OF DIETHYL MERCURYBISDIAZOACETATE IN
CIS- AND *TRANS*-BUTENE-24.1 Results

Cis- and *trans*-butene-2 were chosen as media for the photolysis of DMDA, in order to study in particular the stereospecificity of the addition reaction of carbethoxymethyne. The butene-2 isomers are simple in structure, lack a symmetry axis along the carbon-carbon double bond, and they have been used in numerous investigations to study the mechanism of carbene addition reactions for over a decade^{83,84}. The photolysis of methyldiazoacetate, MDA, in these solvents was carried out by Doering and Mole⁸⁵ in 1960 who demonstrated that singlet state carbomethoxycarbene adds stereospecifically; a certain degree of stereoselectivity was also apparent from the predominant formation of the *exo* addition product. Since similar products were encountered in the photolysis of DMDA, samples of EDA were also photolysed in these solvents for comparison studies and to assist product identification.

When samples of 100 mg of DMDA in about 20 ml butene-2 were prepared for photolysis (cf. Experimental, section 2.3) some crystalline DMDA remained in suspension because of its low solubility, but dissolved readily during photolysis. Otherwise the observations recorded during the photolysis of DMDA in cyclohexene (cf. section 3.1:

precipitation of metallic mercury, quantitative recovery of nitrogen, wavelength effect of the light source on product distribution, EDA intermediacy, and dark reaction in the presence of oxygen) applied to this system as well.

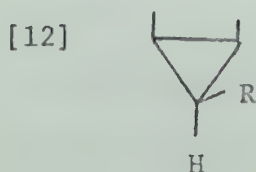
Product characterization after careful evaporation of the solvent and general work-up procedure (cf. Experimental, sections 2.3 and 2.5), was in part assisted by the procedure and results reported by Doering and Mole⁸⁵ who used a 4 meter didecylphthalate column at 130°C for the separation of the isomeric addition products. Temperature programming and the use of a column with XE60 as liquid support, which is intermediate polar like didecylphthalate but allowed higher operating temperatures, was found to give the same sequence of elution of those products observed and identified earlier, but with improved separation. Besides mercury and nitrogen, the following eight products were separated and identified in the photolysis of DMDA butene-2 ($R = -CO_2C_2H_5$):




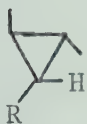


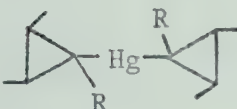
ethyl *cis*-4-hexenate
(*cis*-insertion product)



ethyl *trans*-4-hexenate
(*trans*-insertion product)



ethyl *cis*-2,3-dimethylcyclopropane-*cis*-carboxylate
(α -isomer)

- [13]  ethyl *cis*-2,3-dimethylcyclopropane-*trans*-carboxylate (β -isomer)
- [14]  ethyl *trans*-2,3-dimethylcyclopropane-carboxylate (γ -isomer)
- [15]  ethyl butenyl-*cis*-2,3-dimethylcyclopropane-carboxylate
- [16]  ethyl butyl-*cis*-2,3-dimethylcyclopropane-carboxylate
- [17]  diethyl mercurybis-*trans*-2,3-dimethylcyclopropane-carboxylate (*trans*-mercury adduct)

The retention times (t_R), the parent peak (m/e P), and the ten most intense mass peaks (m/e) listed in Table XIV were determined by combined g.c.-m.s. analysis.

For the isolation of the various products, the reaction mixtures from the photolyses of 0.5 gm DMDA and 1.0 gm EDA in 100 ml butene-2 were submitted to bulb-to-bulb distillation (cf. Experimental, section 2.1). Products [10] - [16] and [10] - [14] from the photolyses of DMDA and EDA respectively were recovered in the fraction distilling at 80 - 95°C/0.5 mm Hg. These products were subsequently separated by preparative gas chromatography. Upon raising the temperature of

TABLE XIV

Combined Gas Chromatographical and Mass Spectral Analysis for Products [10] - [17]

Compound No.	t_R (min)	m/e (P)	m/e and (% of base peak)									
[10]	15.5 ^a	142 (34)	127 (45)	97 (55)	71 (28)	69 (100)	68 (60)	55 (38)	41 (90)	39 (25)	29 (43)	
[11]	14.0 ^a	142 (32)	127 (50)	99 (35)	97 (50)	69 (100)	41 (96)	39 (22)	29 (50)	28 (96)	18 (26)	
[12]	12.2 ^a	142 (5)	114 (10)	99 (60)	97 (65)	69 (70)	43 (15)	41 (80)	39 (16)	29 (30)	27 (15)	
[13]	14.6 ^a	142 (15)	127 (88)	114 (20)	99 (40)	97 (90)	69 (97)	41 (100)	39 (20)	29 (37)	27 (18)	
[14]	9.8 ^a	142 (8)	114 (11)	99 (55)	97 (68)	69 (73)	43 (14)	41 (80)	39 (17)	29 (30)	27 (15)	
[15]	18 ^b	196	169	151	141	123	95	81	67	53	41	
					(some [16] present)							
[16]	17 ^b	198 (7)	181 (24)	169 (100)	153 (25)	123 (55)	95 (46)	69 (35)	55 (35)	41 (50)	29 (60)	
[17]	38 ^c	454	142 (41)	141 (93)	114 (23)	113 (86)	95 (100)	67 (51)	45 (30)	41 (35)	29 (33)	

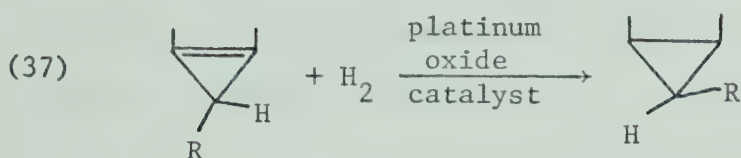
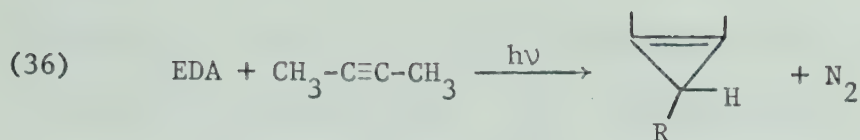
^a Column: 15 ft x 1/8 inch, packed with 12% XE60 on Chromosorb W; flow rate: 50 cc/min helium; Temperature: 80°C. ^b Column and flow rate as in a; temperature 110°C. ^c Column as in a; flow rate: 75 cc/min helium; temperature: 180°C.

the distillation bulb to 175 - 180°C at ~0.5 mm mercury pressure a heavy colorless oil began slowly to distill, and upon extended heating at this temperature or increasing the temperature, metallic mercury was observed, indicating decomposition of a mercury compound. In the samples containing *trans*-butene-2 + DMDA, the heavy distillate partially crystallized in the distillation trap and addition of methanol facilitated crystallization. The white crystalline compound (m.p. 109 - 110°C) was identified as [17]. The remaining high-boiling fraction was subjected to m.s. analysis and found to consist mainly of mercury adduct. By analogy with the DMDA + cyclohexene system, these adducts are probably of the insertion and addition type; it is also likely that small amounts of the isomeric addition products (α, β, γ) are present. The complexity of this fraction was such that isolation of the pure components could not be achieved. The molecular weights, M.Wt., as determined by m.s. measurements, the principal well defined i.r. peaks, and the n.m.r. spectra of all isolated products are recorded in Table XV. The analytical data are in good agreement with the assigned structures for compounds [10] to [17]. The structural distinction between isomeric α and β -addition products, [12] and [13], is based on the application of the principle of surface hindrance in catalytic hydrogenation. Ethyl 2,3-dimethylcyclopropene-carboxylate prepared by the photolysis of EDA in 2-butyne gave predominantly the all-*cis* products:

TABLE XV

Molecular Weights, I.R. and N.M.R. Spectra for Compounds [10] - [17]

Compound No.	Formula	M.Wt.		i.r. γ max	CCl_4 (cm^{-1})	n.m.r. τ (CCl_4)
		calc.	meas.			
[10]	$\text{C}_8\text{H}_{14}\text{O}_2$	142	142	1710(s); 2980(w)		8.90(t, 3H); 8.5(m, 3H); 7.87(m, 4H); 6.10(q, 2H); 4.75(m, 2H).
[11]	$\text{C}_8\text{H}_{14}\text{O}_2$	142	142	1730(s); 2980(w)		8.86(t, 3H); 8.44(d, 3H); 7.83(m, 4H); 6.05(q, 2H); 4.7(m, 2H).
[12]	$\text{C}_8\text{H}_{14}\text{O}_2$	142	142	1770(s); 2980(w)		8.95(m, 9H); 8.88(t, 3H); 6.14(q, 2H).
[13]	$\text{C}_8\text{H}_{14}\text{O}_2$	142	142	1720(s); 2980(w)		9.0 (m, 9H); 8.92(t, 3H); 6.15(q, 2H)
[14]	$\text{C}_8\text{H}_{14}\text{O}_2$	142	142	1720(s); 2980(w)		9.1 (m, 9H); 9.05(t, 2Hz, 3H), 6.24 (q, 7Hz, 2H)
[15]	$\text{C}_{12}\text{H}_{20}\text{O}_2$	196.1463	196.1455	1715(s)		8.82(t, 3H); 8.7-9.2(m, 15H); 6.06 (q, 2H); 5.1-5.3(m, 2H).
[16]	$\text{C}_{12}\text{H}_{22}\text{O}_2$	198	198	1715(s)		8.81(t, 3H); 8.5-9.2(m, 17H); 6.05 (q, 2H).
[17]	$\text{C}_{16}\text{H}_{26}\text{O}_4^{\text{Hg}}$	484.1532	484.1530	1705(s)		8.84(t, 7.2Hz, 6H); 8.89(d, 1.4Hz, 6H); 8.86(m, 2H); 8.83(d, 1.4Hz, 6H); 8.24(m, 2H); 5.98(q, 4H).



In this method, which has been employed by Doering and Mole⁸⁵ for the methyl ester analogs, geometry of adsorption determines the stereochemistry of the hydrogenated product. Hydrogen from the surface of the catalyst adds from the underside to the olefin which is thought to assume the favoured conformation of adsorption with the ethyl carboxylate group *trans* to the catalyst surface, thus yielding the α -isomer.

The n.m.r. spectrum for [17] in carbon tetrachloride is in agreement with the *trans*-configuration of the mercury-adduct. The spectrum features a triplet at $\tau = 8.84$ for the methyl protons of the two carbethoxy groups which collapsed to a singlet when the quartet at $\tau = 5.98$ ($2 \times -\text{CH}_2-$) was irradiated. Furthermore, there were two doublet bands at $\tau = 8.89$ (1.4 Hz) and 8.83 (1.4 Hz) which were assigned to the methyl protons substituted on the cyclopropane ring; the methyl groups which are in the syn-position adjacent to the carbethoxy groups are expected to give a downfield chemical shift. The two multiplets centered around $\tau = 8.86$ and $\tau = 8.24$ were assigned to the methine protons on the cyclopropane ring.

Results of the photolysis of 100 mg samples of DMDA in 25 ml of butene-2 using pyrex filtered light exhibited stereospecific

addition of carbethoxymethyne as demonstrated by the relative yields for products [10] to [14] which are shown in Table XVI. As expected, *cis*-butene gave as major addition products the α - and β -isomers, [12] and [13] respectively, while *trans*-butene-2 yielded only the γ -isomer [14]. More detailed quantitative studies with regard to the effect of wavelength on product distribution were undertaken for *trans*-butene-2 only. The per cent theoretical yield for three different wavelengths are listed in Table XVII (cf. Appendix C for individual photolyses and analytical procedure). The data show an increase of addition products ([14]+[15]+[16]) with increasing energy of irradiating light and at the same time a decrease in the yield of the mercury-adduct, [17], a trend that was also observed in the cyclohexene system. A solution of [17] in *trans*-butene-2 showed no significant decomposition when irradiated under the same conditions and for the same time required to photolyze an equivalent amount of DMDA.

4.2 Discussion

The great similarities in the nature of the products and the effects of experimental conditions on product distributions in the photolysis of DMDA in butene-2 and cyclohexene are quite apparent. The results provide additional evidence for the intermediate formation of carbethoxymethyne, mercurycarbene and EDA, via the three primary steps described by equations (23a-d). A proposed mechanism for the formation of products [10] - [17] from these intermediates

TABLE XVI

Yields of Products [10] - [14] from the Photolysis
EDA and DMDA in *cis*- and *trans*-butene-2

Compound No.	Relative Yields in			
	<i>cis</i> -butene-2		<i>trans</i> -butene-2	
	EDA	DMDA	EDA	DMDA
[10]	10	17	nil	nil
[11]	nil	trace	13	17
[12]	19	39	nil	trace
[13]	73	57	nil	trace
[14]	nil	trace	70	82
[12]/[13]	.25	.69		

TABLE XVII

Wavelength Dependence of the Yields of [14] - [17]

Compound No.	% Yield (theor.) for λ		
	$\overset{\circ}{>2100\text{\AA}}$	$\overset{\circ}{>2800\text{\AA}}$	$\overset{\circ}{>3200\text{\AA}}$
	(vycor)	(pyrex)	(uranium)
[14]	10	2	1
[15]	2	<1	<1
[16]	1	<1	<1
[17]	20	34	40

is outlined and summarized in scheme III (cf. Figure 15) and scheme IV (cf. Figure 16) for the photolysis of DMDA in *cis*-butene-2 and *trans*-butene-2 respectively.

The wavelength dependence of the three major pathways involving carbethoxymethyne, mercury-carbene, and carbethoxymethylene from secondary photolysis of the intermediate EDA, is analogous to the DMDA + cyclohexene system as shown by the variation in product yields. Thus the photolysis of DMDA in *trans*-butene-2 (cf. Table XVII) shows an increase in formation of addition products [14] - [16] and decreased yields of mercury adduct [17] with increased energy of irradiation, which confirms the increased importance of the primary steps (23a) and (23b) (i.e. carbyne formation) as already established for the DMDA + cyclohexene system. Therefore one must conclude that carbethoxymethyne is the main precursor of the addition products [12] - [16] in the photolysis of DMDA at short wavelength and that any observed stereospecificity and stereoselectivity in the products must be related mainly to this intermediate.

In stereospecific addition reactions of carbenes with *cis*- and *trans*-olefins the geometric relationship of the substituents is retained, and *cis*-1,2-dialkylcyclopropanes and *trans*-1,2-dialkylcyclopropanes respectively are produced. Since carbethoxymethyne reacted with *cis*-butene-2 to yield the *cis*-2,3-dimethylcyclopropane-carboxylates [12] and [13] exclusively, and with *trans*-butene-2 only *trans*-2,3-dimethylcyclopropane-carboxylate [14], this addition reaction is also stereospecific. The observed stereospecificity of

REACTION SCHEME IV

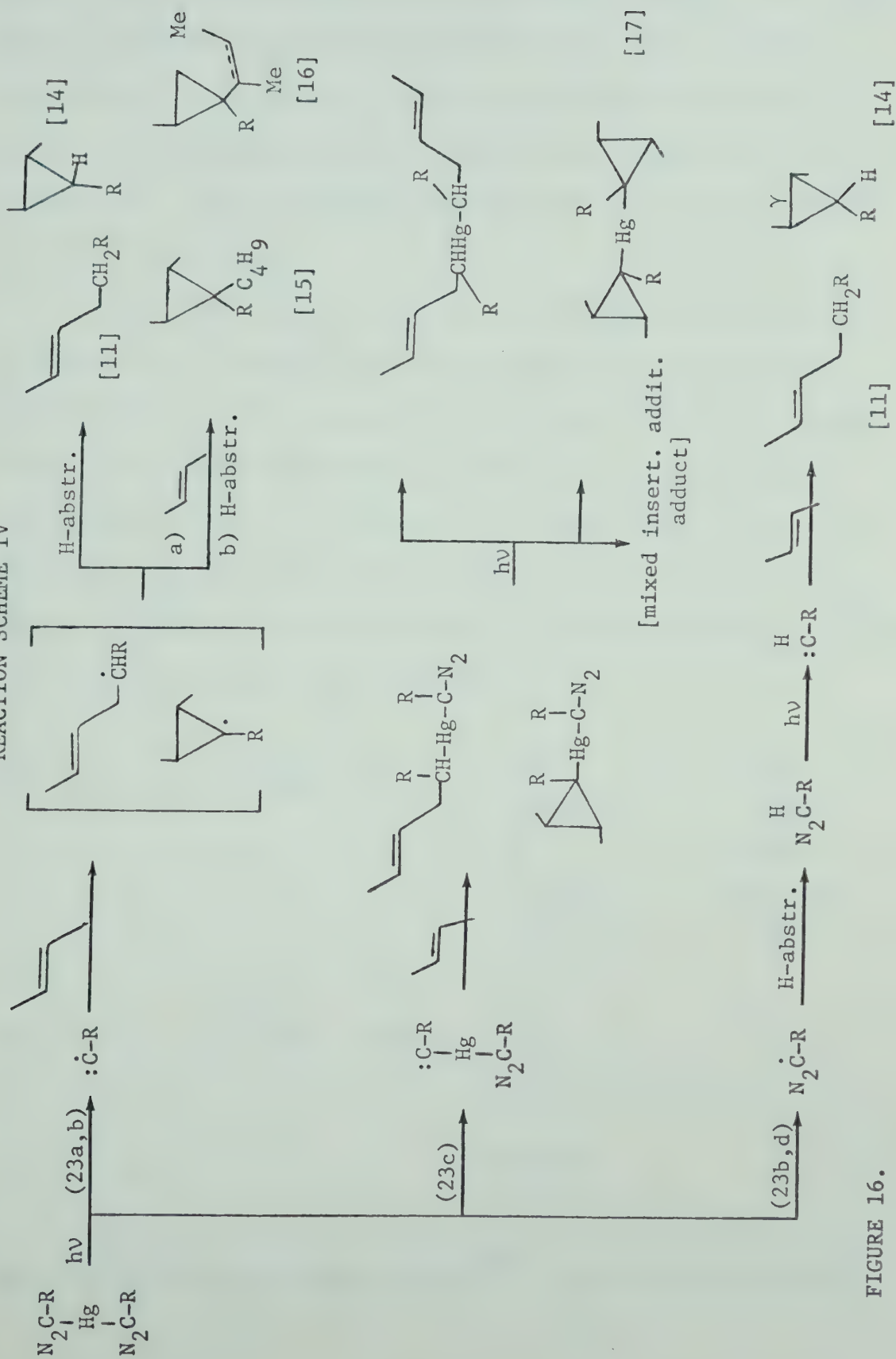
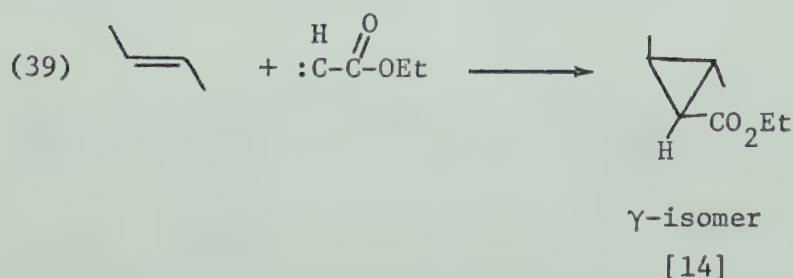
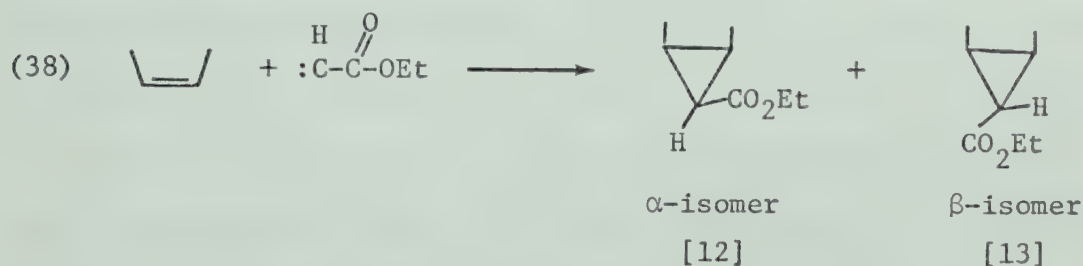


FIGURE 16.

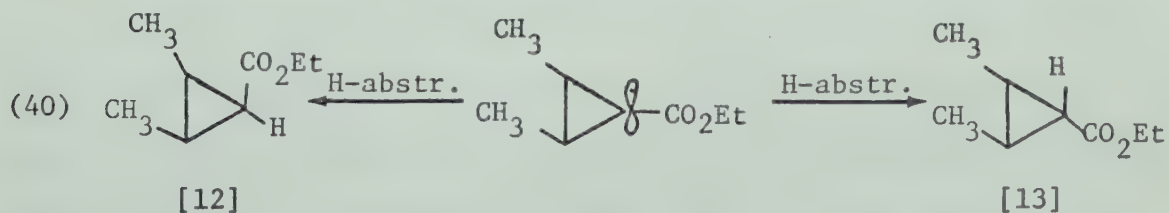
the addition (cf. Table XVI) confirms the involvement of carbethoxymethyne ($\text{:}\dot{\text{C}}\text{-CO}_2\text{Et}$) in its doublet ground state, since a doublet state carbyne is the analog of singlet carbene which has been shown to add stereospecifically to double bonds. Quartet state carbyne, like triplet carbene, would be expected to yield a mixture of *cis*- and *trans*-isomers.

The "stereoselectivity" of the carbethoxymethyne can now be compared with the addition of monosubstituted or unsymmetrical carbenes which, on the assumption of stereospecific addition to *cis*-butene-2, give two stereoisomers, α and β , while in the case of *trans*-butene-2 only the γ -isomer is obtained, provided the mode of addition is *cis* as shown by Doering and Mole⁸⁵ for carbomethoxy carbene ($\text{:}\overset{\text{H}}{\underset{\text{O}}{\parallel}}\text{C-C-OMe}$). This also holds for carbethoxycarbene ($\text{:}\overset{\text{H}}{\underset{\text{O}}{\parallel}}\text{C-C-OEt}$) as pointed out by Skell and Woodworth⁶⁰,




and reflected in the synthesis of [14]⁸⁶. The results obtained in

this study for the photolysis of DMDA and EDA in butene-2, i.e. for carbethoxycarbyne and carbethoxycarbene confirm these expectations. There is, however, a noteworthy difference in the [12]/[13] product ratio (α -isomer/ β -isomer) for the addition reactions with *cis*-butene-2 which is 0.25 for carbethoxycarbene (0.4 for carbomethoxycarbene⁸⁵) and 0.69 for carboethoxycarbyne (cf. Table XVII). In the case of *cis*-addition of the unsymmetrical carbene a second stereochemical choice is available, which leads to endo and exo conformations. They correspond to α - and β -isomers in the addition of carbethoxycarbene to *cis*-butene-2, which is believed to be sterically controlled leading to the predominance of the more stable β -isomer [13], the exo-conformation⁵⁹. The observed increase in the α -isomer, [12], in the photolysis of DMDA in *cis*-butene-2 lends support to the intermediacy of the cyclopropyl radical, $\triangle-R$, arising from addition of carboethoxymethyne to the olefin as outlined in reaction scheme III (cf. Figure 15). The increase in the less stable endo- or α -isomer, [12], can be rationalized by a preferential attack on the more exposed side of the radical intermediate in accordance with the proposed addition-abstraction sequence:



Parenthetically this observation parallels the mechanism proposed for the cyclohexene system, but the stereochemical route here is not as

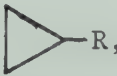
well defined, due to steric factors.

Further evidence for the intervention of the cyclopropyl radical, R, is the occurrence of products [15] and [16] arising from the addition of another solvent molecule to the initially formed radical and subsequent hydrogen abstraction or disproportionation. Analogous reactions have also been proposed in the cyclohexene solvent system.

4.3 Summary

The products formed in the photolysis of DMDA in *cis*- and *trans*-butene and the wavelength dependence of their yields are in good agreement with the results of the DMDA + cyclohexene system and therefore can be rationalized by postulating the same primary processes (23a-d). Two of the primary processes, (23a) and (23b), lead to the formation of ethyl carbethoxymethyne and increase in importance with increasing photon energy.

The observed stereospecificity of the addition reactions of carbethoxymethyne with butene-2 confirm the involvement of the carbyne in its doublet ground state.


The stereoselectivity of the carbethoxymethyne addition to *cis*-butene-2 is reflected in increased yields of the less stable endo- or α -isomer [12] which, together with the occurrence of products [15] and [16], give additional evidence for the intermediacy of the cyclopropyl radical, R, and hence conclusively prove the intervention of ethyl carbethoxymethyne in the photolysis of DMDA.

CHAPTER 5

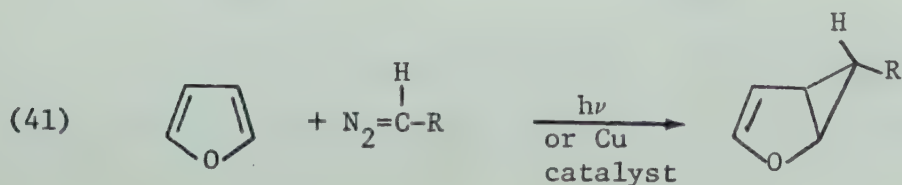
PHOTOLYSIS OF MERCURYBISDIAZOACETATE

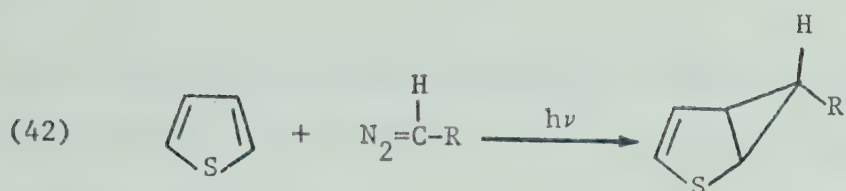
IN PYRROLE

5.1 Solvent Properties and Carbene Reactions of Pyrrole

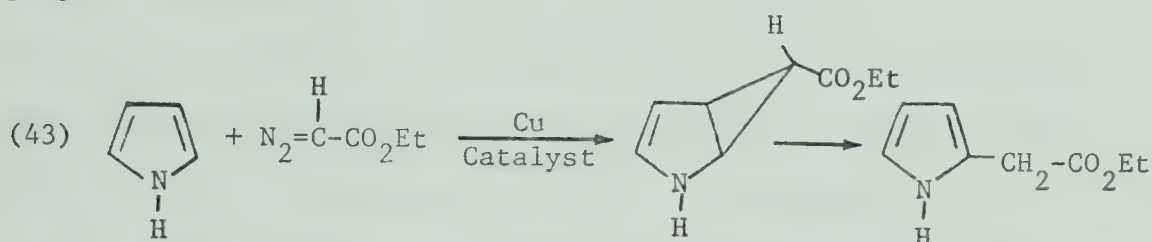
Cyclohexene and *cis*- and *trans*-butene-2 gave a number of characteristic products when used as media for the photolysis of DMDA, but were rather poor solvents for DMDA allowing only small concentrations to be used for the reaction. Pyrrole, , was found to be a good solvent for DMDA and reasonably transparent in the required low wavelength region. The first absorption band is reported to be $\lambda_{\text{max}}^{\circ}$, 2110Å (ϵ 15,000) with an onset at 2200Å⁸⁷. A weak band at $\lambda_{\text{max}}^{\circ}$ 2400Å (ϵ 300) is attributed to impurities⁸⁸. Such undefined impurities and the tendency of pyrrole towards autoxidation, in particular photosensitized autoxidation, have probably been the main reasons militating against its use as solvent in photolytically produced carbene reactions. However, a few catalyst-initiated carbene reactions and accompanying molecular rearrangements are known.

The aromatic heterocyclic compounds furan and thiophen, yield cyclopropanes⁸⁹, upon reaction with carbenes:

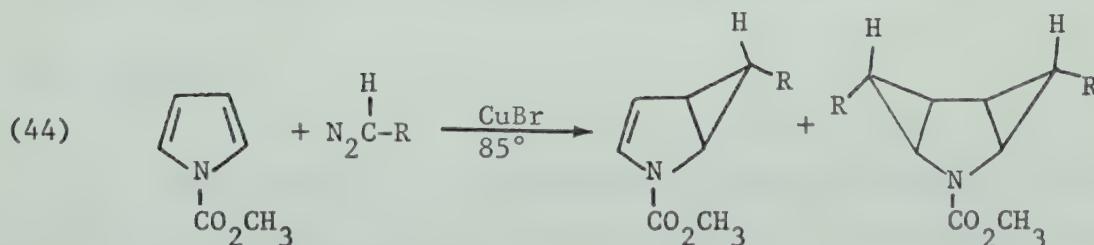




however, catalyzed decomposition of diazo compounds in the presence of pyrrole, and its N-methyl derivatives, produces only substitution products. Piccinini⁹⁰ and later Nenitzescu⁹¹ have shown, for example, that the copper-catalyzed decomposition of EDA in pyrrole leads only to ethyl α -pyrrolylacetate, perhaps by way of an initially formed cyclopropane intermediate:

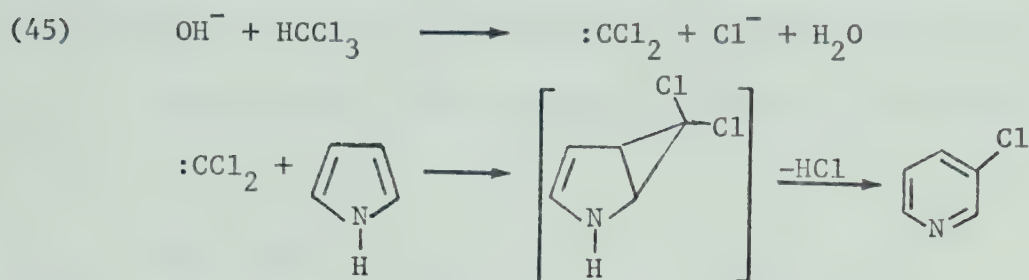


Only pyrroles with a strong electron-withdrawing substituent on the nitrogen atom which gives it diene-like properties at the expense of its aromatic character, were found to give stable addition products. Thus Fowler^{92,93} has recently prepared 2,3-homopyrroles and smaller amounts of the bishomopyrroles by the CuBr-catalyzed decomposition of EDA (also CH_2N_2) in the presence of N-methoxycarbonyl pyrrole:



In addition to insertion and addition reactions of carbenes with pyrrole, a small, though significant mode of reaction involves

ring expansion to yield pyridines⁹⁴. Thus the reaction of haloform and base producing dichlorocarbene when carried out in pyrrole, leads to 3-chloropyridine:



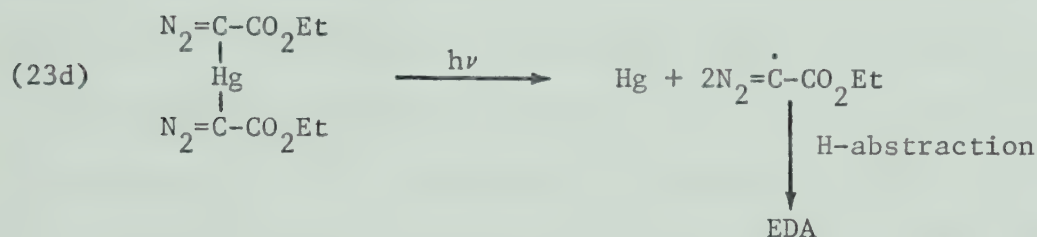
Thermolysis of CHCl_3 leads to improved yields of 3-chloropyridine and also small amounts of 2-chloropyridine^{95,96} which may result from attack at the pyrrole nitrogen or at the carbon.

The reactions of pyrrole with carbenes are not fully understood but can serve as reference systems for the reactions with carbynes. In the addition of carbyne to pyrrole one can envision a 2,3-homopyrrole radical intermediate which does not need to eliminate a group or an ion in order to undergo rearrangement leading to ring expansion, and for this reason it was decided to examine the photolytic decomposition of DMDA in pyrrole.

5.2 Results

The photolytic decomposition of DMDA in freshly distilled pyrrole was accompanied by evolution of nitrogen and precipitation of metallic mercury, as observed earlier in the cyclohexene and butene solvent systems. Completion of the reaction was indicated by the

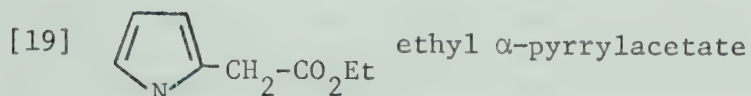
disappearance of the mercury-diazo band (2075 cm^{-1}) in the i.r. spectrum, and also, quantitative recovery of nitrogen (cf. Experimental, section 2.5) resulting from the decomposition of DMDA. When the extent of photolysis was monitored by i.r. analysis, the intermediacy of EDA, which appeared as a separate diazo band (2110 cm^{-1}), became evident. EDA formation arises from the primary step,



and the extent of its intermediacy during the photolysis is assumed to increase with increasing wavelength of the irradiation source, as already established for the cyclohexene solvent system.

The bleaching of the bright yellow colored solution of DMDA during the photolysis was not as apparent in pyrrole as in the cyclohexene and butene solvents, because of the formation of a dark brown polymeric resin which in part precipitated on the wall of the immersion well or, when smaller quartz tubes were used, on the wall adjacent to the irradiation source.

After removal of the metallic mercury, which was in all cases recovered quantitatively within experimental error, pyrrole was removed by flash evaporation at $75^\circ\text{C}/\sim 20\text{ mm Hg}$. Bulb-to-bulb distillation yielded a fraction distilling at $50\text{--}75^\circ\text{C}/\sim 0.1\text{ mm Hg}$, consisting of some pyrrole and the following major reaction products:



Samples of [18] and [19] were isolated by preparative g.c. for spectral analysis and identified by comparison with authentic samples.

Compound [18] was available from Eastman Kodak Co., while [19] was prepared by the Cu-catalyzed decomposition of EDA in pyrrole according to Nenitzescu⁹¹. The predominant i.r. absorption bands as well as the n.m.r. spectra for [18] and [19] are reported in Table XVIII.

TABLE XVIII

I.R. and N.M.R. Spectra for [18] and [19]

Compound No.	Spectra
[18]	i.r. $\nu_{\max}^{\text{CCl}_4}$ (cm^{-1}) 1725(s); 1590(w); 1285(s); 1120(s); 1035(w)
	n.m.r. τ (CCl_4) 8.61 (t, 7H, 3H); 5.62 (q, 7H, 2H); 2.7 (m, 1H); 1.78 (m, 1H); 1.0 (m, 1H); 0.86 (s, 1H).
[19]	i.r. $\nu_{\max}^{\text{CCl}_4}$ (cm^{-1}) 3461(w); 2960(w); 1750(s); 1248(s); 860(w);
	n.m.r. τ (CCl_4) 8.70 (t, 3H); 6.42(s, 2H); 5.87(q, 2H); 4.0 - 4.2 (complex, 2H); 3.48 (m, 1H).

The use of an analytical g.c. column in conjunction with a flame ionization detector made it possible to resolve three further peaks which, however, were too small (0.1% of [18]) for collection and proper structure assignment, but sufficient for combined g.c. - m.s. analysis. The results show one compound [20] with a parent peak of m/e 151 and a fragmentation pattern similar to [18] and two further compounds, [21] and [22], with parent peaks of m/3 153. Table XIX lists the ten most intense mass peaks (m/e) including parent peak (P) and retention times (t_R) for compounds [18] to [22].

The dark brown involatile gummy residue of the photolysis reaction had a molecular weight of 1435 (osmometric determination in acetone) indicating polymerized material which incorporated some pyrrole-nitrogen according to elemental analysis (C:56.8%; H:6.4%; N:8.3%) and also some ester function as evidenced by the strong carbonyl band at 1725 cm^{-1} .

The effect of wavelength of irradiation on the yields of products [18] and [19] using three different cut-off filters are summarized in Table XX. The absolute yields show a near consistent value of 42 - 44% for [18] but an increase in [19] from 4 to 11% with increasing wavelength. For comparison, Table XX includes results of the photolysis of EDA in pyrrole which had not been reported to date. Besides the expected insertion product [19] small yields of the ring expansion product [18] were found which were not detected in the Cu-catalyzed decomposition of EDA⁹¹. The reported value of 8% for [18] includes however, substantial amounts

TABLE XIX

Combined Gas Chromatographical and Mass Spectral Analysis for Products [18] - [22]

Compound No.	t _R (minutes)	m/e (P)	(m/e and % of base peak)											
[18]	31.0 ^a	151 (35)	151 (35)	123 (50)	107 (10)	106 (100)	105 (12)	79 (15)	78 (55)	51 (27)	50 (10)	29 (6)		
[19]	14.5 ^b	153 (18)	153 (18)	81 (7)	80 (100)	53 (16)	52 (7)	32 (12)	29 (10)	28 (55)	27 (11)	18 (5)		
[20]	28.5 ^a	151 (50)	151 (50)	123 (64)	106 (100)	107 (9)	79 (18)	78 (60)	51 (40)	50 (14)	45 (9)	29 (16)		
[21]	29.2 ^a	153 (15)	111 (100)	109 (26)	96 (18)	82 (22)	80 (60)	68 (28)	53 (22)	42 (80)	39 (20)	28 (20)		
[22]	29.8 ^a	153 (40)	153 (40)	109 (8)	81 (17)	80 (100)	67 (8)	53 (16)	31 (12)	29 (9)	28 (8)	27 (9)		

^a Column: 15 ft x 1/8 inch packed with 15% Carbowax 20M on Chromosorb W, 30-60 mesh.
Program: from 140°C - 200°C at 2° per minute, flow rate 60 cc per minute.

^b Column: 3 ft x 1/4 inch packed with 20% Carbowax 20M on Chromosorb W, 30-60 mesh.
Program: 170°C, flowrate 60 cc per minute.

TABLE XX

Per cent Yield of [18] and [19] from the Photolysis of
DMDA and EDA in Pyrrole

Precursor	Filter (λ)	Yield Per cent (Theoretical) ^a	
		[18]	[19]
DMDA	Vycor ($>2100\overset{\circ}{\text{\AA}}$)	44	4
DMDA	Pyrex ($>2800\overset{\circ}{\text{\AA}}$)	42	10
DMDA	Uranium ($>3200\overset{\circ}{\text{\AA}}$)	44	11
EDA	Vycor ($>2100\overset{\circ}{\text{\AA}}$)	8 ^b	18

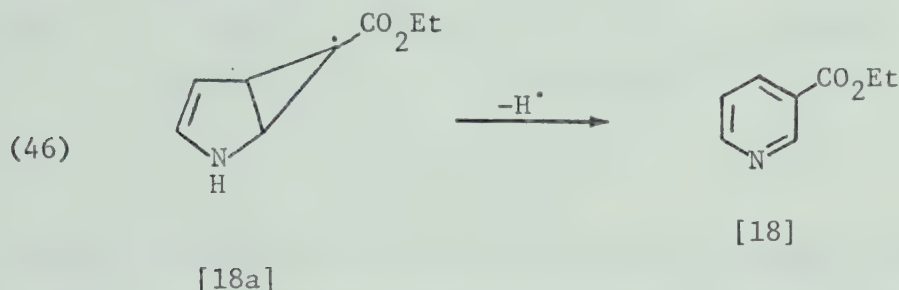
^a The reported values represent averages from several photolysis experiments (cf. Appendix D).

^b Including product [23].

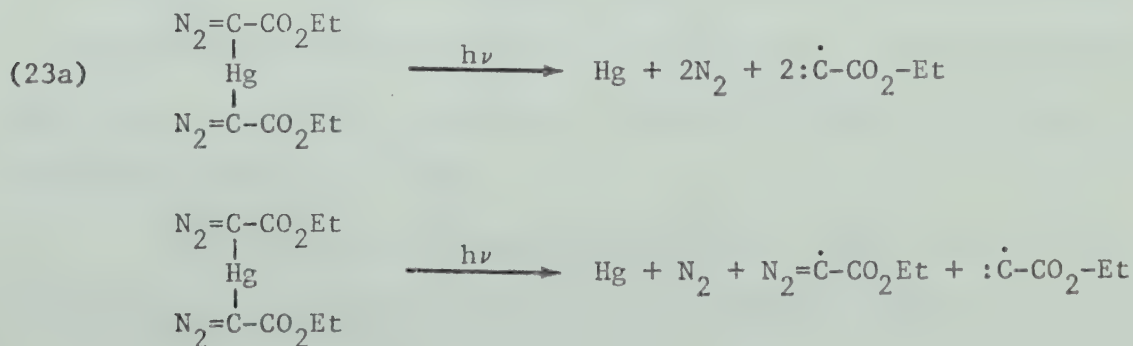
of an uncharacterized solid product, [23], (m.p. 79-80°C) which, like [18], could be obtained by crystallization from the fraction isolated by preparative g.c.

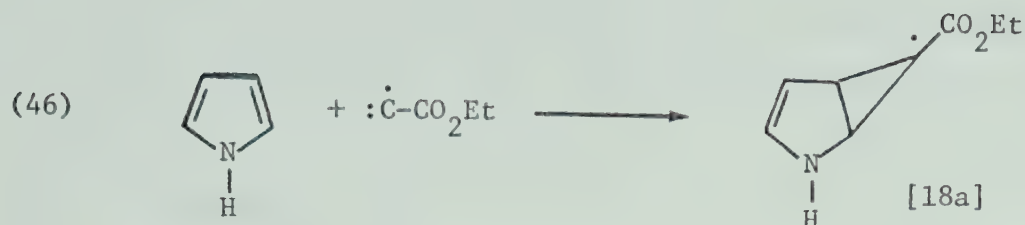
5.3 Discussion

The predominant product of the photolysis of DMDA in pyrrole is ethyl pyridine-3-carboxylate [18] which must arise from facile ring expansion of a cyclopropyl radical intermediate, [18a], to form the more stable pyridine ring system:

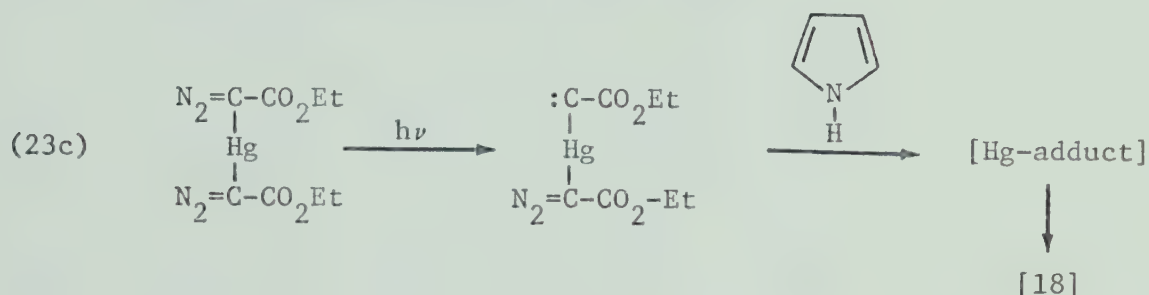


The major route of formation of the cyclopropyl intermediate [18a] is most probably via carbethoxymethyne, $:\dot{\text{C}}\text{-C-OEt}$ formed in the photolytic decomposition of DMDA via the primary steps (23a) and (23b) (cf. Section 3) and subsequent addition of this carbyne to pyrrole:





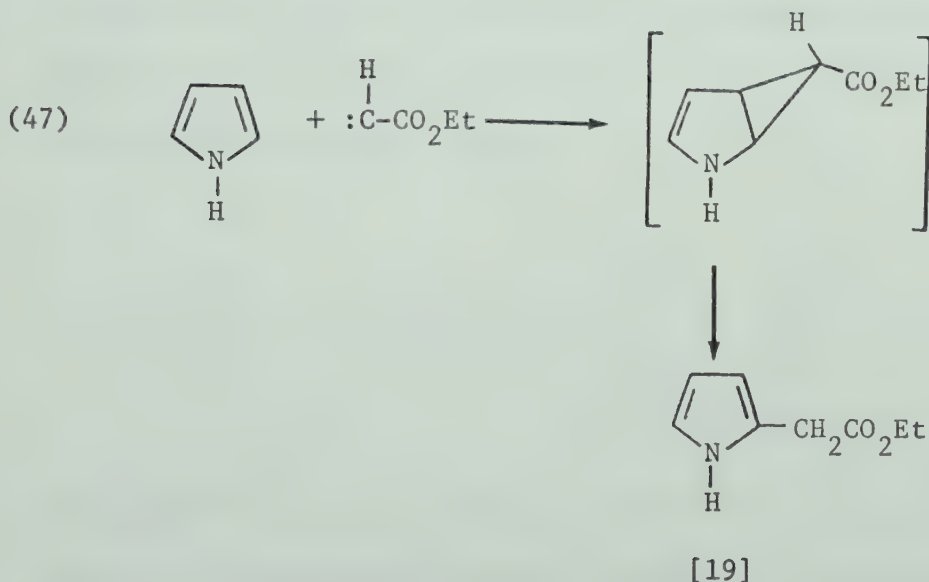
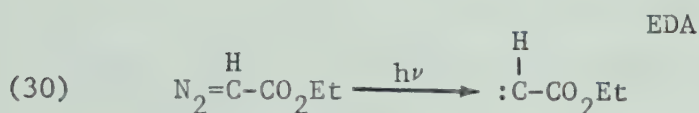
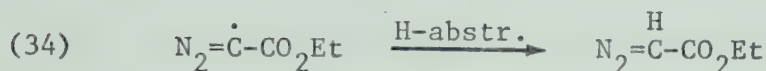
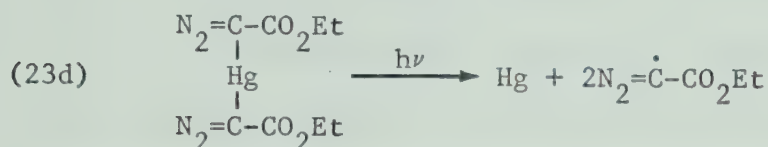
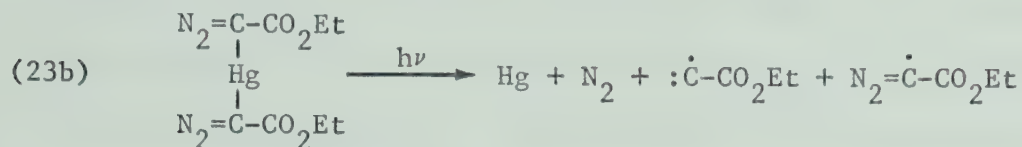
Another possible pathway for the formation of [18a] could be the decomposition of an intermediate mercury adduct arising from the reaction of pyrrole with mercury-carbene formed via primary step (23c) in the following sequence:



The intervention of mercury-carbene as the primary mode of formation of [18] is only possible if the resulting mercury adducts are sufficiently unstable to produce [18a] efficiently. However, all mercury from the starting material, DMDA, was recovered and no mercury adduct could be detected. Furthermore, yields of [18] were independent of the wavelength of the irradiation source, while it was established for the cyclohexene and butene solvent systems that an increase in wavelength resulted in an increase of mercury-adducts via primary step (23c). Therefore, carbethoxymethyne is the only reasonable precursor to [18].

The formation of the insertion product [19] results from the reaction of pyrrole with carbethoxymethylene, $\text{:CH-CO}_2\text{Et}$, which

has been shown to arise in the photolytic decomposition of DMDA via primary steps (23b) and (23d), subsequent hydrogen abstraction and photolysis:

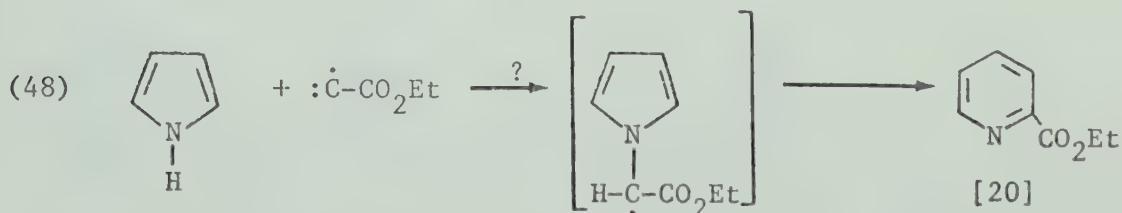


The increased yields of [19] with increasing wavelength of the irradiation source are in agreement with the increasing importance

of EDA with increase wavelength, shown for the cyclohexene system (cf. Section 3.3).

The possible major pathways for the formation of products [18] and [19] are summarized in Reaction Scheme V (cf. Figure 17). The photolysis of EDA in pyrrole yields some [18] and therefore a limited amount of [18] in the photolysis of DMDA may be obtained via an alternative route involving the intermediacy of EDA.

Compounds [20] to [22] were found only in trace quantities and lacking sufficient analytical data, the following structure assignments and mechanism must be considered tentative. Compound [20] has a molecular weight (m/e 151) and a fragmentation pattern in the m.s. analysis similar to [18] and therefore is probably an isomer of [18]. The pyridine-2-carboxylate arising from the reaction of carbethoxymethyne with either pyrrole-nitrogen or the α -carbon of the pyrrole is the favoured isomer, because addition across the 3-4 position of pyrrole followed by ring expansion has not yet been observed and reactions of halocarbenes with pyrrole yield only 2- and 3-substituted pyridine isomers:



Compounds [21] and [22] both have molecular weights of 153, and could be dihydropyridine isomers formed via ring expansion of [18a] and subsequent hydrogen abstraction:

REACTION SCHEME V

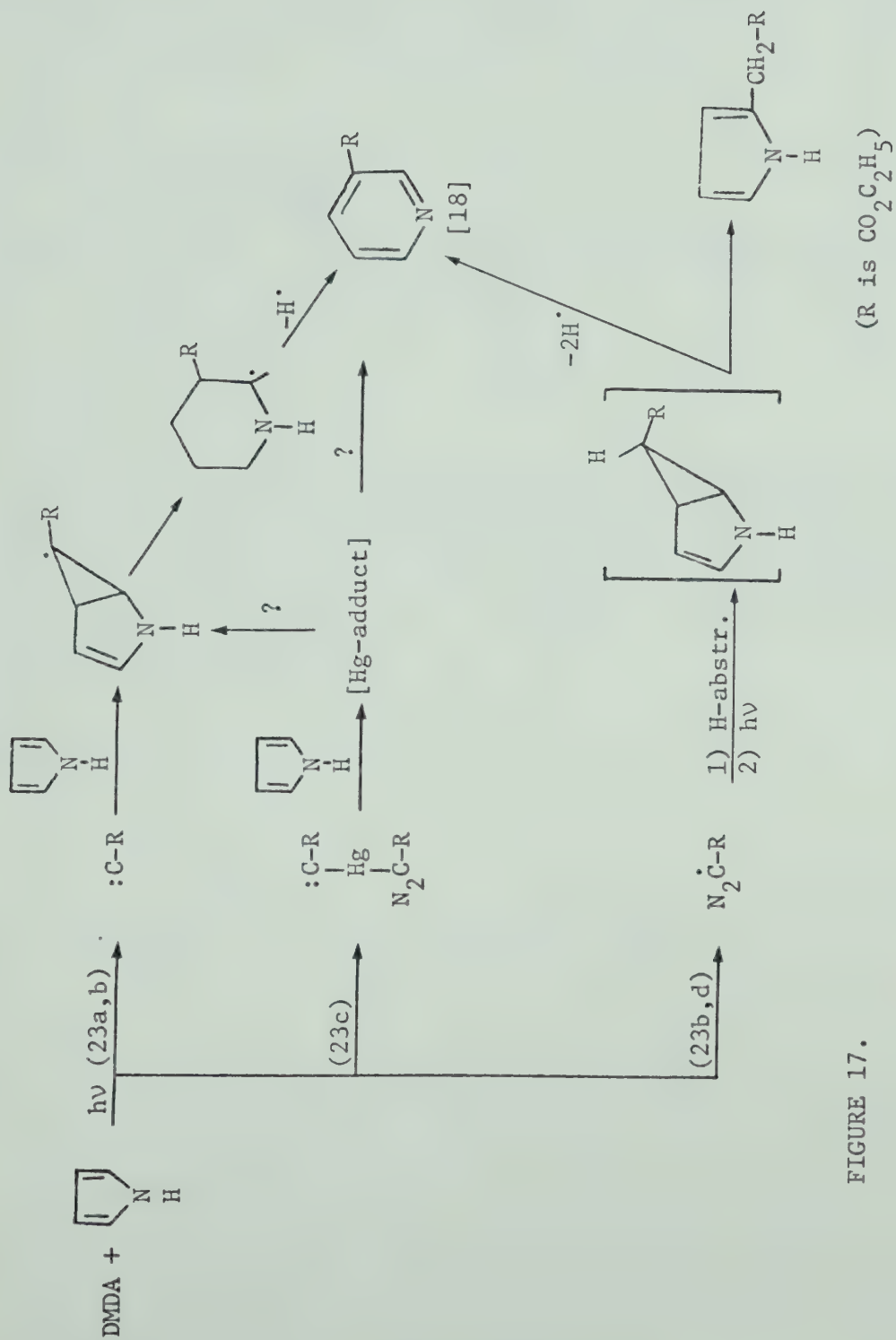
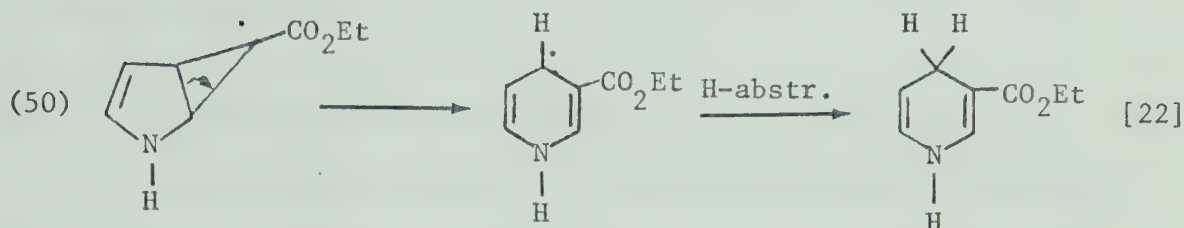
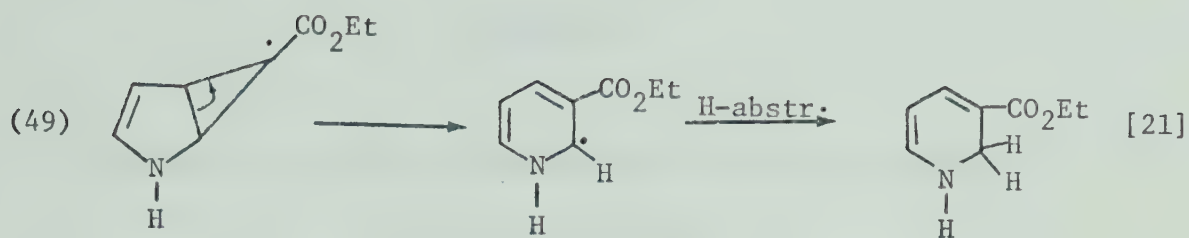


FIGURE 17.



Fowler found similar dihydropyridines to be remarkably stable⁹⁷. The intervention of aziridines and other bicyclo ring systems can be excluded on the basis of n.m.r. spectra of samples containing compounds [20] to [22].

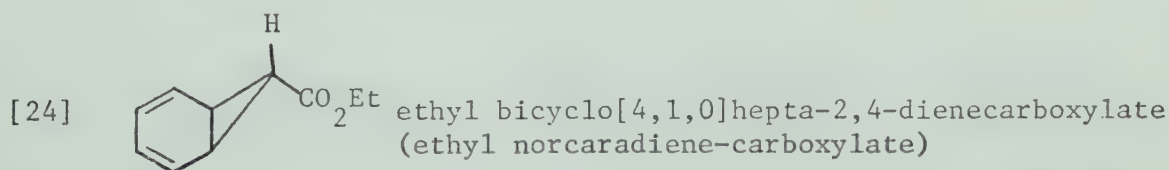
CHAPTER 6

REACTIONS OF CARBETHOXYMETHYLENE AND CARBETHOXYMETHYNE
WITH AROMATIC SOLVENTS

6.1 Carbene Reactions

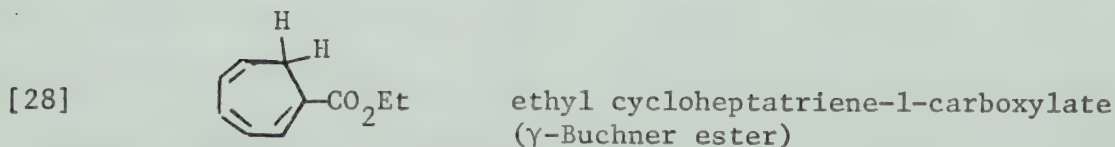
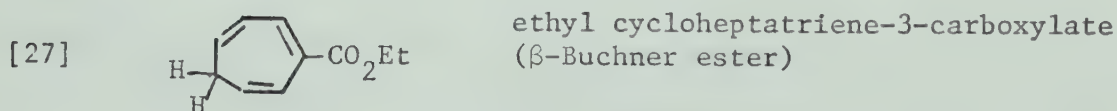
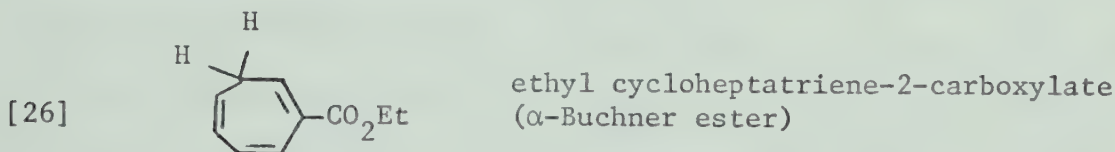
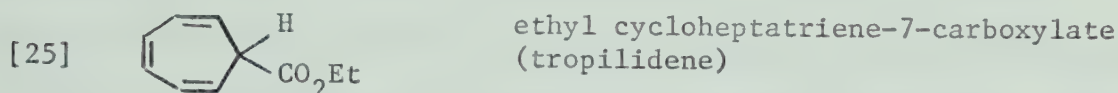
6.1.1 Photolysis of EDA in Benzene

In extending the study of carbethoxymethyne to the aromatic solvents, benzene and hexafluorobenzene, it appeared necessary to review and re-examine the corresponding carbethoxymethylene reactions with these solvents. The decomposition of EDA in benzene is one of the oldest carbene reactions known. The long series of publications started as early as 1885 with the report of the thermal decomposition of EDA in benzene by Büchner and Curtius⁹⁸ who obtained a mixture of esters ("Büchner esters") which appeared to contain as the major product a norcaradiene derivative:



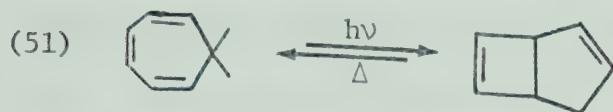
Pyrolysis of EDA in the presence of benzene (130° - 135°C) yields product mixtures which contain at most 20 - 30% of the primary product. Although glass lined autoclaves were used, the omnipresent formation of diethylmaleate and diethylfumarate, which is a competing process in the catalyzed decomposition of EDA, can not be eliminated^{99,100}.

In the photolytic decomposition of EDA in benzene Schenck et al.¹⁰¹⁻¹⁰³ also isolated the same "ethyl norcaradiene-carboxylate" then believed to be the primary product resulting from the addition of carbethoxymethylene to benzene. Investigations of the system were, however, greatly impeded by facile thermal and photolytic isomerization of the primary product in the work-up procedure and the belief in the existence of a norcaradiene type primary product was not abandoned until the advent of n.m.r. Doering¹⁰⁴ repeated Buchner's experiments and found that there are only four "Buchner esters" which are the four positionally isomeric cycloheptatriene esters:



Thus the norcaradiene structure for any of the "Buchner esters" was eliminated, solving for this system what Maier¹⁰⁵, in a review and discussion of relationships between norcaradiene and

cycloheptatriene ring systems, termed the "norcaradiene problem". In 1961 Dauben and Cargill¹⁰⁶ reported photoisomerization of cycloheptatriene to bicyclo[4,2,0]heptadiene,

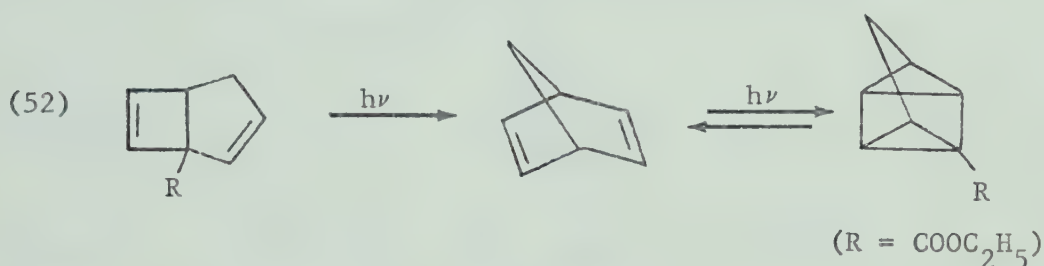


which further complicated the photolysis of EDA in benzene.

When the photolysis of EDA (1%) in benzene was re-examined in this laboratory using Pyrex filtered u.v. light the yield of 30% obtained by Schenck et al. could be increased to 43% (theor.) and the primary product [25] was obtained with at least 90% purity. However, continued irradiation of this product at shorter wavelength resulted in photoisomerisation yielding at least nine isomers which were removed from the reaction mixture by distillation at 50°C/0.1 mm Hg. They were separated by a 4' x 1/4" g.c. column packed with 10% FFAP on Chromosorb W and operated at 100°C and a flow rate of 60 cc/min. Combined g.c.-m.s. analysis gave, for all isomers, the same parent peak (m/e 164) and the same base peak (m/e 91, tropylium ion) and very similar fragmentation pattern i.e. m/e 135 (P-C₂H₅); m/e 119 (P-O-C₂H₅); m/e 65 (). Identical observations were made when deuterated benzene was used as the solvent in the photolysis of EDA, as shown by the molecular and fragment masses of the nine deuterated isomers, i.e. m/e 170 (parent); m/e 97 (base peak; m/e 141 (P-C₂H₅); m/e 125 (P-O-C₂H₅); m/e 69 (D₄H).

The products [25] - [28] were easily identified by their

n.m.r. spectra which are in good agreement with the data reported by Linstrumelle in 1970^{107,108}. When the publications by Linstrumelle appeared the characterization of the remaining isomers was discontinued in this laboratory. Linstrumelle examined the various photolytic and thermal isomerizations of the nine products and suggested that three additional isomers could be involved (cf. Reaction Scheme VI, as advanced by Linstrumelle). Although the proposed bicyclic and tetracyclic structures [30] - [36] are not yet adequately documented supporting evidence for the product assignments can be found in the photochemically induced rearrangements of bicyclodiene systems reported by Gorman and Sheridan¹⁰⁹.



An additional product of major importance in the heavy and viscous residue was the mixture of isomers of carbethoxymethylene tetramer. During liquid (column) chromatography, mixtures with different ratios of tetramer isomers were obtained which gave an osmometric molecular weight determination of 334 (calculated 334 for C₁₆H₂₄O₈) and an elemental analysis of 56.01%C, 7.26%H and 0.0%N (calculated 55.78%C, 7.02%H, and 0.0%N). The mass spectrum consisted of the following major peaks, m/e (%): 196 (9), 168 (9), 128 (42), 103 (12), 99 (20), 98 (10), 87 (40), 75 (20), 71 (13), 69 (100). The parent peak, measured by high resolution techniques, is 344.1470,

REACTION SCHEME VI

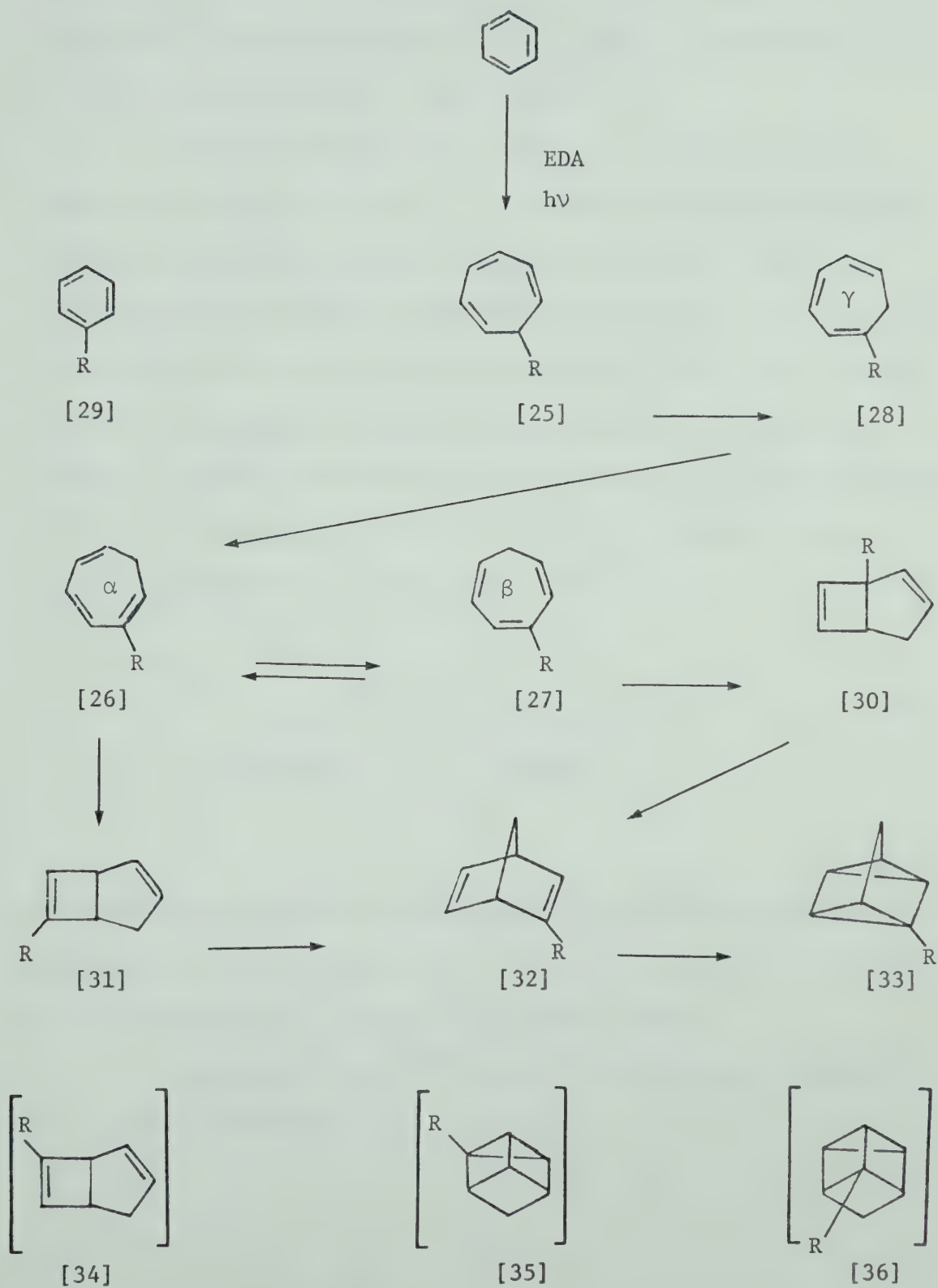
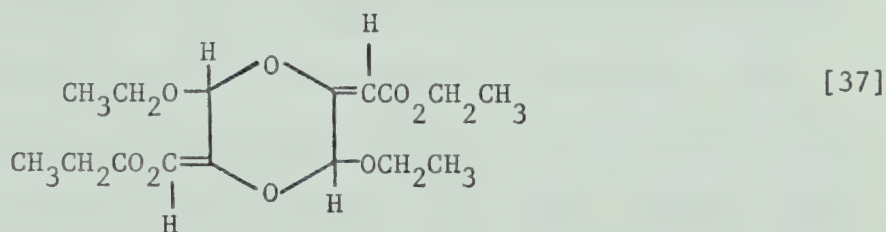


FIGURE 18.

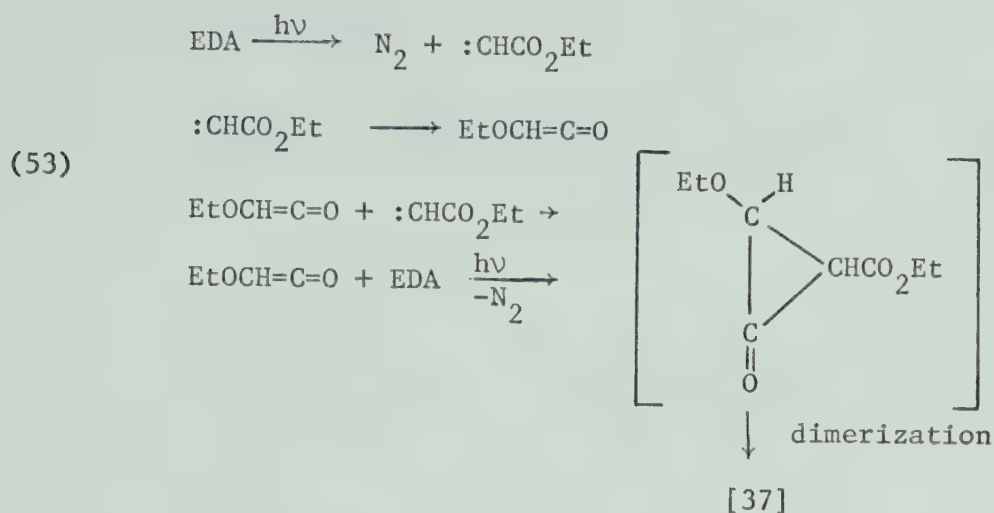
which is in good agreement with the calculated value of 344.1471 for $C_{16}H_{24}O_8$. The i.r. spectrum showed prominent peaks at 1726 and 1711 cm^{-1} (α,β -unsaturated ester), 1660 cm^{-1} ($RO-C=C-CO-$), 1205 cm^{-1} (enol ether) 1125 cm^{-1} (alkyl ether).

The n.m.r. spectra are complex and indicate that the samples are composite mixtures. The methine protons show several different resonance absorption in the region τ 3.3 - 5.0, the methylene protons different quartets in the region τ 5.7 - 6.3, and the methyl protons superimposed triplets at τ 8.9 - 8.5. The main feature of all the different mixtures is the constancy of the methine, methylene and methyl proton ratios, being 1:2:3, respectively. This and the analytical data in general are consistent with the structure postulated by Schenck and Ritter¹¹⁰,



who reported the formation of carbene tetramers (55% theor.) in the photolysis of methyl diazoacetate in benzene and achieved separation of four stereoisomers fitting this general formula.

Schenck and Ritter¹¹⁰ proposed the following mechanism for tetramer formation:



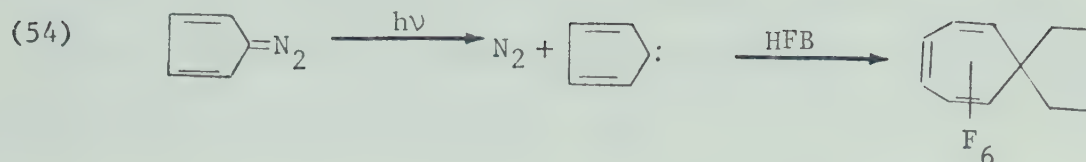
In view of the high reactivity of ethoxyketene¹¹¹ its addition to EDA could possibly occur in the dark, with the simultaneous extrusion of nitrogen.

From this study, combined with published results, it is evident that the photolytic decomposition of EDA in benzene with light of wavelength $\lambda > 2800\text{\AA}$ produces mainly tropilidene, [25], while at shorter wavelength facile isomerization of the primary product [25] occurs to give products [26] - [36]. Finally, about 50% of the produced carbethoxymethylene contributes to the formation of the tetramer [37] in competition with addition to the solvent benzene.

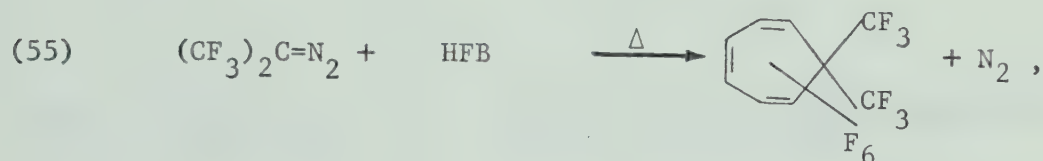
6.1.2 Photolysis of EDA in Hexafluorobenzene (HFB)

It has been shown by Gale¹¹² and independently by Jones¹¹³ in 1968 that divalent carbon radicals add to hexafluorobenzene (HFB). Jones¹¹³ observed that cyclopentadienylidene reacts with HFB

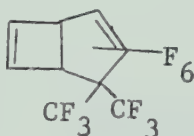
according to the equation



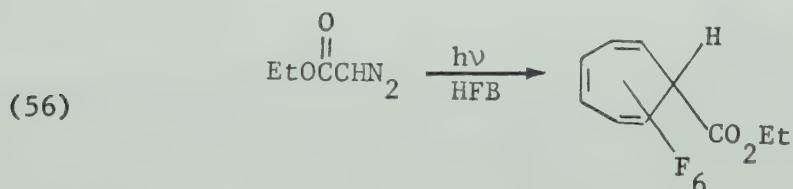
Simultaneously, Gale¹¹² found that the thermolysis of *bis*(trifluoromethyl)diazomethane in HFB gives perfluoro-1,1-dimethyl-2,4,6-cycloheptatriene,



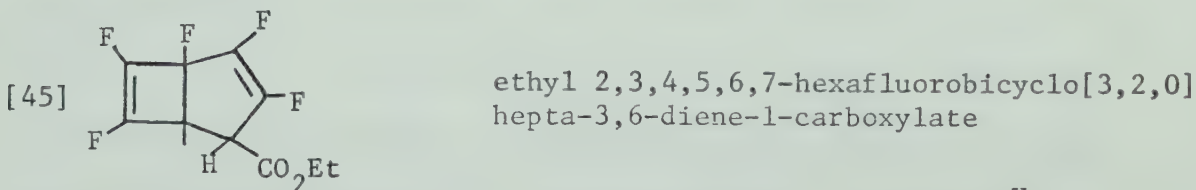
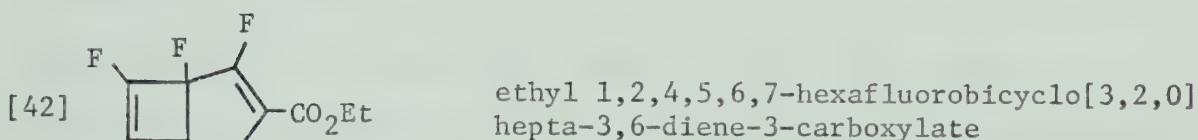
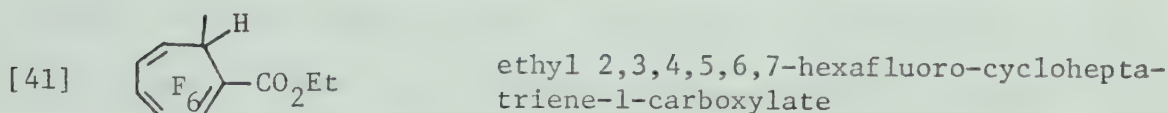
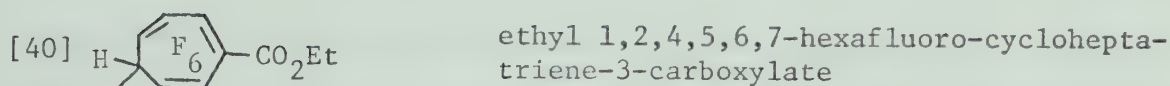
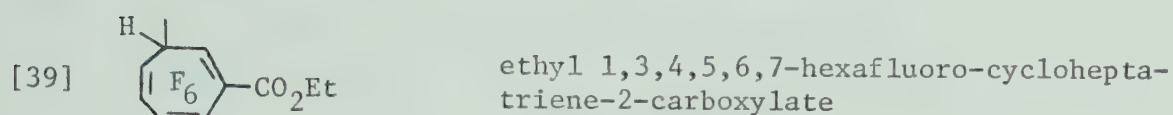
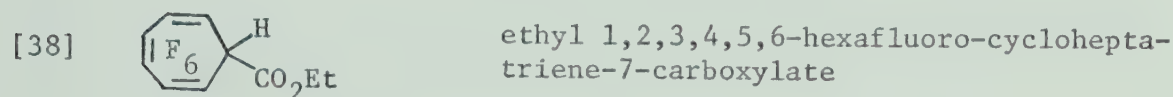
which on photolysis isomerizes to perfluoro-2,2-dimethyl-bicyclo[3,2,0]hepta-3,6-diene,



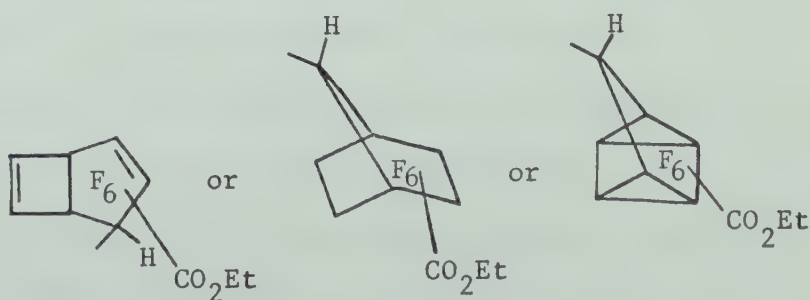
Gale also investigated the photolysis of ethyldiazoacetate (EDA) in HFB and isolated one product, namely ethyl-2,3,4,5,6,7-hexafluoro-2,4,6-cycloheptatriene-carboxylate [38] in 16% (theor.) yield:

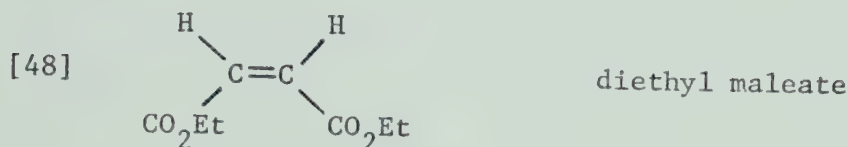
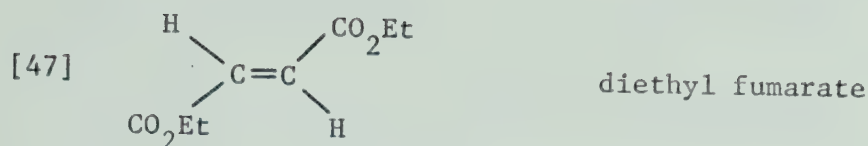


Re-examination of Gale's experiments yielded, in addition to the primary product [38], at least eight isomeric $C_7F_6HCO_2Et$ compounds [39] - [46], diethyl fumarate [47], diethyl maleate [48], and carbethoxymethylene tetramer [37]:



[43], [44], [46]





Distillation of the reaction mixture after removal of HFB at 50°C/100 mm Hg gave a fraction containing products [38] - [48], while the residue, a brown viscous liquid, contained the tetramer [37], which was isolated and characterized as described above (cf. section 6.1.1). The distillate containing the products [38] - [48] was chromatographed using a 15' x 1/8" column packed with 12% XE-60 on Chromosorb W and the isomeric product composition was deduced from g.c. coupled with mass spectrometric analysis. They all show parent ions at m/e 272, peaks at m/e 244 (P-C₂H₄), 227 (P-EtO) and 199 (C₇F₆H), Table XXI. Thus, while it was possible to obtain resolution for g.c. coupled mass spectrometric analyses of the nine isomers, separation by trapping from the effluent could be achieved only for three of the isomers, [38], [42] and [45] owing to thermal instability.

Product [38] was identified by its mass spectrum, Table XXI and n.m.r. spectrum, Table XXII which are in good agreement with

Mass Spectra of $C_7F_6HCO_2Et$ Isomers, Products [38] - [46]

Product	R _t (min)	Relative intensity in % of base peak, m/e 29													
		m/e 31	93	99	130	149	161	168	180	199	200	227	224	272	
[38]	15.6	16.4	6.0	10.4	7.0	7.8	8.0	7.2	14.0	176.0*	24.0	3.6	1.0	4.4	
[39]	13.1	8.6	6.8	12.5	7.0	12.4	9.4	5.6	14.6	47.5	4.2	72.0	5.0	1.8	
[40]	11.7	8.1	2.5	6.1	2.5	2.5	4.7	4.3	19.5	71.0	5.7	0.4	<0.1	1.0	
[41]	9.6	6.0	3.6	13.8	4.5	7.0	3.8	2.0	5.5	25.5	2.4	19.0	0.4	2.2	
[42]	8.8	6.4	2.8	4.6	2.6	2.3	4.0	2.6	46.5	39.0	3.0	4.0	1.0	2.3	
[43]	8.0	7.5	2.5	5.2	2.6	2.9	3.7	3.3	20.5	47.0	5.0	4.6	0.3	0.8	
[44]	6.4	8.5	3.9	6.5	4.8	3.8	7.5	3.8	80.0	77.0	5.5	1.0	2.0	1.5	
[45]	5.4	7.4	4.0	6.7	3.6	3.6	4.6	4.4	22.0	70.5	5.4	6.0	0.8	5.0	
[46]	4.5	3.6	2.0	5.2	2.8	4.1	2.8	0.8	24.0	14.0	2.6	10.0	1.0	0.6	

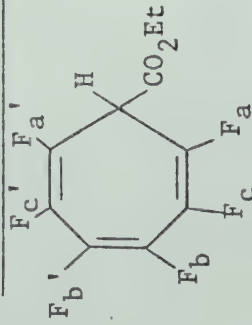
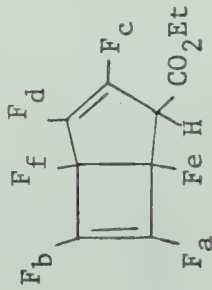
The spectra were obtained on an AEI MS-12 instrument at an ionization voltage of 70 V.

The g.c. column used was an XE-60 on Chromosorb W ($100^\circ C \xrightarrow{1^\circ/\text{min.}} 130^\circ C$).

* Base Peak m/e 199.

TABLE XXII

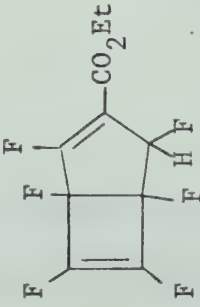
Proton and Fluorine NMR Data

Product	F^{19} in $CFCl_3$		H^1	
	This work	Gale ^a	$CFCl_3/TMS$	CCl_4/TMS^a
<div style="text-align: center;">  <p>[38]</p> <p>I</p> </div>	δ_a 110		τ_3 8.72	8.70
	δ_b 149		τ_4 5.78	5.71
	δ_c 154	155	τ_m 5.75	5.70
<div style="text-align: center;">  <p>[45]</p> <p>VIII</p> </div>	δ_a 120		τ_3 8.70	
	δ_b 126		τ_4 5.75	
	δ_c 136		τ_m 6.12	
	δ_d 156			
	δ_e 165			
	δ_f 175			

$J_{F_e H}$ 21 cps; $J_{F_d H}$ 7 cps; $J_{F_c H}$ 3.5; $J_{F_a H}$ 2 cps

TABLE XXII (cont'd)

Proton and Fluorine NMR Data

Product	F^{19} in $CFCl_3$		H^1	
	This work	Gale ^a	$CFCl_3/TMS$	CCl_4/TMS^a
<div style="text-align: center;">  <p>V</p> </div>	δ			
	119		τ_3 8.63	
	130		τ_4 5.74	
	137		τ_m 6-7	
	155			
	172			
	174			

^a Reference 112.

those reported by Gale¹¹². A cycloheptatriene structure for this product is also supported by the u.v. spectrum depicted in Figure 19, with the onset of absorption at 3600Å and with three distinct maxima at $\lambda_{\text{max}}^{\text{EtOH}}$ 2650Å (ϵ 4422); 2300Å (ϵ 5030), and 2100Å (ϵ 7214). Consistent with this structural assignment is the g.c. retention time. Using an XE-60 on Chromosorb W column which separates primarily according to the number of double bonds in the molecule, the retention time of [38] was the longest among the nine isomers, 15.6 min.

The minor products [39] - [41] with g.c. retention times of 13.1, 11.7 and 9.6 minutes are probably isomeric Buchner acid esters.

Products [42] and [45] have shorter retention times suggesting that they contain fewer number of olefinic bonds. On the basis of their n.m.r. spectra, Table XXII, products [42] and [45] are assigned the bicyclohexadiene structures



respectively.

For [45] the observed chemical shifts of +165 and +175 ppm are in agreement with the predicted value of +175 ppm for the cyclobutenyl fluorines F_e and F_f ¹¹⁴. The four additional observed multiplets centered about 120, 125, 136 and 155 ppm can be assigned to the four vinyl fluorines. Limited information could also be

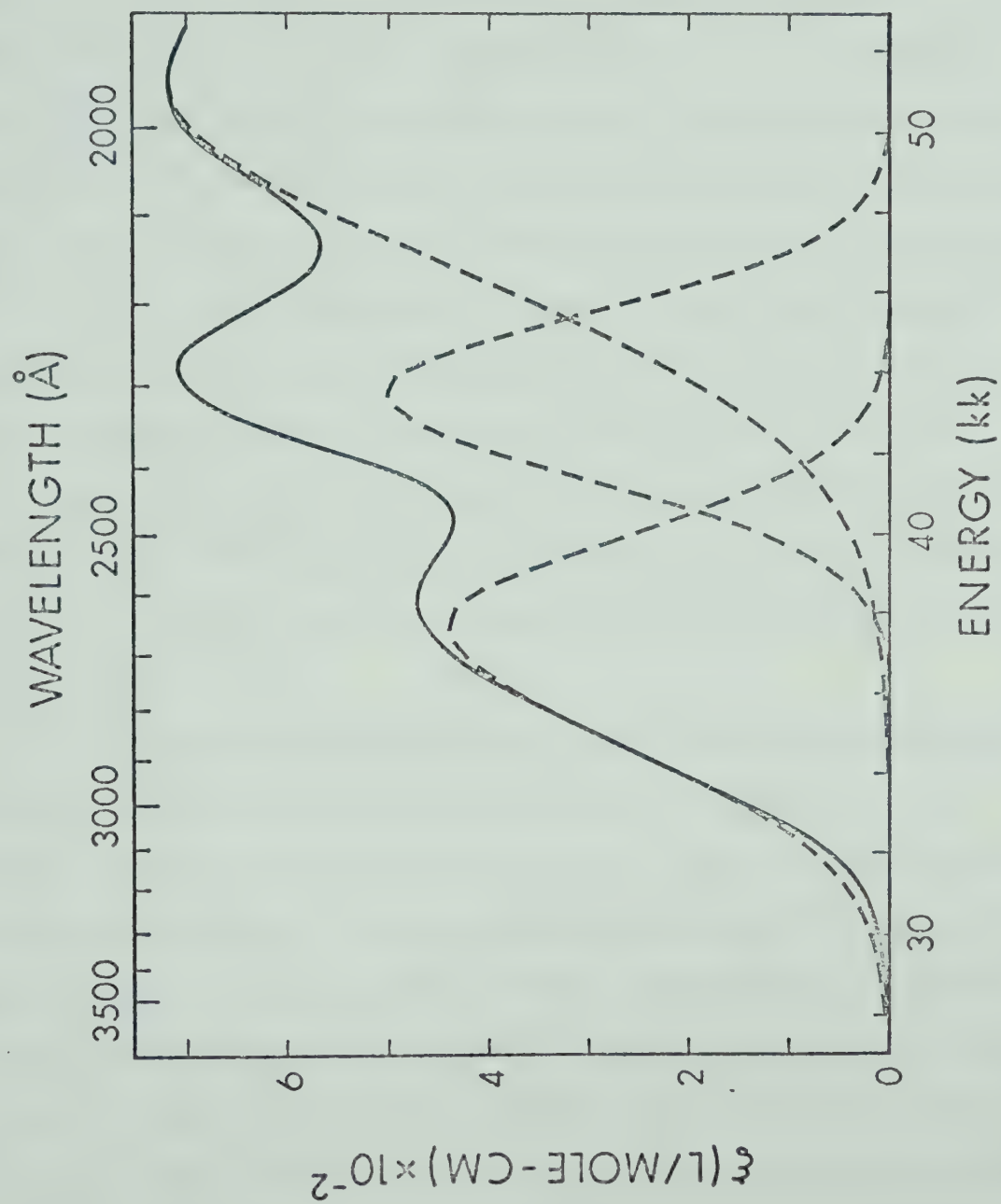


FIGURE 19: U.V. Spectrum of Product [38]

obtained from H^1F^{19} -decoupling experiments. Good decoupling was noted in four cases with $J_{F_eH} = 20$ cps, $J_{F_dH} = 6.5$ cps, $J_{F_cH} = 4$ cps and $J_{F_aH} = 2$ cps. The u.v. spectrum reproduced in Figure 20 features an absorption onset around 2800Å and two distinct maxima at λ_{\max}^{EtOH} 1920Å (ϵ 3972) and 2500Å (ϵ 3377). The simplicity, lower intensity and blue shift of this spectrum as compared to that of [38] are compatible with the proposed bicycloheptadiene structure for [45].

The n.m.r. spectrum of isomer [42] again shows chemical shifts at 172 and 174 ppm which are indicative of the presence of two cyclobutenyl fluorine atoms, and thus of a bicycloheptadiene structure. Four additional multiplets also occur. These are listed in Table XXII. H^1-F^{19} spin-spin decoupling showed only two apparent effects. For more detailed analysis F-F spin-spin decoupling would be required.

Some of the product yields obtained in irradiation using three different cut-off filters are listed in Table XXIII. The results indicate that the primary product is [38] and that secondary photoisomerization of [38] increases with decreasing wavelength of irradiation in a similar fashion as with its unfluorinated analogue, ethyl-cycloheptatriene-carboxylate¹⁰³ which has been studied extensively for several decades. As recently summarized by Linstrumelle¹⁰⁷ not only Buchner acid esters, but also bicyclo and tetracyclo isomeric products have been identified or proposed in the latter reactions.

The secondary photoisomerization of [38] to [42] and [45] has been confirmed by photolyzing pure [38] in a HFB solution under

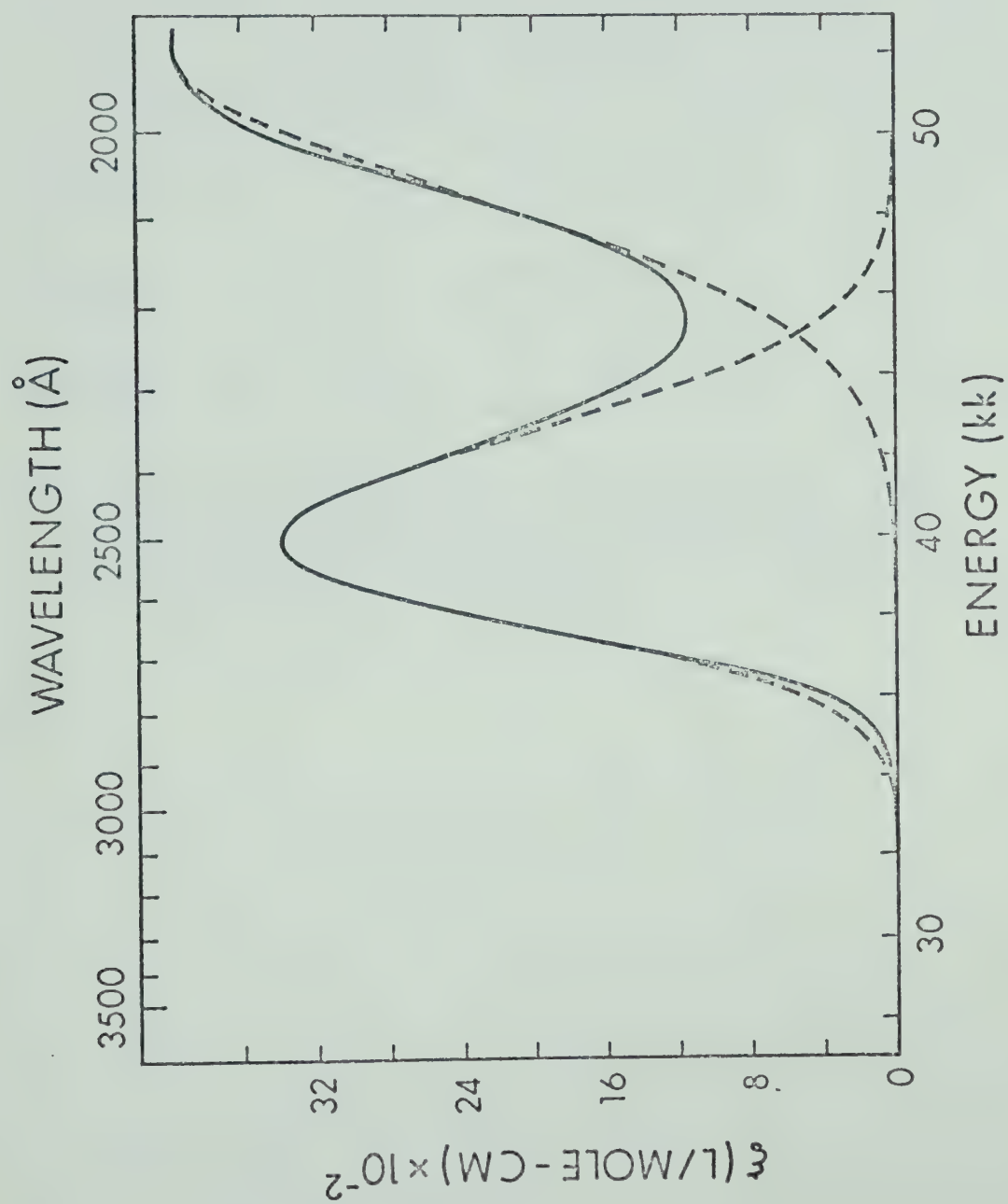


FIGURE 20: U.V. Spectrum of Product [45]

TABLE XXIII

Product Yields from the Photolysis of EDA in HFB*

Filter	Irradiation time (hrs.)	[38]	[42]	[43]	[45]	[47]	[48]
		% Theoretical					
Window glass $\lambda > 3200\text{\AA}$	3	20.0	0.05	2.2	0.7	1.5	1.3
Pyrex. $\lambda > 2800\text{\AA}$	2	5.0	2.8	2.4	12.8	0.6	2.1
Quartz. $\lambda > 2000\text{\AA}$	2	0.8	3.2	2.6	16.4	0.7	2.0

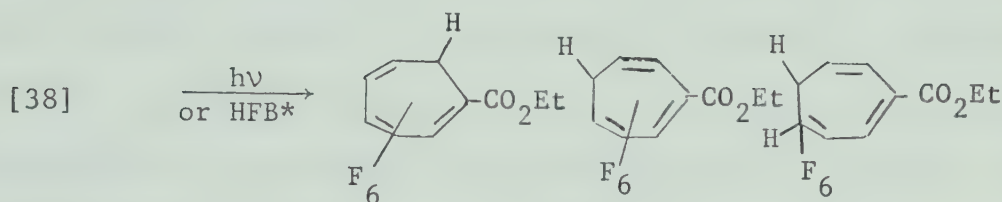
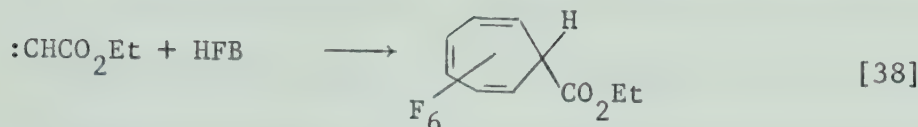
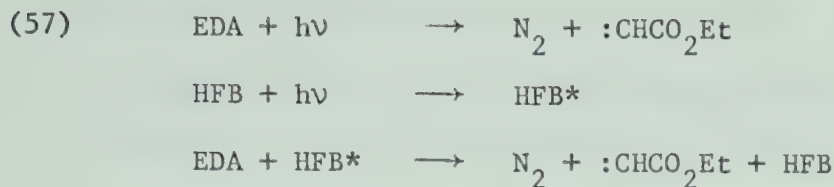
* Solutions of 2% EDA in HFB were irradiated at 15 - 18°C temperature and analyzed by g.c. (column: 12% XE 60 on Chromosorb W, 30 - 60 mesh; program: 100°C $\xrightarrow{1^\circ/\text{min.}}$ 130°C at a helium flow of 50 ccm/min.).

similar conditions as above, using quartz filtered radiation. The two major products observed were [42] and [45]. The isomerization is most likely initiated by photoexcited HFB since most of the light at wavelengths below 2900Å is absorbed by the HFB¹¹⁵. Photosensitized reactions of HFB have been noted previously^{115,116}.

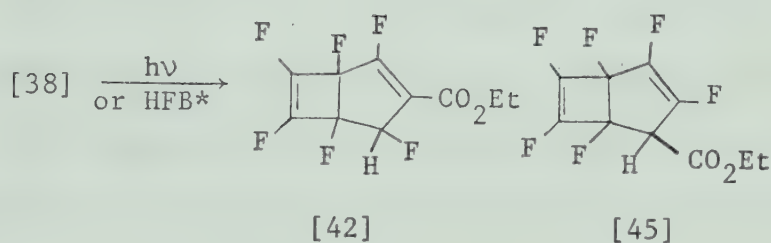
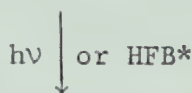
Orbital symmetry arguments indicate that photochemical [1,7] suprafacial sigmatropic migration reactions are allowed in cycloheptatriene^{117,118}. Therefore the presence of a methine proton in the perfluorocycloheptatriene system permits single and consecutive [1,7] suprafacial, sigmatropic hydrogen shifts which can explain the photorearrangement of [38] to the isomeric Buchner acid esters [39] - [41]. Another major mode of photochemical transformation of cycloheptatrienes in solution is photocyclization, which accounts for such valence isomers as bicyclo[3,2,0]hepta-3,6-dienes, i.e. [42] and [45].

The ratio of valence tautomerization to [1,7] hydrogen shift is known to be sensitive to the type of substituents in the cycloheptatriene ring¹¹⁹, which in the present case seems to manifest itself in the predominance of isomer [45]. It also should be noted that the formation of bicycloheptadiene from cycloheptatriene constitutes a photoisomerization reaction which resembles dimerization of olefins to give cyclobutane derivatives and examples of such valence tautomerization have been shown to involve singlet excited states^{120,121}.

Thus, the major steps occurring in the photolysis of HFB solutions of EDA may be summarized by the following sequence:



[39] - [41]



The appearance of the fumarate and maleate esters in a photochemical system is a novel phenomenon since they have been observed before only in catalytic and thermal decompositions of EDA^{108,122}. These dimers of carbethoxymethylene may arise from the attack of the carbene on EDA¹²³ or from dimerization of the carbene. Zimmerman et al.¹²⁴ report olefin formation for the decomposition of dimesityl diazomethane via triplet carbene dimerization. They postulate that due to severe steric hindrance and consequent resistance to external attack by solvent, triplet carbene concentration builds up until dimerization can occur. Formation of triplet

carbethoxymethylene in the present system via triplet HFB sensitization appears unlikely since the combined yield of [47] and [48] is independent of the wavelength of irradiation, because below 3000Å^o the principal absorber is HFB and the decomposition most likely becomes photosensitized. It is, however, possible that triplet carbene is formed not in a primary step but via relaxation of singlet excited carbene by the solvent HFB. This way, a constant yield of triplet carbene and its dimerization products can result independently of wavelength or mode of primary step. Against this militates the observation that neither photolysis nor triplet benzo-phenone sensitized photolysis of EDA in benzene afford detectable amounts of fumarate or maleate.

Analysis of noncondensable gases evolved during the photolysis showed the presence of carbon monoxide in ~2% (theor.) yield. This suggests formation of ethoxyketene via the Wolff rearrangement of singlet carbethoxymethylene and its subsequent photodecomposition^{125,126}.



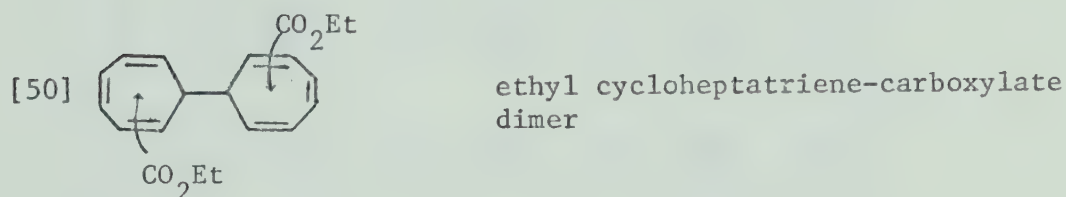
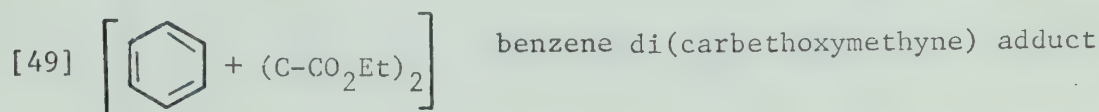
The formation of the ketene and the dimeric tetrameric carbene structures signals the slowness of the addition of carbethoxymethylene to HFB.

6.2 Carbyne Reactions

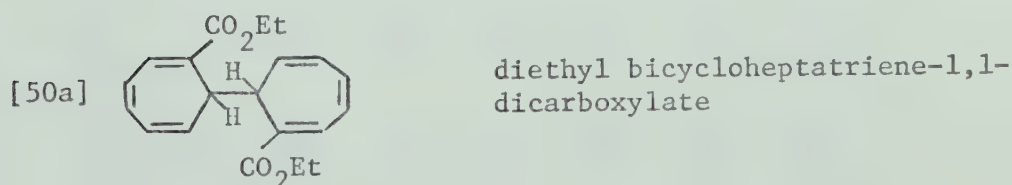
6.2.1 Results of the photolysis of DMDA in benzene

Because there is ample evidence for photoisomerization of products in the photolytic decomposition of EDA in benzene at wavelengths less than $2800\overset{\circ}{\text{\AA}}$, the photolysis of DMDA was carried out with Pyrex filtered light ($\lambda > 2800\overset{\circ}{\text{\AA}}$). Solutions containing 0.5% DMDA were irradiated in the immersion well assembly to completion (3 hrs), as indicated by bleaching of the yellow color, subsidence of the evolution of molecular nitrogen, and complete disappearance of the diazo band in the i.r. spectrum. After removal of metallic mercury which was recovered nearly quantitatively (~90%) and evaporation of benzene, a viscous dark-brown residue remained and attempts to fractionate by high vacuum distillation ($200^{\circ}\text{C}/\sim 0.1$ mm Hg) were unsuccessful. However, g.c. analysis of the reaction mixture using a FFAP or SE-30 column afforded small amounts of ethyl cycloheptatriene-carboxylate isomers [24] and [28] which were identified by comparison with g.c. retention times and m.s. analysis of standard samples (cf. section 6.1.1). Using multiple t.l.c. techniques (20 x 20 cm glass plates with 1 mm Silica Gel layer) and benzene as solvent it was possible to separate the total reaction mixture into eight bands. The isolated bands consisted of mixtures of products having ester groups (i.r. 1700 cm^{-1} ; n.m.r. superimposed triplets at τ 8.6 - 8.8 and quartets at τ 5.7 - 5.9), which were difficult to identify without further separation and purification. The first band (12% wt) was enriched in the products

[25] and [28]. Analytical data (Tables XXIV and XXV) of the next major band (28%) gave ample evidence that it consisted mainly of a mixture of compounds having molecular weights of 248 and 326 and the general formulae:



While attempts to isolate and purify [49] for structural assignments were unsuccessful, it was possible to obtain from the dimeric product [50] one crystalline compound (m.p. 120-122°C):



The structure assignment was assisted by decoupling experiments on the n.m.r. spectrum (Table XXIII). Irradiation of the ring juncture protons at τ 7.91 effected decoupling of the olefinic protons at τ 4.71 only, while irradiation of these protons affected the ring juncture protons at τ 7.91 and also the olefinic protons at τ 3.67. Hydrolysis of the cycloheptatriene-carboxylate dimer [50] with 10% ethanolic potassium hydroxide gave the solid diacid (m.p. 165-175°C),

TABLE XXIV

Mass Spectra of Products [49] - [53]

Compound No.	m/e (P)	m/e and (% of base peak)									
[49]	248 (38)	248 (38)	175 (43)	174 (25)	147 (31)	133 (24)	119 (25)	103 (36)	102 (44)	77 (22)	29 (100)
[50]	326 (1)	207 (12)	179 (14)	178 (11)	164 (16)	163 (100)	135 (25)	105 (17)	103 (15)	77 (18)	29 (26)
[50a]	326 (1)	207 (11)	179 (15)	178 (16)	163 (100)	135 (25)	105 (18)	103 (17)	91 (10)	77 (24)	29 (26)
[50b]	270 (3)	135 (100)	122 (18)	105 (34)	91 (15)	77 (41)	51 (18)	44 (28)	39 (16)	28 (14)	18 (23)
[51]	254 (36)	254 (36)	181 (61)	153 (54)	138 (55)	125 (31)	110 (38)	109 (51)	108 (64)	82 (27)	29 (100)
[52]	338 (7)	291 (16)	218 (13)	190 (28)	188 (20)	169 (100)	141 (30)	110 (26)	96 (21)	82 (22)	29 (55)

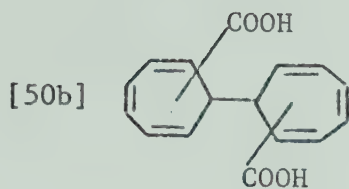
TABLE XXV

Molecular Weights, I.R. and N.M.R. Spectra* for Compounds [49]-[53]

Compound No.	Formula	Molecular Weight		i.r. ν_{\max} CCl_4 (cm^{-1})	n.m.r. (CCl_4)
		Calc.	Meas.		
[49]	$\text{C}_{14}\text{H}_{16}\text{O}_4$	248.1049	248.1041	2998(w); 1705(s) 1260(s);	8.75(superimposed t); 7.95, 6.65(ring juncture proton) 5.8(superimp. q); 4.7, 4.0, 3.7, 3.2, 2.8, 2.3(olefinic protons, m)
[50]*	$\text{C}_{20}\text{H}_{22}\text{O}_4$	326.1518	326.1511		
[50a]	$\text{C}_{20}\text{H}_{22}\text{O}_4$	326.1518	326.1515	2998(w); 1705(s) 1260(s)	8.72(t, 7 Hz, 6H); 7.91(m, 2H) 5.75(q, 7 Hz, 4H); 4.71(m, 2H) 3.67(m, 4H); 3.17(m, 2H); 2.70(m, 2H)
[50b]*	$\text{C}_{16}\text{H}_{14}\text{O}_4$	270.0892	270.0900	3520-3200(broad, s) 1680(s); 1275(m)**	7.7(m, 2H); 4.5(m, 4H); 3.6(m, 2H); 3.1(m, 2H); 2.25(m, 2H); 0.65(broad m, 2H)

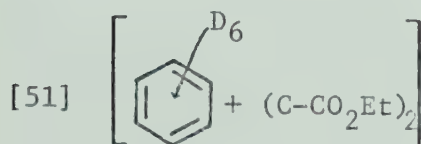
* Elementary Analysis for [50] calculated: C 73.62%, H 6.75%; measured: C 71.83%, H 6.56%
[50b] calculated: C 71.11%, H 5.19%; measured: C 65.57%, H 4.72%

** Matrix used was KBr.

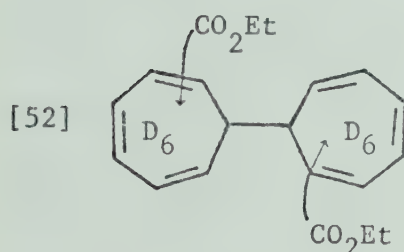


bicycloheptatriene-dicarboxylic acid

which is probably a mixture of isomers as indicated by the wide melting point range and the complex nature of the n.m.r. spectrum. Experiments with deuterated benzene gave products analogous to [49] and [50], with molecular weights 254 and 338:

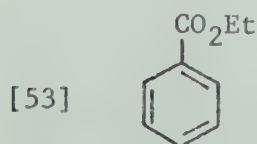


d_6 -benzene di(carbethoxymethyne) adduct

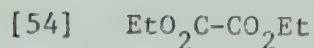


ethyl d_6 -cycloheptatriene-carboxylate dimer

Photolysis of a more concentrated (3%) suspension of DMDA in benzene yielded the following products in addition to those described above,



ethyl benzoate



diethyloxalate

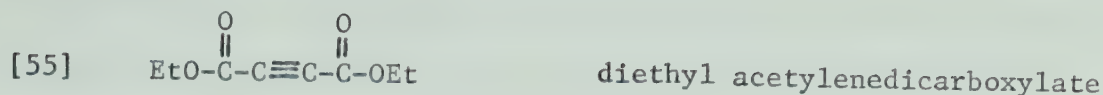
of which the yield of [54] was markedly increased in the presence of oxygen.

The intervention of unstable mercury intermediates was evidenced by continued precipitation of metallic mercury during the work-up procedure and also by characteristic patterns of mercury fragment ions in the mass spectrum of the reaction mixture.

6.2.2 Results of the photolysis of DMDA in hexafluorobenzene

The irradiation of a solution of DMDA (0.3% wt) in hexafluorobenzene was carried out with Pyrex filtered light to avoid or minimize photoisomerization. After complete photodecomposition of DMDA (1 hr) only 52% of the mercury was recovered as metallic mercury. An insoluble flocculent precipitate formed during the photolysis which, after separation and drying, gave a yellow solid (14%) which decomposed above 200°C. Analysis indicated that it was a polymeric organic material containing mercury and fluorine (C: 23.34%; H: 3.26%; F: 1.37%; Hg: 46.90%). After evaporation of hexafluorobenzene the total liquid product (48%) was distilled at 100°C/~0.1 mm Hg to yield colorless liquid (20%) which consisted mainly of the products [38] - [48]. These products were also detected in the photolysis of EDA in hexafluorobenzene and therefore were characterized in the same fashion (cf. section 6.1.2). However, g.c. analysis on the XE-60 column indicated the presence of several additional products in smaller quantities which were eluted immediately following products [38] - [48]. One compound (2-3% of the distillate) could be isolated and

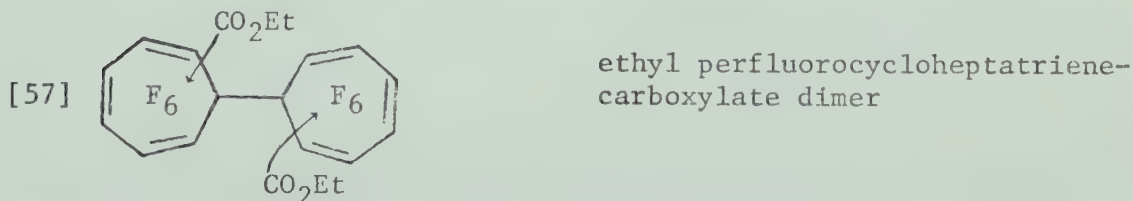
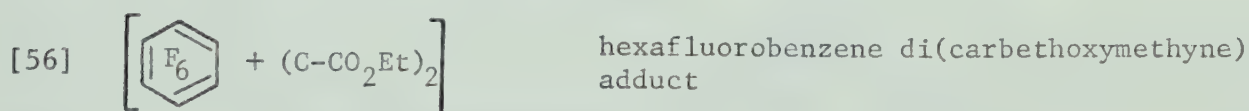
identified as:



The g.c. retention time, the m.s., i.r., and n.m.r. spectra for [55] were identical with those of a standard sample (K&K Laboratories, lot #55190) and with published data¹²⁷.

The involatile gummy residue (27%) contained some metallic mercury which was formed during the distillation indicating the presence of a thermally unstable mercury intermediate. Organically bonded mercury was also evidenced by the fragmentation pattern of the mass spectrum and the elemental analysis (C: 28.54%; H: 2.21%; F: 3.16%; Hg: 33.77%). The presence of the carbethoxy group was shown by the i.r. (1700 cm^{-1}) and n.m.r. spectra (superimposed triplets at τ 8.65 - 8.85 and quartets at τ 5.60 - 5.80).

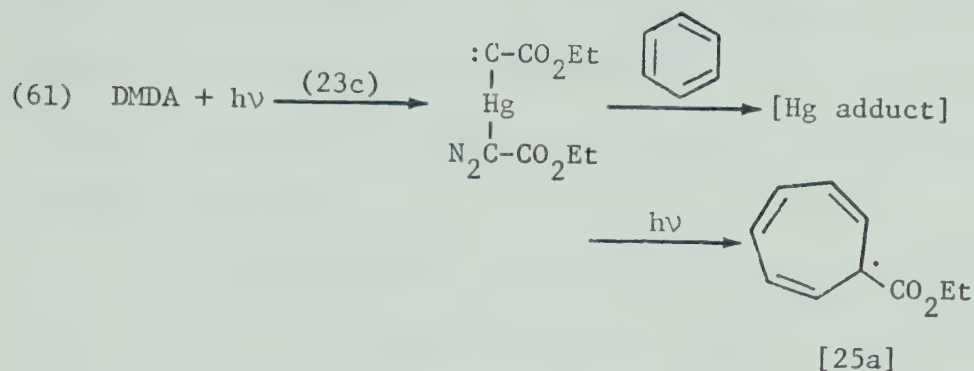
Compounds analogous to [49] and [50], i.e.



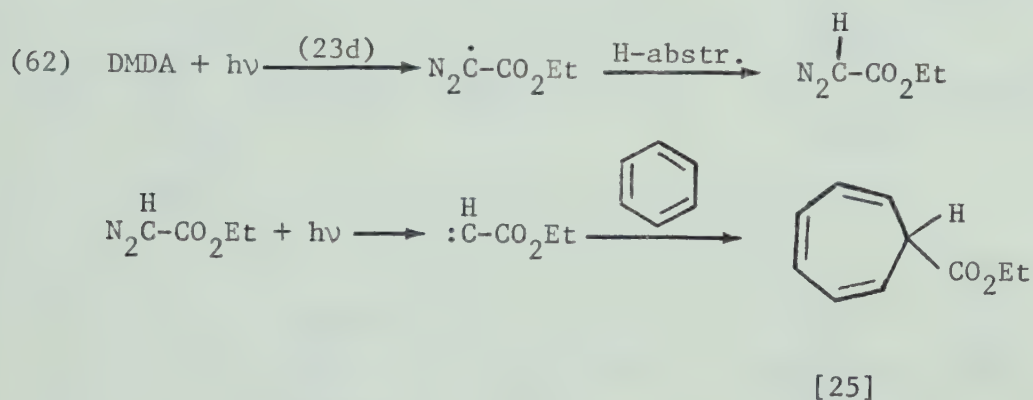
were not isolated but are probably present since the m.s. of the residue showed parent ions corresponding to [56] and [57].

In summary, the photolysis of DMDA in hexafluorobenzene

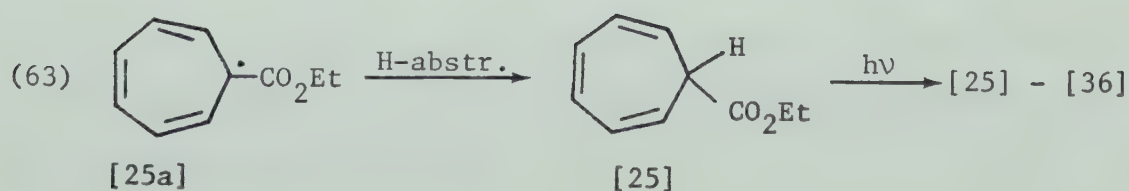
or, in part, depending on the photon energy of the actinic light from the addition of mercury-carbene to benzene:



Neither the photolytic decomposition of DMDA via primary step (23d) nor intermediacy of EDA can lead to the formation of [25a]; only [25] can be formed as the primary product:



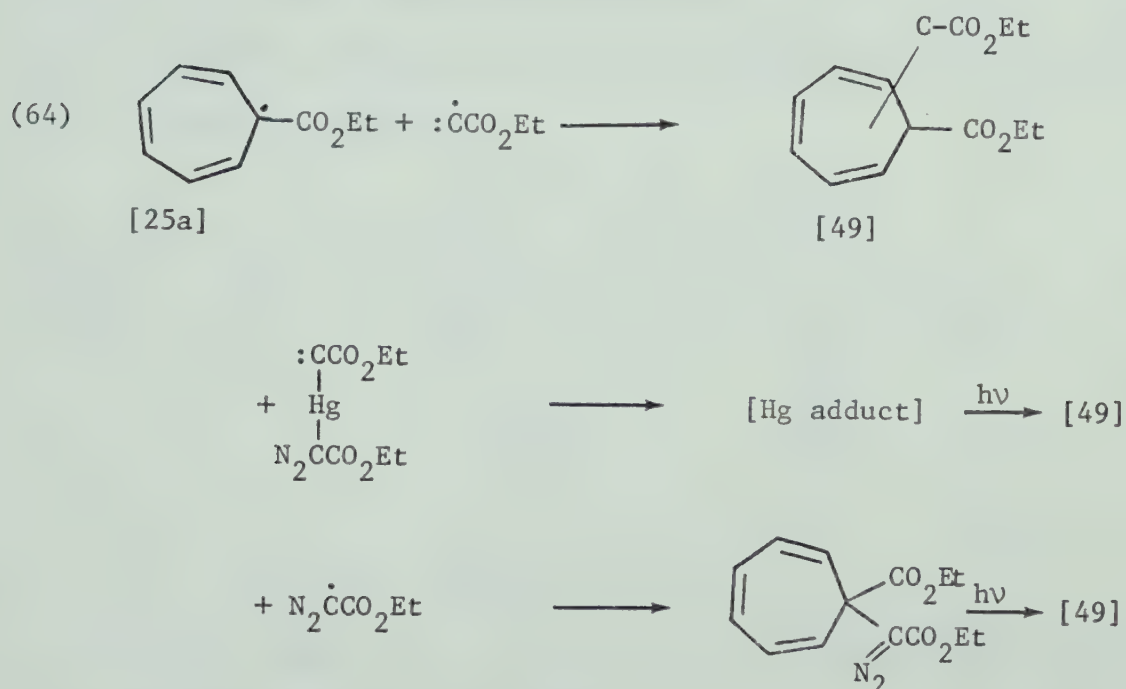
Besides dimerization, [25a] may undergo hydrogen abstraction to give products [25] - [36]:



The fact that dimerization of [25a] can compete in this solvent with

H abstraction must be due to the reduced availability of hydrogen for abstraction, i.e. the carbon-hydrogen bond is relatively strong in benzene and the ethyl group of the starting material DMDA is present only in low concentration (0.5%). In the case of hexafluorobenzene as solvent the ethyl group in DMDA is the only source for hydrogen abstraction.

A third possible reaction pathway for the cycloheptatrienyl radical [25a] is combination with mono-, di-, or trivalent carbon intermediates such as carbethoxymethyne, mercury-carbene, and the EDA radical, $\text{N}_2\dot{\text{C}}\text{CO}_2\text{Et}$, to yield product [49] either directly or after secondary photolysis:

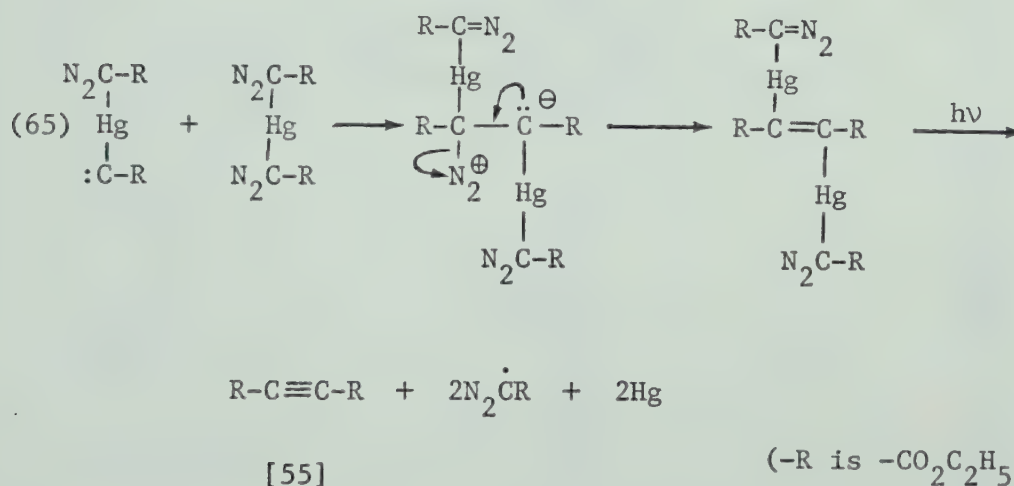


This reaction sequence is only speculative since the structure of [49] is not known. There is some evidence however, that [49] is a cyclo-octatetraene derivative,



Thus, the occurrence of ethyl benzoate [53] in the DMDA + benzene system and of diethyl acetylenedicarboxylate [55] in the DMDA + hexafluorobenzene system support the cyclooctatetraene structure for [49] since thermal and photolytical decomposition of cyclooctatetraene has been reported to give benzene and acetylene¹²⁸.

The formation of product [55] need not necessarily involve an aromatic solvent molecule but could result from an intermolecular reaction of DMDA intermediates with DMDA followed by intramolecular rearrangements and photolysis:



Dimerization of carbethoxymethyne could also lead to [55] but this is somewhat unlikely. The suggested mechanism that leads to the formation of the observed products is summarized in Reaction Scheme VII (Figure 21). Due to the instability of the primary

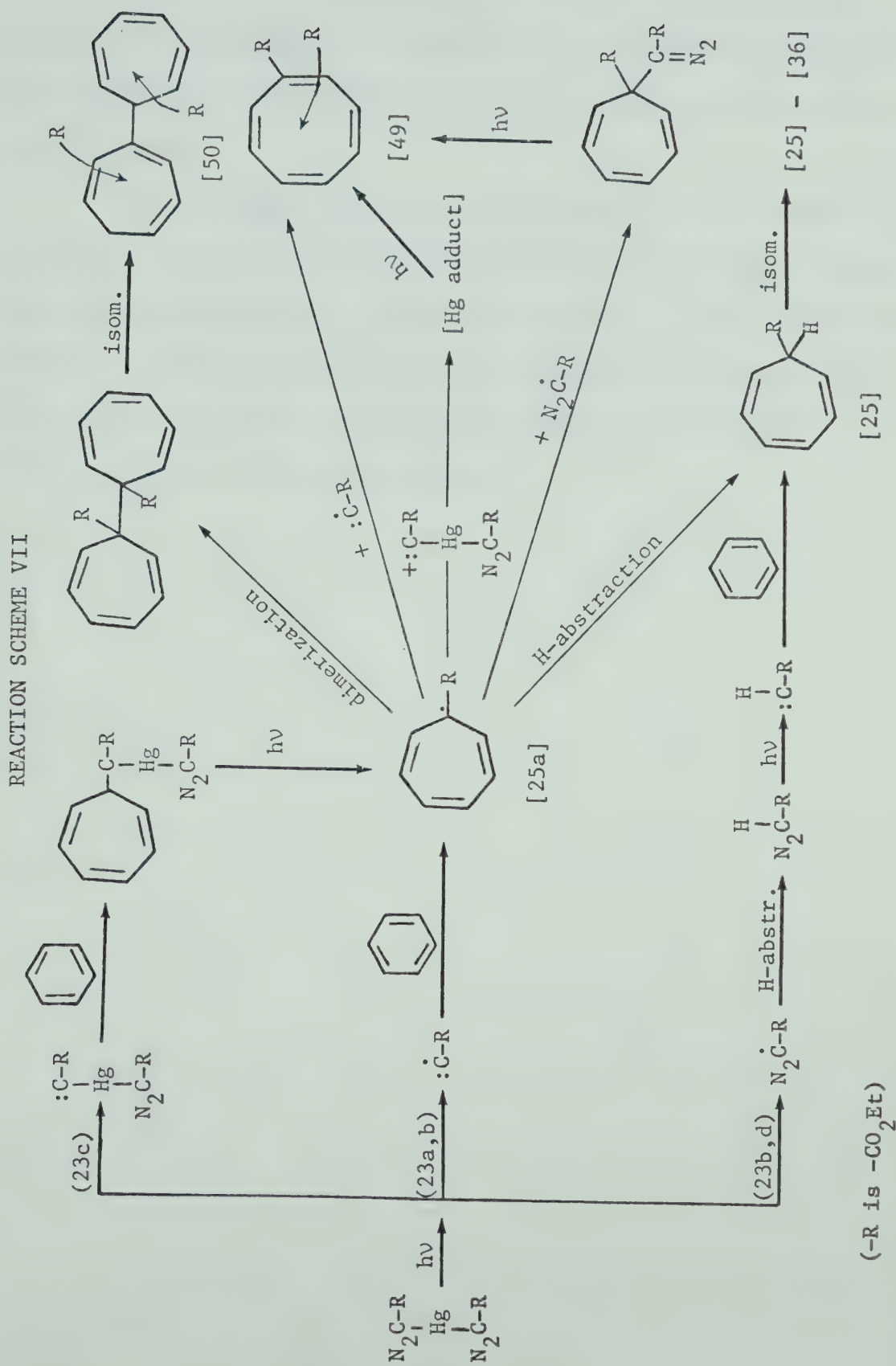


FIGURE 21

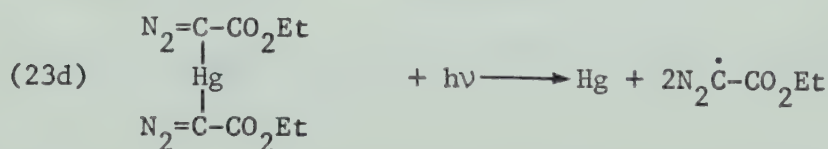
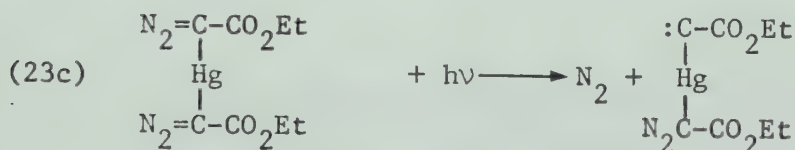
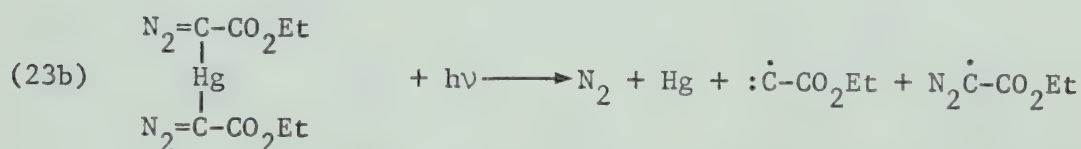
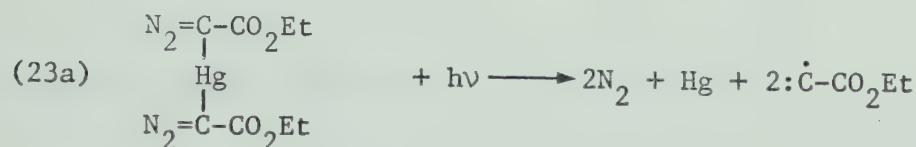
products in the photolysis of DMDA in hexafluorobenzene and the tendency of intermediates to polymerize, the results are incomplete and hence do not allow the assumption of a similar reaction scheme for this system.

It is assumed that oxygen is involved in the formation of diethyl oxalate [54] because the yields increased when no attempts were made to exclude air. However, the effect of oxygen on the decomposition of DMDA in benzene was not investigated further and therefore the mechanism for the formation of [54] and possibly [53] involving oxygen can only be alluded to.

CHAPTER 7

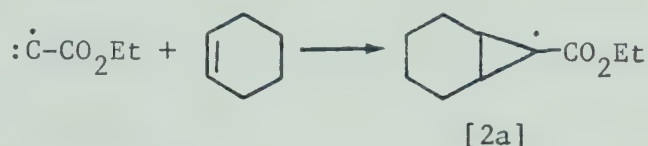
SUMMARY AND CONCLUSION

A systematic study has been undertaken to establish suitable experimental conditions for the generation of carbethoxymethyne by the photolysis of diethyl mercurybisdiazooacetate, DMDA, and to examine its chemical properties in a variety of substrates by means of product characterization. DMDA has two extremely labile linkages, C-N₂ and C-Hg, which can be broken simultaneously and also individually leading to mono-, di-, and trivalent carbon intermediates via the four postulated primary steps:

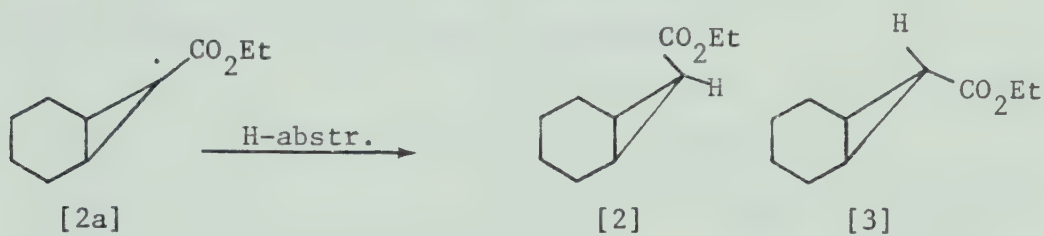


The first two of these primary steps produce carbethoxymethyne and increase in importance with increasing photon energy.

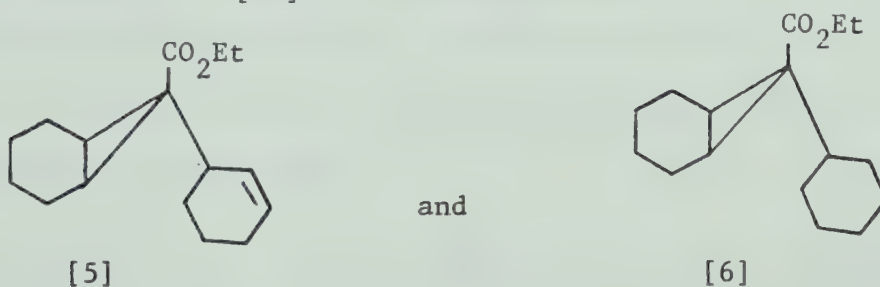
The main feature of the reaction of carbethoxymethyne with cyclohexene and hence the key argument for carbyne formation, is the involvement of the cyclopropyl radical [2a],



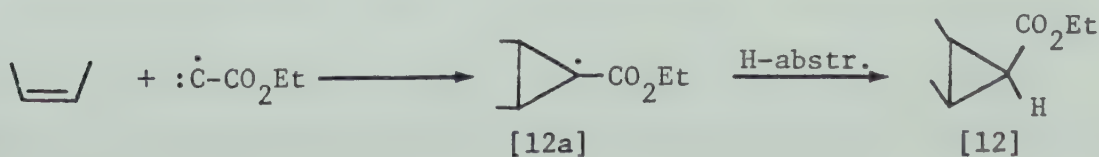
which is unequivocally demonstrated by the high endo/exo addition product ratio which results from hydrogen abstraction by [2a]:



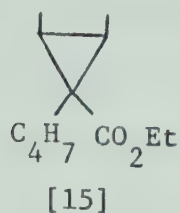
Further evidence for [2a] is the formation of



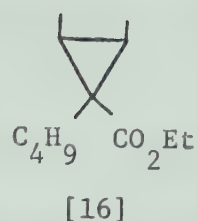
In the addition reaction of carbethoxymethyne to butene-2 the intermediacy of a cyclopropyl radical [12a] is evidenced by the increased yield of the less stable all-*cis* or α -isomer, [12]



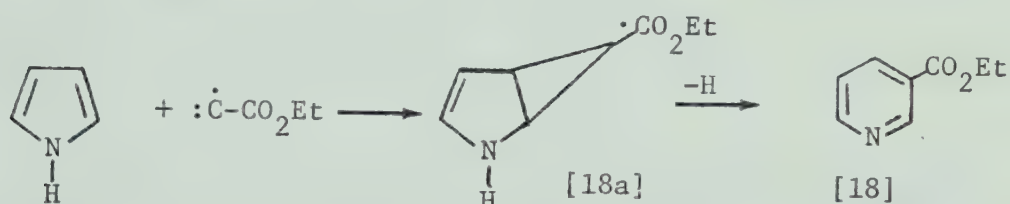
and also by the presence of products



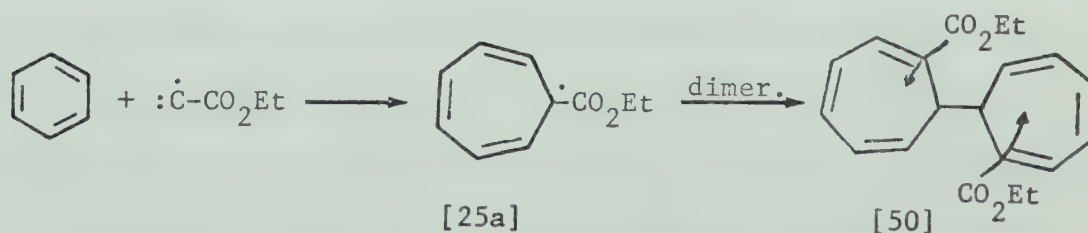
and



which are formed by the reaction of [12a] with solvent. The pre-dominant product of the photolysis of DMDA in pyrrole is ethyl pyridine-3-carboxylate [18] which is derived from the addition of carbethoxymethyne to pyrrole to form a cyclopropyl radical intermediate [18a] followed by facile ring expansion:



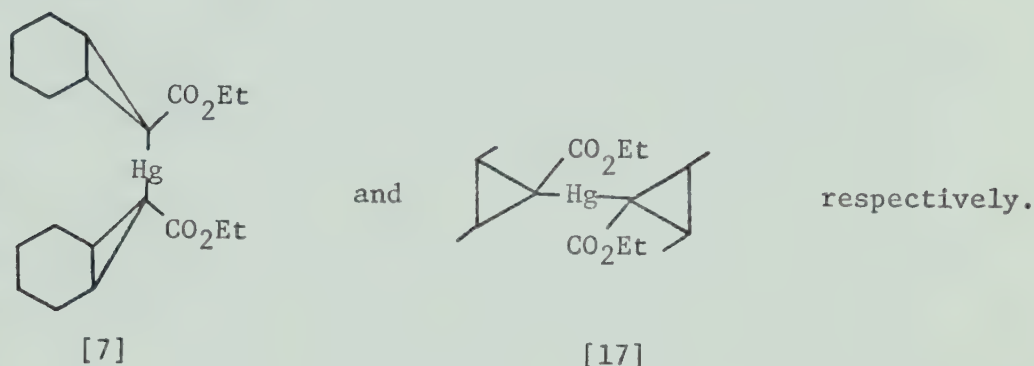
The characteristic intermediate formed by the addition of carbethoxycarbyne to benzene is the cycloheptatriene radical [25a] which is evidenced by its dimer [50]:



The observed stereospecificity of the addition reaction of carbethoxymethyne to *cis*- and *trans*-butene-2 is characteristic for doublet multiplicity of the monovalent carbon species in analogy to the well established singlet carbene addition reaction. The carbynes

were also observed to undergo insertion reaction with the allylic C-H bonds of cyclohexene and butene-2, and the C-H bonds of pyrrole, which is a reaction common to singlet carbenes.

Divalent carbon intermediates were observed and characterized by the formation of stable mercury adducts from a novel mercurycarbene via primary step (23c). The extent of the mercurycarbene reaction in cyclohexene and also in *trans*-butene-2 was assessed by the yields of



The intermediacy of an ethyl diazoester radical, $\text{N}_2\dot{\text{C}}\text{CO}_2\text{Et}$, was verified and also measured by direct monitoring of its characteristic product, ethyl diazoester, $\text{N}_2\text{CHCO}_2\text{Et}$.

After having recognized and quantitatively assessed the extent of the primary steps (23a-d) in the photolytic decomposition of DMDA in olefinic and aromatic solvents, it is concluded that the intervention of a monovalent carbon intermediate has been established, and that the extent of such carbyne intermediate can be estimated by the yields of the characteristic addition products. Such products arise from the addition of carbyne to the π system of unsaturated bonds in olefins and aromatics followed by either hydrogen abstraction, loss of hydrogen, scavenging by the substrate, or dimerization of the intermediate radicals.

Secondary photolysis of primary products, especially in aromatic solvent systems yielded a complex reaction mixture and complicated product characterization and interpretation of results. Therefore, the experimental conditions and the nature of the precursor must be planned carefully for future work and the solvents will have to be chosen judiciously in order to minimize the extent of primary steps which lead to divalent and trivalent carbon transients and to avoid photoisomerization of primary products. Solvents are required which are transparent in the required wavelength region ($>2100\overset{\circ}{\text{\AA}}$) and also dissolve DMDA readily and at the same time yield photostable and characteristic products. Since such solvents, owing to the poor solubility of DMDA, are limited it would be advantageous to modify the structure of the metal diazoester in a way that its solubility and volatility would increase. This would allow gas phase studies and a larger variation in the choice of reactants and kinetic parameters.

BIBLIOGRAPHY

1. A. P. Wolf in *Advances in Physical Organic Chemistry*, V. Gold, ed., Vol. II, Academic Press (1964), p. 201.
2. G. M. Meaburn, D. Perner, *Nature*, 212, 1042 (1966).
3. a) P. S. Skell, R. R. Engel, *J. Amer. Chem. Soc.*, 87, 1135 (1965); b) J. L. Sprung, S. Winstein, W. F. Libby, *J. Amer. Chem. Soc.*, 87, 1812 (1965); c) P. S. Skell, R. R. Engel, *J. Amer. Chem. Soc.*, 93, 2699 (1971).
4. G. W. Spangler, S. K. Lott, M. J. Jonich, *Chem. Comm.*, 842 (1966).
5. A. R. Fairbairn, *J. Quant. Spectros. Radiat. Transfer*, 9, (7), 943 (1969).
6. F. Martinotti, M. J. Welch, A. P. Wolf, *Chem. Comm.*, 115 (1968).
7. Von K. H. Hommann, W. Lange, H. G. Wagner, *Ber. Buns. Ges.*, 75(2), 121 (1971).
8. a) L. J. Stief, V. J. De Carlo, *J. Chem. Phys.*, 43, 2552 (1965).
b) D. E. Milligan, M. E. Jacox, *J. Chem. Phys.*, 48, 2265 (1968).
9. a) W. Braun, A. M. Bass, D. D. Davis, J. D. Simmons, *Proc. Roy. Soc.*, A312, 417 (1969); b) E. Tschuikow-Roux, S. Kodama, *J. Chem. Phys.*, 50, 5292 (1969).
10. Ph. B. Shevlin, A. P. Wolf, *Tetr. Letters*, No. 46, 3987 (1970).
11. G. Herzberg, *Molecular Spectra and Molecular Structure*, Vol. I, D. van Nostrand Co., Inc., Princeton (1967) p. 491.
12. P. C. Keenan, W. W. Morgan, *Astrophys. J.*, 94, 501 (1941).
13. E. Hulthén, *Z. f. Phys.*, 11, 284 (1922).
14. A. Kratzer, *Z. f. Phys.*, 23, 298 (1924).

15. R. Fortrat, *Chem. Rev.*, 178, 1272 (1924).
16. R. S. Mulliken, *Phys. Rev.*, 30, 785 (1927).
17. T. Hori, *Z. J. Phys.*, 59, 91 (1929).
18. L. Gerö, *Z. J. Phys.*, 117, 709 (1941).
19. T. Shidei, *Japanese J. Phys.*, 11, 23 (1936).
20. L. Gero, *Z. J. Phys.*, 118, 27 (1942).
21. R. G. W. Norrish, G. Porter, B. A. Thrush, *Proc. Roy. Soc., London*, A216, 165 (1953).
22. J. H. Callomon, R. A. Ramsay, *Can. J. Phys.*, 35 (2), 129 (1957).
23. G. Herzberg, J. W. Johns, *Astrophys. J.*, 158, 399 (1969).
24. G. Herzberg, *The Spectra and Structure of Simple Free Radicals*, Cornell University Press, Ithaca (1971).
25. C. MacKay, R. Wolfgang, *J. Amer. Chem. Soc.* 83, 2399 (1966).
26. E. P. Rack, A. F. Voigt, *J. Phys. Chem.*, 67, 198 (1963).
27. G. S. Stöcklin, A. P. Wolf, *J. Amer. Chem. Soc.*, 85, 229 (1963).
28. A. P. Wolf, G. Stöcklin, *Abstracts, 146th National Meeting of Amer. Chem. Soc., Denver, Col., (1964) p. 32.*
29. A. P. Wolf in *Advances in Physical Organic Chemistry*, Vol. II, p. 255 (1964) and papers cited therein.
30. D. E. Clark, A. F. Voigt, *J. Amer. Chem. Soc.*, 87, 5558 (1965).
31. C. MacKay, R. Wolfgang, *Science*, 148, 899 (1965).
32. R. Wolfgang, *Progr. React. Kinetics*, 3, 159 (1965).
33. J. Nicholas, C. MacKay, R. Wolfgang, *J. Amer. Chem. Soc.*, 88, 1065 (1966).
34. C. MacKay, J. Nicholas, R. Wolfgang, *J. Amer. Chem. Soc.*, 89, 5758 (1967).

35. A. G. Gaydon, *Spectroscopy of Flames*, Chapman and Hall Ltd., London (1957).
36. D. R. Safrany, R. R. Reeves, P. Harteck, *J. Amer. Chem. Soc.* 86, 3160 (1964).
37. a) H. F. Calcote, S. C. Kurzins, J. W. Miller, *Tenth Symposium on Combustion*, The Combustion Institute, Pittsburgh, Pa., (1965) p. 605; b) A. Fontijn, W. J. Miller, J. M. Hogan, *ibid.*, p. 545; c) G. P. Glass, G. B. Kistiakowsky, J. V. Michael, H. Niki, *ibid.*, p. 513.
38. W. Braun, K. H. Welge, J. R. McNesby, *J. Chem. Phys.*, 45, 2650 (1966).
39. W. Braun, J. R. McNesby, A. M. Bass, *J. Chem. Phys.*, 46, 2071 (1967).
40. M. W. Bosnali, D. Perner, *Z. Naturforsch.*, 26a, 1768 (1971).
41. R. W. B. Pearse, A. G. Gaydon, *Identification of Molecular Spectra*, Chapman and Hall, London (1965).
42. T. L. Porter, D. E. Mann, N. Acquista, *J. Molec. Spectr.*, 16, 228 (1965).
43. J. P. Simons, A. J. Yarwood, *Trans. Far. Soc.*, London, 57, 2167 (1961).
44. J. P. Simons, A. J. Yarwood, *Trans. Far. Soc.*, 58, 90 (1962).
45. J. P. Simons, A. J. Yarwood, *Proc. Chem. Soc.*, 62 (1962).
46. R. N. Dixon, H. W. Kroto, *Trans. Far. Soc.*, 59, 1484 (1963).
47. W. J. R. Tyerman, *Spectrochimia Acta*, 26A, 1215 (1970).
48. M. E. Jacox, D. E. Milligan, *J. Chem. Phys.*, 50, 3252 (1969).

49. M. E. Jacox and D. E. Milligan, *J. Chem. Phys.*, 53, 2688 (1970).
50. A. Carrington and B. J. Howard, *Molec. Phys.*, 18, 225 (1970).
51. A. J. Merer and D. N. Travis, *Can. J. Phys.*, 43, 1795 (1965).
52. W. J. R. Tyerman, *Trans. Farad. Soc.*, 65, 2948 (1969).
53. W. J. R. Tyerman, *J. Chem. Soc. (A)*, 2483 (1969).
54. R. Dickson, unpublished work.
55. a. Thap DoMinh, H. E. Gunning and O. P. Strausz, *J. Amer. Chem. Soc.*, 89, 6785 (1967).
b. O. P. Strausz, Thap DoMinh and J. Font, *J. Amer. Chem. Soc.*, 90, 1930 (1968).
56. W. M. Huo, *J. Amer. Chem. Soc.*, 49, 1482 (1968).
57. R. Hoffmann, G. D. Zeiss and G. W. von Dine, *J. Amer. Chem. Soc.*, 90, 1485 (1968).
58. W. Kirmse, "*Carbene, Carbenoide und Carbenanaloge*," Verlag Chemie, Ginlett, Weinheim/Bergstr. (1966) and references cited therein.
59. W. Kirmse, "*Carbene Chemistry*," second ed., Vol. I of Organic Chemistry Series, Academic Press, New York (1971).
60. P. S. Skell and R. C. Woodworth, *J. Amer. Chem. Soc.*, 78, 4496 (1956); *ibid*, 81, 3383 (1959).
61. R. Hoffmann, *J. Amer. Chem. Soc.*, 90, 1475 (1968).
62. R. Gosavi, unpublished work.
63. T. L. Cottrel, "*The Strength of the Chemical Bond*," Butterworth Scientific Publication, London (1958), p. 249.
64. H. V. Carter, E. I. Chappel and E. Warhurst, *J. Chem. Soc.*, 106 (1956).

65. A. S. Kallend and J. H. Purnell, *Trans. Farad. Soc.*, 60, 103 (1964).
66. K. J. Irvin and E. W. R. Steacie, *Proc. Roy. Soc.*, A208, 25 (1951).
67. L. C. Fischer and G. J. Mains, *J. Phys. Chem.*, 68, 2522 (1964).
68. G. von Büнау, P. Potzinger and G. O. Schenck, *Tetrahedron*, 1293 (1965).
69. Thap Do Minh, O. P. Strausz and H. E. Gunning, *Tetr. Letters*, No. 50, 5237 (1968).
70. J. G. Calvert and J. N. Pitts, "*Photochemistry*," J. Wiley & Sons (1967).
71. N. E. Searle, *Org. Synth.*, Coll. IV, p. 424 (1964).
72. G. S. Skinner, *J. Amer. Chem. Soc.*, 46, 733 (1924).
73. G. Wieland, *Ann.*, 367, 61 (1907).
74. H. E. Ungnade and L. W. Kissinger, *J. Org. Chem.*, 24, 666 (1959).
75. H. E. Ungnade and E. D. Longhran, *J. Heterocycl. Chem.*, 1 (2), 61 (1964).
76. E. Buchner, *Ber.*, 28, 215 (1895).
77. P. S. Skell and R. M. Etter, *Proc. Chem. Soc.* 443 (1961).
78. W. R. Moser, *J. Amer. Chem. Soc.*, 91, 1135 (1969).
79. R. Hoffmann, *Tetrahedron*, 22, 539 (1966).
80. R. E. Dessey and W. Kitching in "*Advances in Organometallic Chemistry*," Academic Press, New York (1966) p.304 and references quoted therein.
81. R. Fusco in "*Pyrazoles, Pyrazolines, Pyrazolidines, Indazoles, and Condensed Rings*," Interscience Publishers, New York (1967).

82. C. J. Jarboe, in *"Pyrazoles, Pyrazolines, Pyrazolidines, Indazoles, and Condensed Rings,"* Interscience Publishers, New York (1967).
83. H. M. Frey, *Proc. Roy. Soc., Ser. A*, 250, 409 (1959).
84. H. M. Frey, *Proc. Roy. Soc., Ser. A*, 251, 575 (1959).
85. W. von Doering and T. Mole, *Tetrahedron*, 10, 65 (1960).
86. J. M. Walbrick, J. W. Wilson, Jr. and W. M. Jones, *J. Amer. Chem. Soc.*, 90, 2895 (1968).
87. A. R. Katritzky, ed., *"Physical Methods in Heterocyclic Chemistry,"* Academic Press, New York (1963), p. 59.
88. H. H. Jaffe and O. Milton, *"Theory and Application of Ultraviolet Spectroscopy,"* John Wiley, New York (1962).
89. G. O. Schenck and R. Steinmetz, *Ann.*, 668, 19 (1963).
90. A. Piccinini, *Gazz. Chim. Ital.* 29, 363 (1899)
91. C. D. Nenitzescu and E. Solomonica, *Ber.*, 64, 1924 (1931).
92. F. W. Fowler, *Chem. Commun.*, 1359 (1969).
93. F. W. Fowler, *Angew. Chem. Internat. Edit.*, 10, 135 (1971).
94. C. W. Rees and C. E. Smithen in *"Advances in Heterocyclic Chemistry,"* Vol. 3 (1964), p. 66.
95. H. L. Rice and T. E. Londergan, *J. Amer. Chem. Soc.*, 77, 4678 (1955).
96. F. S. Baker, R. E. Busby, M. Igbal, J. Patrick and C. J. G. Shaw, *Chem. Ind. (London)*, p. 1344 (1969).
97. F. W. Fowler, *J. Org. Chem.*, 37, 1321 (1972).
98. E. Buchner and Th. Curtius, *Chem. Ber.*, 18, 2377 (1885).

99. A. Loose, *J. prakt. Chem.*, 79, 509 (1909).
100. C. Grundmann and G. Ottmann, *Ann.*, 582, 163 (1953).
101. G. O. Schenck, *Z. Electrochem. Angew. Phys. Chem.*, 55, 505 (1951).
102. G. O. Schenck, *Angew. Chem.* 64, 19 (1952).
103. G. O. Schenck and H. Ziegler, *Ann.*, 584, 221 (1953).
104. W. von Doering, G. Laber, R. Vanderwahl, N. F. Chamberlain and R. B. Williams, *J. Amer. Chem. Soc.*, 78, 5448 (1956).
105. G. Maier, *Angew. Chem., Internat. Edit.*, 6, 402 (1967).
106. W. G. Cauben and R. L. Cargill, *Tetrahedron*, 12, 186 (1961).
107. G. Linstrumelle, *Tetrahedron Letters*, 85 (1970).
108. G. Linstrumelle, *Bull. Soc. Chim.*, 3, 920 (1970).
109. A. H. Gorman and J. B. Sheridan, *Tetrahedron Letters*, 2569 (1969).
110. G. O. Schenck and A. Ritter, *Tetrahedron Letters*, 3189 (1968).
111. T. Do Minh and O. P. Strausz, *J. Amer. Chem. Soc.*, 92, 1766 (1970).
112. D. Gale, *J. Org. Chem.*, 6, 2536 (1968).
113. M. Jones, Jr., *J. Org. Chem.*, 6, 2538 (1968).
114. J. W. Emsley, J. Feeny and L. H. Sutcliffe, "*High Resolution Nuclear Magnetic Resonance Spectroscopy*," Pergamon Press Ltd. London, 1960, p. 871.
115. A. K. Basak, G. P. Semeluk and I. Unger, *J. Phys. Chem.*, 70, 1337 (1966).
116. D. Phillips, *J. Chem. Phys.*, 46, 4679 (1967).
117. R. B. Woodward and R. Hoffmann, *J. Amer. Chem. Soc.*, 87, 395 (1965).

118. R. B. Woodward and R. Hoffmann, *J. Amer. Chem. Soc.*, 87, 2511 (1965).
119. H. Klosterziel, A. P. ter Borg and E. Razenberg, *Chem. Comm.* 1210 (1967).
120. R. Srinivasan, *J. Amer. Chem. Soc.*, 84, 3432 (1962).
121. O. L. Chapman, G. W. Borden, R. Swindell and T. Tezuka, *J. Amer. Chem. Soc.*, 89, 2980 (1967).
122. W. Kirmse, "*Carbene Chemistry*," Academic Press, New York (1964), p. 95.
123. W. Kirmse, "*Carbene, Carbenoxide and Carbenanaloge*," Verlag Chemie, (1969), p. 43.
124. H. E. Zimmerman and D. H. Paskovich, *J. Amer. Chem. Soc.*, 86, 2149 (1964).
125. I. G. Csizmadia, H. Font and O. P. Strausz, *J. Amer. Chem. Soc.*, 90, 7360 (1968).
126. G. Frater and O. P. Strausz, *J. Amer. Chem. Soc.*, 92, 6654 (1970).
127. Beil. Bd. 2-III, 1993 (1961).
128. G. Schroeder, "*Cyclooctatetraen*," Verlag Chemie b.m.b.H., Weinheim/Bergstrasse (1965).

APPENDIX A

Quantitative Determination of [1]-[7]

For the quantitative determination of compounds [1]-[7] a series of samples was irradiated at 18°C in quartz tubes (16 mm diameter) containing 0.1 gm DMDA per 20 ml cyclohexene and also in the larger immersion vessel assembly containing 0.8 gm DMDA in 200 ml cyclohexene. After complete decomposition of DMDA, removal of metallic mercury, and partial removal of the solvent by flash evaporation the volume of the total reaction mixture of each sample was made up to 1.0 ml and 10.0 ml respectively with cyclohexene. Aliquots of these stock solutions were then analyzed by comparison of g.c. peak areas with standard solutions of the purified compounds [1]-[7] in cyclohexene. It was assumed that the g.c. detector response would be identical for the isomers [1]-[4]. The standard solution used for analysis of [1]-[4] contained 5.95×10^{-2} M/ltr. of [3]; that for [5] and [6] contained 2.53×10^{-2} M/ltr. of [6]; and the one for [7], 1.05×10^{-1} M/ltr. of [7].

A summary of yield data for various photolyses including type of photolysis cell used, filter, and irradiation time is given in Table XXVI.

TABLE XXVI

Analytical Data for Products [1] - [7]

Sample No.	Filter	Type of Photo-lysis Cell	Irradiation Time (min.)	% Yield, (theoretical)							Hg-metallic recovered
				[1]	[2]	[3]	[4]	[5]	[6]	[7]	
I-a	Vycor	16 mm dia. tube	30	8.5	6.5	2.0	16.3	4.7	3.6	-	-
I-b	Vycor	16 mm dia. tube	30	7.5	5.8	1.8	15.3	-	-	-	-
I-c	Vycor	Immers. vessel	37	10.8		1.3	25.0	(12.0)	(10.0)	-	-
I-d	Vycor	Immers. vessel	90	10.9	6.1	1.8	100	-	-	-	-
I-e	Vycor	Immers. vessel	30	9.1	14.8	1.4	8.0	4.0	3.5	14.3	65
I-f	Vycor	Immers. vessel	30	9.2	12.3	1.9	11.2	2.8	1.9	18.4	27
II-a	Corex	16 mm dia. tube	30	4.5	2.4	1.0	12.5	-	-	-	-
II-b	Corex	Immers. vessel	30	11.2	8.1	0.6	13.5	3.9	2.6	26.0	23
II-c	Corex	Immers. vessel	30	5.5	5.1	0.9	5.1	2.0	1.1	27.9	37
III-a	Pyrex	16 mm dia. tube	45	6.4	3.0	1.4	10.6	2.2	0.8	-	-
III-b	Pyrex	Immers. vessel	40	6.5	2.6	0.4	8.3	1.6	0.5	39.0	114
III-c	Pyrex	Immers. vessel	40	4.3	1.8	<0.1	4.5	1.4	0.4	38.1	18.3
IV-a	Uranium	16 mm dia. tube	60	2.6	1.2	0.7	5.1	0.4	<0.1	-	-
IV-b	Uranium	Immers. vessel	65	3.1	1.4	0.2	4.9	0.6	<0.1	36.2	2.1
IV-c	Uranium	Immers. vessel	65	2.8	1.2	0.3	3.9	0.6	<0.1	39.0	5.1

APPENDIX B

Calibration Procedure and Method of I.R. Measurement

Concentration measurements of DMDA and EDA in cyclohexene were made with the PE-421 i.r. instrument using the sharp infrared diazo bands at 2075 cm^{-1} and 2110 cm^{-1} for DMDA and EDA respectively. The instrument was operated at a very low scan rate (position 16) and an expansion of 100°A per 8 cm (linear scale). Calibration curves for EDA and DMDA were prepared by measuring the peak heights of the corresponding diazo bands for solutions containing known amounts of the two diazoesters. (cf. Table XXVII and Figure 22)

Baseline adjustments were necessary during the i.r. measurements of photolysed samples due to the fogging of the sodium chloride windows of the i.r. cell by precipitated mercury and increasing opacity of the solution owing to a suspension of metallic mercury.

TABLE XXVII

Concentration and Absorbance Measurements for EDA and DMDA

Calibration Point	EDA		DMDA	
	Concentration M/l x 10 ⁻³	Absorbance	Concentration M/l x 10 ⁻³	Absorbance
1	1.05	0.11	2.0	0.15
2	1.45	.16	4.0	.26
3	2.25	.25	6.0	.34
4	2.80	.28	8.0	.45
5	2.85	.27	10.0	.55
6	3.30	.32	12.0	.66
7	4.50	.43		
8	5.80	.52(0.55)		
9	7.05	.62		
10	10.01	.90		
11	11.25	.99		
12	12.0	1.06		

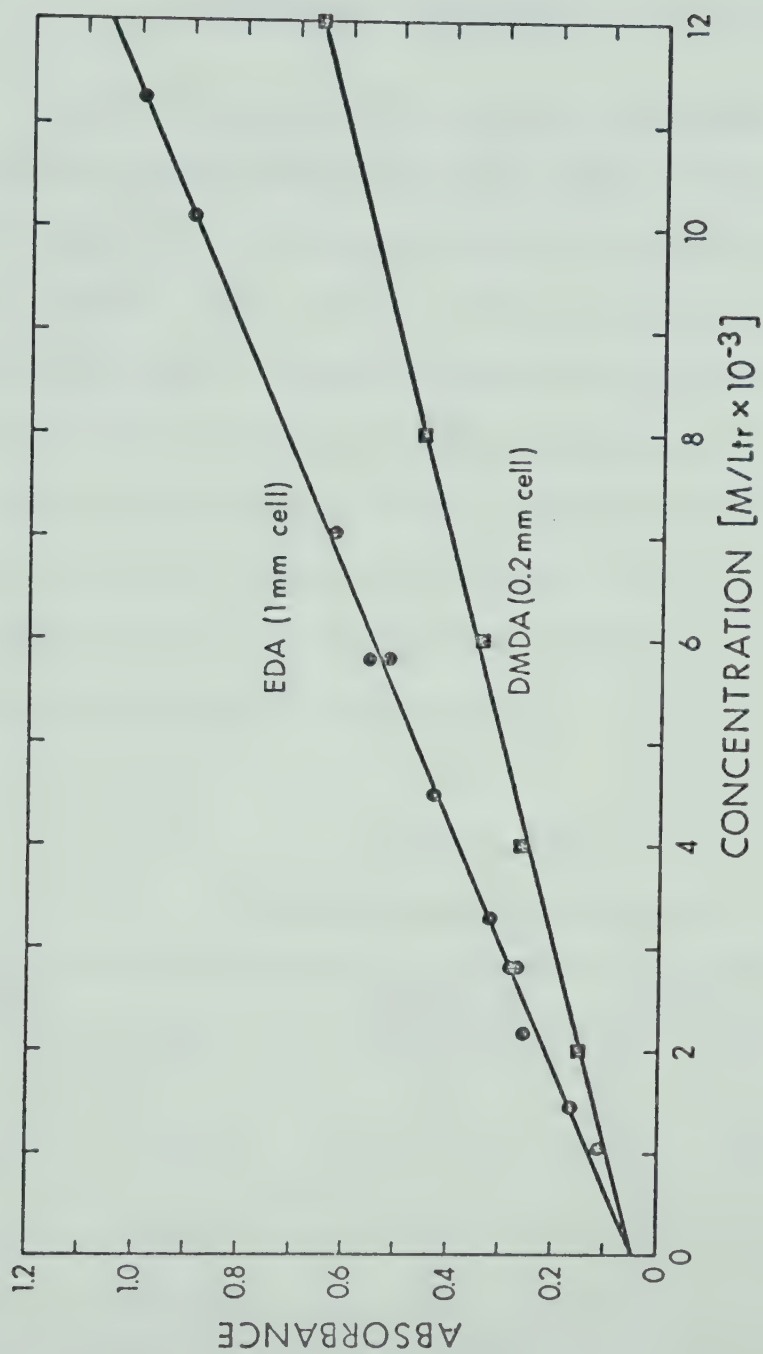


FIGURE 22: Calibration Curves for EDA and DMDA.

APPENDIX C

Quantitative Determination of [14]-[17]

A series of samples containing 0.1 gm DMDA per 25 ml trans-butene-2 was irradiated at 18°C using a quartz tube (16 mm diameter) and three different cut-off filters (Vycor, Pyrex and Uranium glass). After removal of the solvent at 0°C and of metallic mercury, the volume of each reaction mixture was made up to 1.0 ml with chloroform. For quantitative determination by g.c. the peak areas were compared with standards containing 1.60×10^{-2} M/ltr. of [14], 1.90×10^{-2} M/ltr. of [16], and 1.40×10^{-2} M/ltr. of [17]. The yields obtained for the different photolyses and the reaction conditions are listed in Table XXVIII.

TABLE XXVIII

Product Yields for [14]-[17]

Sample No.	Filter	Irradiation Time (hrs.)	% Yield (theoretical)			
			[14]	[15]	[16]	[17]
I-a	Vycor	1	8.7	1.3	2.1	20
I-b	Vycor	1	10.5	0.9	1.8	-
II	Pyrex	3	1.9	<0.1	0.13	34
III	U-glass	8	0.97	<0.1	0.11	40

APPENDIX D

Quantitative Determination of [18] and [19]

For the quantitative determination of ethylpyridine-3-carboxylate [18] and ethyl α -pyrrolylacetate [19], a series of samples containing ~0.4 and ~0.2 gm of DMDA and EDA, respectively, dissolved in 20 ml of freshly distilled pyrrole were photolyzed in a small quartz tube (16 mm diameter). Each sample was carefully degassed to exclude oxygen and the photolysis temperature was kept at 18°-20°C (cf. Experimental, section 2.3).

After the photolysis, aliquots of the 20.0 ml reaction mixture were compared by g.c. with a standard containing 0.160 M/ltr. of [18] and 0.047 M/ltr. of [19] in pyrrole. The column used was a 3 ft. x 1/4 inch tubing packed with 20% carbowax 20M on chromosorb W (30-60 mesh) and operated at a column temperature of 170°C and a helium flow rate of 60 cc/min. All samples including the standards were run in duplicate and on the same day allowing 2 to 3 hour intervals for reconditioning on column at elevated temperature. The peak areas, measured by a planimeter, were found to be directly proportional to concentration as per experiments with diluted standards, and also reproducible within $\pm 2\%$ of the total area. The per cent theoretical yields, based on the amount of the starting material for [18] and [19] recovered metallic mercury and photolysis conditions, are summarized in Table XXIX.

TABLE XXIX

Analytical Data for the Photolysis of DMDA and EDA in Pyrrole

Photolysis Number	Filter	Irradiation Time (hrs.)	% Yield (theoretical)		% Metallic Mercury Recovered
			[18]	[19]	
Photolysis of DMDA					
I-a		3	45.5	-	98
I-b		3	43.2	4.10	90
II-a	Pyrex	8	42.1	10.3	100
II-b	Pyrex	8	40.7	10.1	100
III-a	Uranium	11	43.3	-	-
III-b	Uranium	11	45.2	11.2	100
III-c	Uranium	11	42.1	11.2	100
Photolysis of EDA					
IV		3	8.5	18.0	

B30040